

**Electroosmosis and Electrochromatography in  
Narrow Bore Packed Capillaries**

by

**Iain Henry Grant**

A thesis presented for the degree of  
Doctor of Philosophy in the  
Faculty of Science at the  
University of Edinburgh  
1990



## **DECLARATION**

This thesis is the original work of the author, unless otherwise stated, and has not been submitted previously for any other degree.

Iain H. Grant.

## ACKNOWLEDGEMENTS

First and foremost I would like to sincerely thank my supervisor, Professor J. H. Knox for his patience, enthusiasm and helpful advice during the course of this work, and also for initiating my interest in this area of research.

I would also like to thank the Science and Engineering Research Council and Kratos Analytical Instruments (Manchester, U.K.) for funding the project as a SERC CASE award.

The services of the chemistry department mechanical workshop, which were required on several occasions, are also greatly appreciated.

Finally I would like to thank the staff and students, past and present, of the University of Edinburgh chemistry department physical chemistry section, particularly those involved with research into chromatography and related areas, for helpful discussions and their friendship during my course of study.

## ABSTRACT

Electroosmosis, the electrically induced flow of liquid, can be used as an alternative to pressure driven flow in liquid chromatography. Consideration of the physical nature of this type of flow suggests that less peak dispersion should result than with conventional flow. In addition theoretical considerations indicate that it should be possible to work with particles far smaller than those currently used in high performance liquid chromatography.

This work describes the use of electroosmosis to propel electrolyte through narrow capillaries packed with typical chromatographic packing materials. The resistive heating generated by the passage of electric current through the medium dictates that this must be carried out in capillaries of less than 200 $\mu$ m i.d.. The experimental methods used with such capillaries, including the production of packed capillaries are discussed.

Experiments carried out in capillaries packed with particles as small as 1.5 $\mu$ m in diameter demonstrate that adequate linear flow velocities can be obtained with particles which are too small for use in conventional chromatography due to pressure limitations. Measurements of the linear velocity of electroosmotic flow show that there is no evidence of a relationship between linear velocity and particle diameter, for particles ranging from 1.5 $\mu$ m to 50 $\mu$ m in diameter.

The direct comparison of plate heights obtained using both pressure driven flow and electroosmotic flow shows that in the latter case considerably enhanced efficiencies are obtained. In some cases reduced plates heights as low as 0.7 have been achieved, providing strong evidence of a negligible contribution to the overall plate height from the van Deemter A-term. Using 1.5 $\mu$ m diameter particles plate numbers of 300,000 have been obtained for an unretained analyte in a time of approximately 5 minutes.

The implications of the results together with the performance limitations of electrically driven chromatography (electrochromatography) are discussed.

**To My Parents**

## Table of Contents

<b>1 INTRODUCTION</b>	<b>2</b>
1.1 Description of Chromatography and Electrophoresis.	2
1.2 Definition of Electrochromatography.	4
1.3 Experimental Objectives.	5
1.4 Basic Concepts in Chromatography.	5
1.4.1 Resolution	8
1.4.2 Plate Number	9
1.4.3 Reduced Parameters	10
1.5 Basic Concepts in Electrophoresis	11
<b>2 THEORETICAL ASPECTS OF CHROMATOGRAPHY</b>	<b>14</b>
2.1 Introduction	14
2.2 The Plate Theory of Chromatography.	14
2.3 Factors Contributing to Band Broadening in Liquid Chromatography.	19
2.3.1 Axial Diffusion	20
2.3.2 Slow Equilibration	21
2.3.3 Band Broadening Due to Flow	25
2.4 Limitations of Chromatographic Performance	30
2.5 Capillary Chromatography	32
<b>3 ELECTROKINETIC PHENOMENA</b>	<b>36</b>
3.1 Introduction	36
3.2 The Electrical Double Layer	37
3.2.1 Stern-Gouy-Chapman Model of the Electrical Double Layer	38
3.2.2 Diffuse Layer	38
3.2.3 The Rigid Layer or Stern Layer	43
3.3 Debye - Hückel Theory	44
3.4 Zeta Potential ( $\zeta$ )	47
3.5 Electroosmosis	48
3.5.1 The Smoluchowski Equation for Electroosmosis	49
3.5.2 Comparison of Electroosmotic Flow and Pressure Induced Flow	53
3.5.3 Effect of Double Layer Overlap on Electroosmotic Flow	55
3.5.4 Electroosmosis in a Packed Capillary	59
3.6 Electrophoresis	61
3.6.1 Large $\kappa a$ - The von Smoluchowski Equation	61
3.6.2 Small $\kappa a$ - The Hückel Equation	61
3.7 Band Broadening in Electrophoresis and Electrochromatography	63
3.7.1 Band Broadening due to Self-Heating	66
3.7.2 Trans-Column Temperature Profile	66
3.7.3 Correlation of $\Delta T$ with H	68
3.8 Optimisation of Analysis Time in Electrophoresis	71
3.9 Self Heating in Electrochromatography	77
<b>4 MODES OF CHROMATOGRAPHY AND ELECTROPHORESIS</b>	<b>80</b>
4.1 Introduction	80
4.2 Traditional Electrophoretic Methods	80
4.2.1 Moving Boundary Electrophoresis	80
4.2.2 Slab Gel Electrophoresis	81
4.2.3 Isoelectric Focusing	81
4.2.4 Isotachophoresis	82



4.3 Column Liquid Chromatographic Techniques	84
4.3.1 Frontal Chromatography	84
4.3.2 High Performance Liquid Chromatography (HPLC)	84
4.3.3 Displacement Chromatography	86
4.4 Capillary Electroseparation Methods	87
4.4.1 Capillary Zone Electrophoresis (CZE)	88
4.4.2 Complexation Electrophoresis	90
4.4.3 Capillary Gel electrophoresis	91
4.4.4 Micellar Electrokinetic Capillary Chromatography	92
4.5 Electrochromatography	94
<b>5 EXPERIMENTAL METHODOLOGY</b>	<b>100</b>
5.1 Introduction	100
5.2 Production of Packed Capillary Columns	100
5.2.1 Production of Drawn Packed Capillaries	102
5.2.2 Derivatisation of Drawn Capillaries	108
5.2.3 Slurry Packing of Capillaries	111
5.3 Instrumentation	113
5.3.1 Sample Introduction Techniques	114
5.3.2 Sample Introduction in Capillary Chromatography	115
5.3.3 Sample Introduction in Capillary Electrophoresis	116
5.3.4 Experimental - Capillary Chromatography Injection Method	117
5.3.5 Experimental - Electrochromatography Injection Method	121
5.3.6 Detection in Capillaries	123
5.3.7 Experimental - Detection System for Electrochromatography	124
5.3.8 Experimental - Dispersion due to Injection and Detection	125
5.3.9 Apparatus for Electrochromatography	127
5.4 Data Handling	131
5.4.1 Calculation of Plate Numbers from Fronts and Gaussian Peaks	131
5.4.1.1 Analysis of Fronts	131
5.4.1.2 Analysis of Gaussian Peaks	134
<b>6 EXPERIMENTAL MEASUREMENTS</b>	<b>138</b>
6.1 Introduction	138
6.2 Pressure Driven Experiments	139
6.2.1 Drawn Packed Capillaries	139
6.2.2 Slurry Packed Capillaries	147
6.3 Measurements in Electrochromatography	151
6.3.1 Experimental Procedure	151
6.3.2 Plate Height Measurements	153
6.3.2.1 Drawn Packed Capillaries	153
6.3.2.2 Slurry Packed Capillaries	155
6.3.3 Separations by Electrochromatography	163
6.3.4 Effect of Particle Size on Electroosmosis	171
6.3.5 Results for 1.5µm Diameter Particles	176
6.3.6 Effect of Ionic Strength in Electrochromatography	184
<b>7 DISCUSSION AND CONCLUSIONS</b>	<b>192</b>
7.1 Introduction	192
7.2 Electroosmotic Flow Rates	192
7.3 Comparison of Electrochromatography with HPLC	194
7.4 Comparison of Electrochromatography with CZE	196

7.5 Potential of Electrochromatography	196
7.6 Limitations of Electrochromatography	205
7.6.1 Dependence on $\zeta$ -Potential	205
7.6.2 Detection	207
7.7 Conclusions	208
<b>LITERATURE CITED</b>	<b>209</b>
<b>APPENDIX I - Calculation of <math>h, \nu</math> Coefficients</b>	<b>215</b>
<b>APPENDIX II - Datasystem for Electrochromatography</b>	<b>220</b>
<b>APPENDIX III - Optimal Analysis Time for a Fixed <math>d_p</math></b>	<b>227</b>
<b>APPENDIX IV - Glossary of Symbols Used</b>	<b>229</b>
<b>APPENDIX V - Courses Attended</b>	<b>233</b>



## Index of Figures

2.1	Factors Contributing to Flow Term in Plate Height Equation.	26
2.2	Knox $h, \nu$ Plot.	29
3.1	Schematic View Electrical Double Layer.	39
3.2	Variation of Potential within the Electrical Double Layer.	45
3.3	Electroosmotic Flow Profile.	50
3.4	Pressure Driven Laminar Flow Profile.	54
3.5	Electroosmotic Flow Profiles Predicted for Various $\kappa a$ Values.	56
3.6	Mean Linear Velocity of Electroosmotic Flow as a Function of $\kappa a$ .	58
5.1	Schematic View of Glass Drawing Process.	104
5.2	Photomicrograph of Drawn Packed Capillary.	106
5.3	Photomicrograph of Drawn Packed Capillary.	107
5.4	Schematic View Apparatus used for In-Situ Silanisation.	109
5.5	Principle of Heart-Cut Injection Procedure.	119
5.6	Injection and Solvent Delivery System for Capillary LC.	120
5.7	Injection Components for Electrochromatography.	122
5.8	Taylor Plot for Dispersion due to Laminar Flow in an Open Tube.	126
5.9	Schematic View of Complete System for Electrochromatography.	128
5.10	Analysis of Chromatographic Fronts.	133
5.11	Example Datasystem Report for a Chromatographic Peak.	136
6.1	Pressure Drive $h, \nu$ Plot for a 40 $\mu\text{m}$ i.d. Drawn Capillary ( $d_p = 5\mu\text{m}$ ).	141
6.2	Separation of Aromatic Hydrocarbons of 'In-Situ' Derivatised Drawn Packed Capillary ( $d_p = 5\mu\text{m}$ ).	145
6.3	Separation of Aromatic Hydrocarbons on Slurry Packed Capillary ( $d_p = 5\mu\text{m}$ , 2005 $\mu\text{m}$ i.d.).	150

6.4	Comparison of $h, v$ Plots for $5\mu\text{m}$ Particles in Drawn Packed Capillaries for Pressure and Electrically Driven Flow.	161
6.5	Summary of $h, v$ data for 3 and $5\mu\text{m}$ Particles in Drawn Packed Capillaries with Electrically and Pressure Driven Flow.	162
6.6	Separation of PAHs on ODS-Drawn Capillary ( $d_p = 5\mu\text{m}$ ) Electroosmotic.	165
6.7	Separation of PAHs on ODS-Drawn Capillary ( $d_p = 5\mu\text{m}$ ) Pressure Driven.	166
6.8	Overlay of Peaks from Electrochromatography and Pressure Driven Chromatography.	167
6.9	Electrochromatogram and First Derivative with Respect to Time.	168
6.10	Separation of PAHs on ODS-Drawn Capillary ( $d_p = 3\mu\text{m}$ ) Pressure Driven.	169
6.11	Separation of PAHs on ODS-Drawn Capillary ( $d_p = 3\mu\text{m}$ ) Electroosmotic.	170
6.12	Linear Velocity as a Function of Applied Field ( $d_p = 3\text{-}5\mu\text{m}$ ).	173
6.13	Linear Velocity as a Function of Applied Field (All Materials).	180
6.14	Reduced Plate Height as a Function of Reduced Velocity ( $d_p = 1.5\mu\text{m}$ .)	181
6.15	Rising (or leading) Front ( $d_p = 1.5\mu\text{m}$ .)	182
6.16	Falling (or trailing) Front ( $d_p = 1.5\mu\text{m}$ .)	183
6.17	Effect of Ionic Strength on Plate Height.	189
6.18	%Change in Electroosmotic Flow Velocity for a 1% Change in $\kappa a$ as a function of $\kappa a$ .	190
7.1	Minimum Analysis Times in Electrochromatography as a Function of $N$ .	201

## Index of Tables

	PAGE
3.1 Theoretical Minimum Analysis Times for $N=10^6$ (in electrophoresis).	75
6.1 Drawn Packed Capillary - Plate Height verses Linear Velocity Pressure Driven Data ( $d_p = 5\mu\text{m}$ )	140
6.2 Drawn Packed Capillary - Plate Height verses Linear Velocity Pressure Driven Data ( $d_p = 5\mu\text{m}$ ) (High Efficiency Batch).	142
6.3 Drawn Packed Capillary - Plate Height verses Linear Velocity Pressure Driven Data ( $d_p = 3\mu\text{m}$ ).	146
6.4 Slurry Packed Capillary - Plate Height verses Linear Velocity Pressure Driven Data ( $d_p = 5\mu\text{m}$ ).	148
6.5 Slurry Packed Capillary - Plate Height verses Linear Velocity Pressure Driven Data ( $d_p = 3\mu\text{m}$ ).	149
6.6 Drawn Packed Capillary - Plate Height verses Linear Velocity, and Linear Velocity verses Applied Field ( $d_p = 5\mu\text{m}$ ).	156
6.7 Drawn Packed Capillary - Plate Height verses Linear Velocity, and Linear Velocity verses Applied Field ( $d_p = 5\mu\text{m}$ ). (Batch with Particularly High Efficiency).	157
6.8 Drawn Packed Capillary - Plate Height verses Linear Velocity, and Linear Velocity verses Applied Field ( $d_p = 3\mu\text{m}$ ).	158
6.9 Slurry Packed Capillary - Plate Height verses Linear Velocity and Linear Velocity verses Applied Field ( $d_p = 5\mu\text{m}$ ).	159
6.10 Slurry Packed Capillary - Plate Height verses Linear Velocity and Linear Velocity verses Applied Field ( $d_p = 3\mu\text{m}$ ).	160
6.11 Drawn Packed Capillary - Plate Height verses Linear Velocity, and Linear Velocity verses Applied Field ( $d_p = 20\mu\text{m}$ ).	174
6.12 Drawn Packed Capillary - Plate Height verses Linear Velocity, and Linear Velocity verses Applied Field ( $d_p = 50\mu\text{m}$ ).	175
6.13 Slurry Packed Capillary - Plate Height verses Linear Velocity and Linear Velocity verses Applied Field ( $d_p = 1.5\mu\text{m}$ ).	179

6.14	Plate Height in Electrochromatography as a Function of Ionic Strength.	187
7.1	Theoretical Analysis Times in Electrochromatography for Non-Ionic Species.	204

# CHAPTER 1

## INTRODUCTION

## Chapter 1 INTRODUCTION

### 1.1 Description of Chromatography and Electrophoresis.

Chromatography and electrophoresis are the terms given to two, essentially independent, physical processes, by which the separation of chemical substances, for analytical or preparative purposes, is achieved via their differential migration through one of several possible media. After a given time, as a result of this differential migration, different species will be found at different locations within the medium resulting in a spatial separation. Both methods are widely used in the analysis and purification of an enormous range of compounds.

In the case of chromatography the process is based on a thermodynamic partitioning between two distinct phases, which are moving relative to each other. In general one of these phases is fixed and is termed the stationary phase, which can be either solid or liquid. The mobile phase can be liquid, in which case it is referred to as the eluent, or gaseous, where it is referred to as the carrier gas. Substances with a high affinity for the stationary phase migrate slower than those which spend a greater proportion of their time in the mobile phase. From this definition it is clear that the substances to be separated must possess different distribution ratios between the two phases if any degree of separation is to be obtained.

The process was first described at the turn of this century by the Russian botanist Michael S. Tswett<sup>1</sup>, to whom its discovery is accredited. Tswett also formulated



the name chromatography, from the Greek words *khroma* (colour) and *graphein* (to write), for he had employed his newly discovered phenomenon in the separation of plant pigments, which could be observed as a series of coloured bands.

In electrophoresis, separation takes place, in an electrolyte, due to the migration of ionic species induced by an electric field. The ions of each species migrate at velocities determined by their effective size and the charge carried. Although the phenomenon of electrical migration of colloidal particles had been known since the middle of the nineteenth century, the study of ion transport was first reported in 1886 by Oliver Lodge<sup>2</sup>, through an experiment in which the progress of a moving boundary of hydrogen ions within an indicator-containing gel was observed. The term electrophoresis (which literally means being carried or transported electrically) was conceived by the German bacteriologist Leonor Michaelis<sup>3</sup>, who, in 1909, investigated the "electrical transportation" of enzymes.

The earliest forms of electrophoresis were carried out in aqueous electrolyte solutions. However, the need to suppress the unwanted convection currents, resulting from heat generated within the medium, led to the introduction of stabilising media to electrophoresis in the form of paper<sup>4</sup> and gel electrophoresis<sup>5</sup>. This step enabled considerable advances to be made in the technique and as a result electrophoresis in slabs of gel is at present the most commonly used form of electrophoresis.

## 1.2 Definition of Electrochromatography.

The presence of a stationary support within the separation vessel also created the possibility of an interaction between the separating species and the stabiliser, which, although normally an undesirable effect, led to the possibility of a superimposition of electrophoretic and chromatographic separation mechanisms. In 1939, prior to the introduction of stabilising gels, the combination of electrophoretic and chromatographic methods was reported by H. Strain<sup>6</sup>. In this case an improvement over the chromatographic separation of the time, was recorded for several ionic dyes. Several years later the "electrophoretic" separation of electrically neutral carbohydrates was reported by Synge and Tiselius<sup>7</sup> using a technique which they named "electrokinetic ultrafiltration". In the latter case, the carbohydrates were carried through the pore structure of an agar gel by electroosmosis, which is the term used to describe the electrically induced flow of liquid often observed in electrophoretic experiments. The separation was attributed to the molecular sieving action of the agar gel.

Both of the above observations could be considered as examples of electrochromatography which is the main theme of this thesis. Although electrochromatography has previously been defined by H. Lecoq in 1944<sup>8</sup> as *"chromatography carried out with the aid of electromotive force"*, for the purposes of this thesis it shall be defined as *"chromatography in which electroosmosis is responsible for the flow of mobile phase."*

### **1.3 Experimental Objectives.**

Despite these early experiments, electrochromatography has been largely ignored as a research topic, presumably due to the intense development in both electrophoresis and chromatography in the years following. However, the physical properties of electroosmotic flow suggest that electroosmosis could be used to considerable advantage in liquid chromatography.

The objective of the work described within this thesis has been an investigation of the use of electroosmosis in liquid chromatography. This includes the measurement of electroosmotic flow rates in real chromatographic systems, and a direct comparison of the performance of conventional and electroosmotic systems, including the influence of parameters which affect this. The work involves aspects of both chromatography and electrophoresis.

### **1.4 Basic Concepts in Chromatography.**

Chromatography can be carried out on inert plates coated with an adsorbent or on strips of adsorbent, in which case the technique is referred to as thin layer chromatography (TLC). Alternatively the adsorbent material can be packed into open tubes, or columns, giving rise to the term column chromatography. In the later case a pressure difference between the inlet and outlet of the column generates the flow of mobile phase.

Ideally, the mixture to be separated would be introduced to the separation system as a zone of infinitesimal width, and would be separated into several bands, one



for each component of the mixture, after a very short migration distance. However, as the separation proceeds the individual zones are broadened, due to a number of kinetic processes (which are discussed in section 2.3) which hinders the separation. In most cases the separating zones rapidly take on a concentration distribution having a Gaussian form, which becomes wider as each band migrates along the length of separation system. Provided that the distribution ratio is constant along the length of the separation system, the distance between any two zone concentration maxima will increase linearly with the mean distance migrated. However, the width of each band is observed to increase only in proportion to the square root of the distance covered by that band, and in this way, provided that the process takes place over a sufficiently long distance, an effective spacial separation of the substances will be obtained.

If one considers a substance which has a distribution coefficient  $K$  between the two phases, the relative amounts ( $q$ ) of that species in each of the phases is given by equation 1.1,

$$q_s/q_m = K.(V_s/V_m) \quad 1.1$$

where  $V$  represents the volume of the phase and the subscripts  $s$  and  $m$  denote the stationary and mobile phases respectively.

In a chromatographic system in which the mobile phase moves at a mean velocity  $u$ , relative to the stationary phase, the velocity of a zone of a particular substance will be given by the fraction of that substance in the mobile phase at any time, multiplied by the mean mobile phase velocity, as shown in equation 1.2,

$$u_b = u. ( q_m / (q_s + q_m) ) \quad 1.2$$

where  $u_b$  denotes the mean velocity of a given zone or band.

The above can also be expressed in terms of time spent in the mobile and stationary phases, as in,

$$u_b = u. ( t_m / (t_s + t_m) ) \quad 1.3$$

where  $t_s$  and  $t_m$  represent the mean residence times in the stationary and mobile phases respectively. Equations 1.2 and 1.3 can both be expressed as 1.4a in which  $k'$  replaces  $q_s/q_m$  and  $t_s/t_m$  respectively.

$$u_b = u / ( 1 + k' ) \quad 1.4a$$

The ratio  $k'$  is termed the phase capacity ratio. From the above it is clear that if substances are to be easily separated they must have a significantly different  $k'$ .

In many forms of column chromatography the stationary phase is, or is supported on, a porous structure, and frequently it is necessary to distinguish between parts of the mobile phase which are actually moving and stagnant mobile phase within the pores. Thus, the term mobile zone is used to describe the portion of the mobile phase outwith the porous structure, whereas the term stationary zone denotes the stationary phase plus stagnant regions of the mobile phase. By analogy with equation 1.4a the following can be written,

$$u_b = u_o / ( 1 + k'' ) \quad 1.4b$$

where  $u_0$  is the mean velocity in the mobile zone and  $k''$  the zone capacity ratio.

#### 1.4.1 Resolution

The degree of separation of any two substances can be quantified by the term resolution ( $R_s$ ), which is defined as distance between the two band centres ( $\Delta z$ ) divided by the mean band width ( $w$ ) as in equation 1.5,

$$R_s = 2 (\Delta z) / (w_1 + w_2) \quad 1.5$$

where  $w_1$  and  $w_2$  represent the widths of bands 1 and 2 respectively.

Evidently in order to maximise the resolution between two substances it is necessary to choose conditions under which  $\Delta z$  will be large, i.e., vastly different  $k'$ , or a situation where the rate of band broadening is minimised. It is clear that the smaller the band broadening effect, the shorter the mean migration distance required for a given resolution. The degree of band broadening can be quantified by the concept of efficiency which is measured, by analogy with fractional distillation, in terms of the "number of theoretical plates" (usually written  $N$ ) to which the chromatographic arrangement is equivalent. This abstraction was introduced to chromatography by the Nobel laureates Martin and Synge in 1941<sup>9</sup>, whose plate theory of chromatography is considered in more detail in section 2.2.



### 1.4.2 Plate Number

The number of theoretical plates of a given system is expressed by equation 1.6,

$$N = L^2 / \sigma^2 \quad 1.6$$

Where  $\sigma$  refers to the standard deviation of the Gaussian concentration distribution in length units, and  $L$  the distance covered by a given zone. In the case of column chromatography  $L$  generally corresponds to the length of the column. A more useful indication of the efficiency of the chromatographic process is the "Height Equivalent to a Theoretical Plate" (HETP) which is also referred to as the plate height, denoted  $H$ . The plate height can be expressed as the rate of change of peak variance with respect to the distance migrated, as shown by equation 1.7a,

$$H = d\sigma^2/dz \quad 1.7a$$

If this is constant throughout the system  $H$  can be determined from,

$$H = L / N = \sigma^2 / L \quad 1.7b$$

Clearly the smaller the value of  $H$  the greater the degree of separation for a given migration length.

The relationship between  $N$  and the peak width (effectively  $4\sigma$ ), together with dependence of the relative migration rates on  $k'$  permits equation 1.5 for the resolution of two components to be expressed as,

$$R_s = ( (\alpha-1)/\alpha ) . ( k'/(1+k') ) . N^{1/2}/16 \quad 1.8$$

where  $\alpha = k'_1/k'_2$  and is referred to as the selectivity for two components with capacity factors  $k'_1$  and  $k'_2$  and  $k'$  denotes the mean value of the capacity factor. A resolution of 1.5 corresponds to an almost complete separation of two components.

This expression clearly shows the need for high plate numbers in cases where the selectivity is close to unity.

### 1.4.3 Reduced Parameters

For comparison of different chromatographic systems it is often convenient to express  $H$  in units of packing material particle diameters, in the form of the dimensionless quantity reduced plate height ( $h$ ).

Thus,

$$h = H / d_p \quad 1.9$$

Theoretical considerations and experimental observations show that  $H$  is a function of the mobile phase velocity and the particle diameter of the stationary phase support. The nature of the relationship between these parameters allows the reduced plate height to be expressed as a universal function of the reduced velocity, where the reduced velocity is defined as,

$$v = u_0 \cdot d_p / D_m \quad 1.10$$

and represents the ratio of the time taken by a molecule in the mobile zone to travel the distance equivalent to a particle diameter to the time taken to diffuse the same distance in the mobile phase. The convenience of such parameters becomes apparent in section 2.3.

## 1.5 Basic Concepts in Electrophoresis

An ionic species of charge  $q$ , when placed in an electric field will experience a force causing it to accelerate towards one of the electrodes, the direction of this force depending on the sign of the charge. The magnitude of this force is given by equation 1.11

$$F = q.E \quad 1.11$$

If the ion is in a viscous medium it will continue to accelerate until this force is balanced by an equal in magnitude but opposing force due to the viscous drag of the surrounding fluid. If the ion is considered to be spherical with radius  $a$ , the viscous drag can be expressed by Stokes law, which formulates this as a function of the linear velocity ( $u$ ), as in equation 1.12,

$$f = -6\pi.\eta.a.u \quad 1.12$$

where  $\eta$  represents the viscosity of the medium.

When these two forces are balanced the ion will continue to migrate at a constant velocity ( $u$ ) given by equating 1.11 and 1.12 to give,

$$u = q.E/(6\pi.\eta.a) \quad 1.13$$

From equation 1.13 it is clear that the terminal velocity of the ion is directly proportional to the strength of the applied field. The constant of proportionality, which is equivalent to  $q/(6\pi.\eta.a)$ , is referred to as the electrophoretic mobility of the ion and is denoted  $\mu_{ep}$ . Hence, the previous equation may be written as,

$$u = \mu_{ep}.E \quad 1.14$$

Electrophoretic mobility has a significance in electrophoresis equivalent to that of the phase capacity ratio in chromatography, whereby an obvious prerequisite for a separation by electrophoresis is a difference in electrophoretic mobility.

## **CHAPTER 2**

# **THEORETICAL ASPECTS OF CHROMATOGRAPHY**



## Chapter 2

# THEORETICAL ASPECTS OF CHROMATOGRAPHY

### 2.1 Introduction

As the degree of chromatographic resolution of two substances depends on their relative migration rates and on the rate at which band spreading occurs as the individual bands migrate, a theoretical approach to chromatography must be concerned with these factors.

The first theoretical treatment of chromatographic separations was presented by Wilson<sup>10</sup> in 1940. In this model equations were derived correlating the migration rates with the partition coefficient. However, no explanation of peak broadening, other than that caused by a non-uniform partition coefficient was given. The following year a more extensive treatment was presented by A.J.P. Martin and R.L.M. Synge which led to the plate theory of chromatography<sup>9</sup>.

### 2.2 The Plate Theory of Chromatography.

In this model the chromatographic column is likened to a fractional distillation column in which separations can be achieved which are equivalent to those obtained through several individual distillation stages. The efficiency of such a column could be described by the number of stages, known as "theoretical plates", to which the column is equivalent. For the distillation process the theoretical plate is defined as the section of the column over which the vapour in its lower boundary is in thermodynamic equilibrium with the liquid in its upper



boundary.

Martin and Synge<sup>9</sup> developed this idea into a theoretical model of the chromatographic process. According to their model the process could be visualised in the following manner. The column is divided into imaginary isolated sections known as plates and the effect of transferring small quantities ( $\delta v$ ) of eluent to adjacent plates, in the direction of migration, is considered. By placing a solute into the first plate and successively transferring quantities ( $\delta v$ ) of eluent, resulting in the transfer of a fraction  $\delta x$  of the plate contents to the next plate, and assuming that sufficient time is available between transfers for full equilibration between the two phases, the progress of a migrating zone can be simulated. After  $n$  such transfers it can be shown that the amount( $q$ ) of solute in each plate is described by a binomial distribution function as in equation 2.1,

$$q(r) = (n! / (n-r)! \cdot r!) \cdot (\delta x)^r \cdot (1-\delta x)^{n-r} \quad 2.1$$

where  $r$  corresponds to the serial number of the plate. The mean of such a distribution, which can be regarded as a discrete form of the Gaussian distribution, is equivalent to  $n \cdot \delta x$ . The profile of such a distribution is known to be symmetrical, and thus, the position of the concentration maximum ( $r_{\max}$ ), is equivalent to the mean.

Thus,

$$r_{\max} = n \cdot \delta x \quad 2.2$$

where  $r_{\max}$  denotes the serial number of the plate containing the highest

concentration of solute, and thereby marks the position of the band centre.

Here,  $\delta x$  can be expressed in terms of the volume transferred as in equation 2.3,

$$\delta x = (\delta v/v_A).R \quad 2.3$$

where  $v_A$  represents the volume of mobile phase in each plate and  $R$  the fraction of solute in the mobile phase at equilibrium. The total number of transfers  $n$  is given by the total volume transferred  $V_R$  divided by the transfer volume  $\delta v$ . By making the appropriate substitutions for  $n$  and  $\delta x$  the "mean" ( $r_{\max}$ ) can be expressed by equation 2.4.

$$r_{\max} = V_R.R / v_A \quad 2.4$$

The total volume of mobile phase ( $V_A$ ) through which the zone maximum has been displaced is given by  $r_{\max}.v_A$ . Thus, by substituting  $V_A$  for  $r_{\max}.v_A$ , and using the fact that  $R$  is equivalent to  $1/(1+k')$  (cf section 1.4), one obtains,

$$V_A = V_R / (1 + k') \quad 2.5$$

If eluent transfer were continued until the band maximum reached the end of the column  $V_A$  would correspond to  $V_m$  (the total volume of mobile phase contained within the column) and the resulting  $V_R$  would be termed the retention volume of the substance. Equation 2.5 describes the same relationship for the zone migration rate relative to the eluent front as that expressed by equation 1.4 (cf section 1.4).

The variance of the binomial distribution described by equation 2.1 is given by,

$$\sigma^2 = n.(\delta x).(1-\delta x) \quad 2.6$$

Using the fact that  $(1-\delta x) \simeq 1$ , the above can be reduced to equation 2.2. Thus, the standard deviation of the concentration distribution, in terms of plates, is equivalent to  $r_{\max}^{1/2}$ .

$$\sigma = r_{\max}^{1/2} \quad 2.7$$

In order that this may be expressed in length units, the standard deviation must be multiplied by the plate height(H). The variance, being equivalent to  $r_{\max}$ , can be expressed as  $Z/H$ , where  $Z$  represents the distance migrated. Inserting this value into equation 2.7 and multiplying by  $H$  gives the following expression for the peak standard deviation in units of length,

$$\sigma = (H.Z)^{1/2} \quad 2.8$$

Thus, for a constant value of  $H$  the zone widths are proportional to the square root of the distance migrated.

The implications of the plate theory are:

- The zones broaden in proportion to the square root of the distance migrated.
- The zones possess an approximately Gaussian profile.
- The migration rate is related to the distribution coefficient between two phases.

However, the theory has several drawbacks in that it is largely qualitative and offers no means of predicting the plate height ( $H$ ). The theory does nevertheless acknowledge that the rate of equilibration plays a decisive role in determining the dimensions of the plate height, in fact Martin and Synge define the chromatographic equivalent of plate height as, *"the thickness of the layer such that the solution issuing from it is in equilibrium with the mean concentration of solute in the non-mobile phase throughout the layer"*.

In other words the finite rate of equilibration results in the mobile phase profile being slightly ahead of its equilibrium counterpart in the stationary phase, by a displacement proportional to  $H$ . This suggests that the plate height increases with increasing flow velocity of the mobile phase. It also indicates that factors affecting the rate at which equilibrium is established, such as the fineness of the particles or the diffusion coefficients in both phases, have an influence on the plate height.

However, the plate theory does nothing to suggest which processes are involved in achieving equilibrium and says nothing with regard to other factors which may be involved in band spreading. The plate number  $N$  and the related parameter  $H$  however, remain useful indices for quantifying the separating power of chromatographic systems.

Later theoretical treatments of the chromatographic process separate the thermodynamic aspects, concerned with the relative migration rates, and the kinetic aspects responsible for band spreading.



## 2.3 Factors Contributing to Band Broadening in Liquid Chromatography.

The kinetic factors contributing to zone broadening are the following.

1. Axial diffusion
2. Non instantaneous equilibrium
3. Flow Tortuosity

Of the three listed above only the second, non instantaneous equilibrium, is hinted at by the plate theory.

If all processes independently bring about a Gaussian concentration profile, having started from an infinitely thin zone, the variance of the resultant profile is the sum of the independent variances, in accordance with the theory of errors. Since the plate height  $H$  is proportional to the profile variance, the total plate height is the sum of the individual plate heights arising from each process.

Hence,

$$H_{\text{total}} = H_1 + H_2 + \dots + H_n \quad 2.9$$

where  $H_x$  represents the plate height resulting from a given process.

The analysis of each process in turn leads to an expression for the total plate height. The first such treatment of band spreading was given by J. J. Van Deemter.

### 2.3.1 Axial Diffusion

The random thermal movement of the components of a given zone leads to zone broadening by axial diffusion. If the zone begins as a plane, having zero width in the direction of migration, the variance ( $\sigma_L^2$ ) of the resultant Gaussian distribution, after diffusion for a time  $t$ , is given by the Einstein diffusion equation, where  $D$  is the diffusion coefficient.

$$\sigma_L^2 = 2D.t \quad 2.10$$

In a chromatographic system it is necessary to take into account both diffusion in the mobile and stationary zones.

Thus,

$$\sigma_L^2 = 2D_m.t_m + 2D_s.t_s \quad 2.11$$

where the subscripts  $m$  and  $s$  denote properties of the mobile and stationary zones respectively.

Using the fact that  $k'' = t_s/t_m$ , the above can be written as,

$$\sigma_L^2 = 2(D_m + k''.D_s).t_m \quad 2.12$$

From the above definition of plate height,  $H$  can be obtained by dividing equation 2.12 by the migration distance ( $L$ ) to give equation 2.13 where  $L/t_m$  has been replaced by  $u_0$ , the mobile zone velocity.



$$H_{\text{diff}} = 2(\gamma_m D_m + k'' \gamma_s D_s) / u_0 \quad 2.13$$

The geometric constants  $\gamma_m$  and  $\gamma_s$  must be added to allow for the fact that diffusion within a packed chromatographic column will be obstructed to some extent by the particles. Using the reduced parameters defined in chapter 1, the above can be expressed in a dimensionless form as,

$$h = B / v \quad 2.14$$

where B corresponds to  $2(\gamma_m + k'' \gamma_s (D_s / D_m))$ .

Basically the magnitude of this effect depends solely on the time spent undergoing diffusion, and thus, as equation 2.13 suggests, the effect can be minimised by carrying out the chromatography at very high linear flow rates.

### 2.3.2 Slow Equilibration

As mentioned regarding the plate theory of chromatography, the finite time taken for equilibrium between the phases to be established leads to a finite size for the plate height for this model. In qualitative terms molecules spending a finite time in the mobile zone will be carried ahead of their "equilibrium" position whereas the reverse is true for a molecule residing in the stationary zone.

This effect can be modelled by a method known as the random walk model. The basis of this can be explained by the following thought experiment. For an observer moving on the crest of a chromatographic peak at the mean velocity of

the peak ( $u_0/(1+k'')$ ), his perception of his environment would be one of molecules (of that species representing the peak) moving in steps away from him at a constant velocity and towards him at a constant, although different, velocity. If the observer is looking forward (in the direction of flow), molecules in the mobile zone will seem to move away at a velocity of ( $u_0 - u_0/(1+k'')$ ) whereas molecules in the stationary zone will appear to move towards the observer at a velocity of  $u_0/(1+k'')$ . If looking backwards, stationary zone molecules will move away from, and mobile phase molecules will move towards the observer at their respective velocities.

For the sake of convenience let the forward and backward steps be of equal length. For an individual molecule, after taking  $n$  such steps, the probability of it being a net number of steps  $r$  away from the observer in the forward or reverse direction is given by a form of the binomial distribution where  $f$  corresponds to the actual number of forward steps ( $f=(r+n)/2$ ) and  $p$  and  $q$  are the probabilities of a forward and backward step respectively. Thus, the probability,  $p(r)$ , of a net  $r$  steps in a given direction is given by,

$$p(r) = (n! / (n-f)!f!) . p^f . q^{n-f} \quad 2.15$$

The variance of the above distribution, in units of steps, is  $n.p.q$ , which if  $p$  and  $q$  are equal, i.e. both are 0.5, is simply  $n/4$ . Thus, the variance in length units is given by,

$$\sigma^2 = n.l^2/4 \quad 2.16$$

where  $l$  is the actual step length.

The estimation of the contribution to band broadening from this effect requires expressions for  $n$  and  $l$ .

In a real system molecules do not move by conveniently taking steps of a fixed length, and so the mean step length  $l$  must be considered. The mean step lengths in the mobile zone and in the stationary zone are given by equations 2.17 and 2.18 respectively,

$$l_m = (u_o \cdot k'' / (1 + k'')). \tau_m \quad 2.17$$

and

$$l_s = (u_o / (1 + k'')). \tau_s \quad 2.18$$

where  $\tau$  denotes the mean duration of a step.

Using the fact that  $k''$  must equal  $\tau_s / \tau_m$ ,  $\tau_s$  can be replaced in equation 2.18 by  $k'' \cdot \tau_m$  to give the same result as equation 2.17. Thus, the step lengths in each zone are indeed equivalent. The probability of a molecule making a step in either zone is related to the probability of a particular molecule being in that zone divided by the length of time required for the step, which leads to an equal probability, i.e., both 50% for each event, confirming the applicability of the model.

The total number of mobile zone excursions is given by  $t_m$  divided by  $\tau_m$ . Since the steps are equally probable the overall number of steps is given by,

$$n = 2 \cdot t_m / \tau_m \quad 2.19$$

Substitution of the results for  $n$  and for  $l$  into equation 2.16 to give an expression for the variance, followed by division by the migration length leads to the following expression for the plate height,

$$H = u_0 \cdot k'' \cdot \tau_s / 2(1 + k'')^2 \quad 2.20$$

In the case where desorption from the stationary zone is limited by diffusion within it, the mean residence time  $\tau_s$  can be related to the stationary zone diffusion coefficient and the particle size ( $d_p$ ) by,

$$\tau_s = q \cdot d_p^2 / D_s \quad 2.21$$

where, for porous particles  $q \approx 1/15$ .

The replacement of  $\tau_s$  in equation 2.20 by the above yields,

$$H = (1/30) \cdot u_0 \cdot (k'' / (1 + k'')^2) \cdot (d_p^2 / D_s) \quad 2.22$$

or in reduced terms,

$$h = (1/30) \cdot (k'' / (1 + k'')^2) \cdot (D_m / D_s) \cdot v = C_s v \quad 2.23$$

The dependence of  $H$  on  $D_s^{-1}$  has led to this term being known as resistance to mass transfer in the mobile zone. This expression confirms the implication of the plate theory that high velocities will result in large plate heights. It also demonstrates the need for using small particles, since  $H \propto d_p^2$ .



### 2.3.3 Band Broadening Due to Flow

The inhomogeneity of a packed chromatographic bed, in conjunction with the properties of hydrodynamic flow give rise to an additional source of band spreading. The mean linear velocity of pressure induced flow in a cylindrical channel is proportional to the square of the channel diameter. In addition the velocity within any one channel varies, in a parabolic fashion, from zero at the channel wall to twice the mean velocity in the channel core.

This contributes to band spreading in two ways:

1. The interparticular channels within a chromatographic bed will have varying diameters and thus, the mean velocity will vary accordingly. Also the channels themselves will be randomly orientated, and will therefore deviate from the actual forward direction. This effect is known as eddy diffusion.
2. The variation of the linear velocity with axial position within a given channel will also lead to zone broadening. The detrimental effect on plate height arising from this phenomenon is counteracted by diffusion across the channel axis, which averages out the velocity differences, and thus, becomes more significant as the diffusion coefficient in the mobile phase decreases. For this reason the term mass transfer resistance in the mobile phase is used to describe this effect.

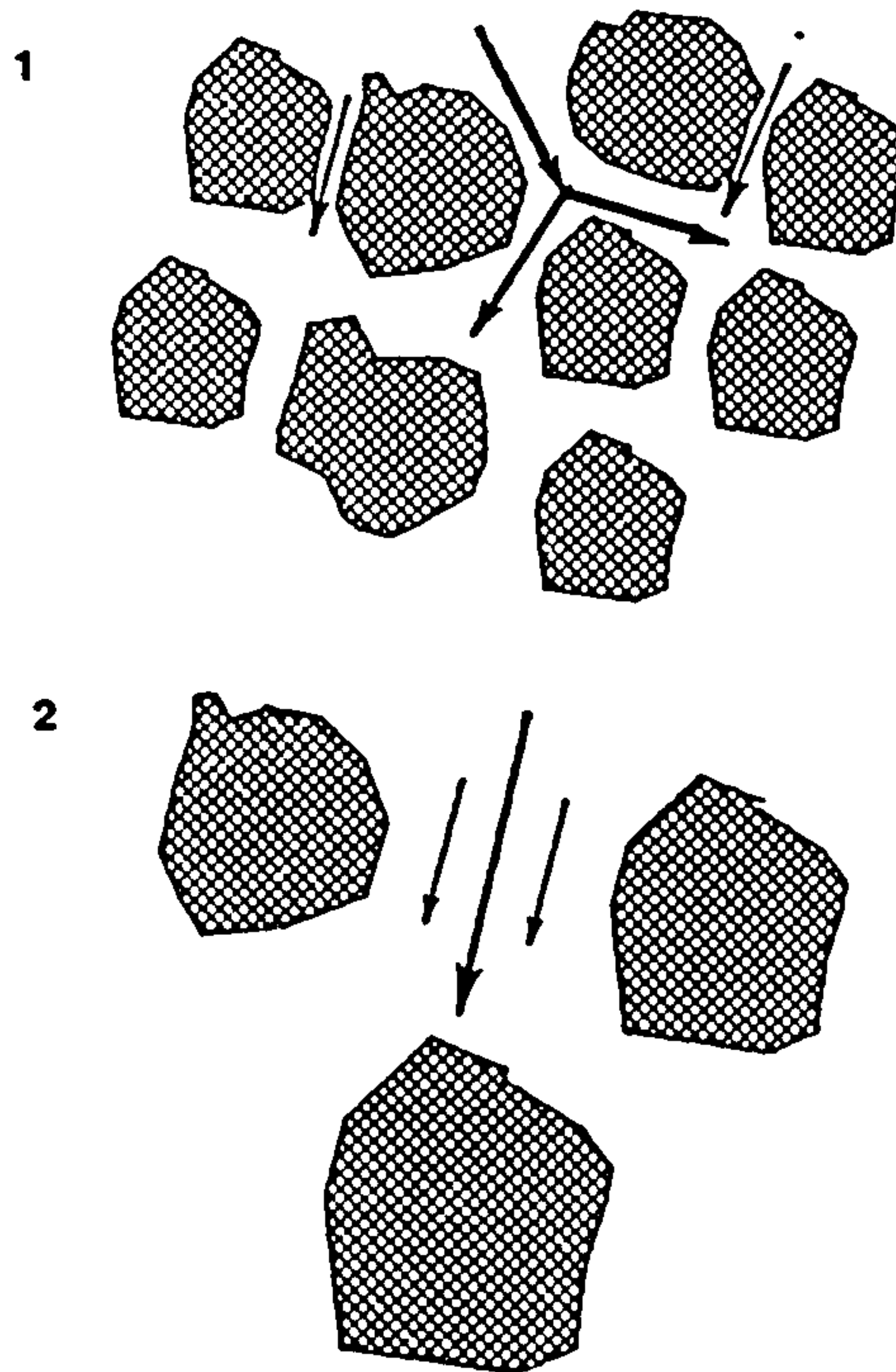
Both of these phenomena are depicted by figure 2.1.

In the original Van Deemter equation<sup>11</sup> only the first, eddy diffusion, is

FIGURE 2.1

Factors contributing to the A-term in the  $h, v$  relationship.

1. The flow velocity in channels wider and narrower than the mean channel diameter will be larger and smaller, respectively, than the mean velocity.
2. The flow velocity within a given channel is a function of the radial position within the channel.





considered. The situation can be treated by the random walk method whereby a molecule in a velocity region of less than the mean velocity can be considered as making a backward step and vice versa, and leads to,

$$H = 2\lambda \cdot d_p = A \cdot d_p \quad 2.24$$

or in reduced form,

$$h = A \quad 2.25$$

where  $\lambda$  is a geometric factor which depends on the uniformity of the column packing.

Combination of the reduced plate heights arising from all three processes considered leads to the original Van Deemter equation,

$$h_{\text{total}} = B/v + C_s \cdot v + A \quad 2.26$$

Consideration of the mobile phase mass transfer resistance, in an isolated channel leads to an additional factor<sup>12</sup> ( $C_m$ ), which is analogous to  $C_s$  in the above, whereby  $C_m \propto d_p^2/D_m$ . However, since the random nature of the flow, and not only mobile phase diffusion, effects the transport of solutes across the internal channels, the two factors cannot be regarded as independent.

The combination of both effects into a single expression for the plate height due to flow, which also takes into account the possibility of diffusion from one channel to another becomes a rather complex problem<sup>13,14</sup>. However, Knox<sup>15</sup> has shown that the overall contribution to the plate height, from flow effects, can be described by an expression of the form,

$$h_{\text{flow}} = A.v^{1/3} \quad 2.27$$

where the coefficient  $A$  has an approximate value of unity for a well packed bed.

Thus, the total plate height can be described by a modified form of the Van Deemter equation, sometimes referred to as the Knox equation,

$$h_{\text{total}} = B/v + C_s v + A v^{1/3} \quad 2.28$$

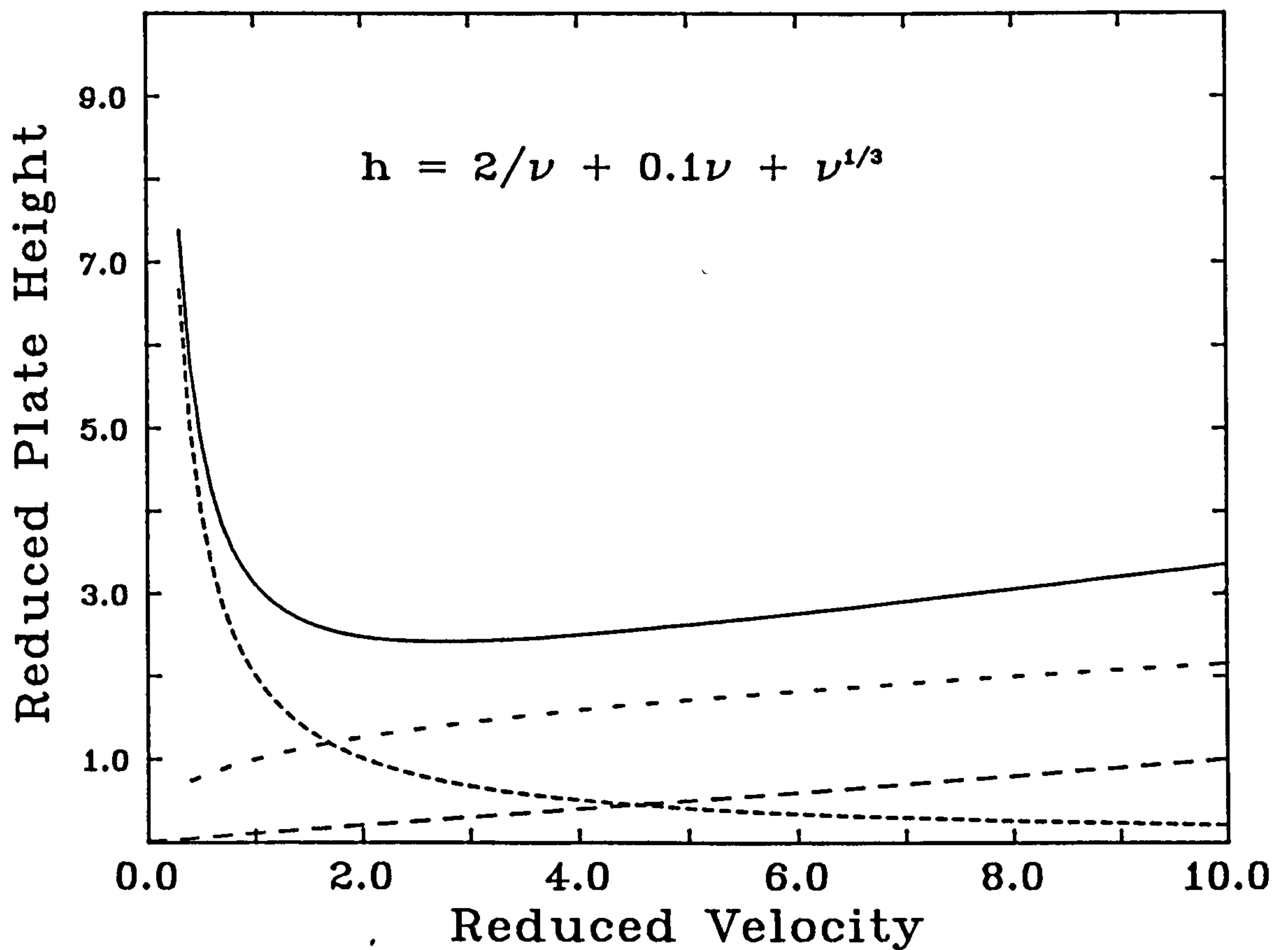
Thus, the plate height can be expressed by the above equation as a dimensionless parameter as a function of another dimensionless parameter. This is therefore a universal expression and as such should be valid for all types of chromatography and for all particle sizes. Figure 2.2 shows graphically the form of this function, for typical values of the coefficients  $A$ ,  $B$  and  $C_s$ , together with the contributions from the individual processes.

It is clear from the above expression that there exists a reduced velocity for which the plate height is a minimum and therefore if one operates with a very low or very high reduced velocity a loss of efficiency will be encountered. It is also readily apparent that with the use of smaller particles and a correspondingly higher flow rate, the same reduced velocity and plate height are maintained. This leads to smaller actual plate heights, and furthermore to a shorter analysis time for a given number of plates. It was realised by Giddings<sup>16</sup> and Knox<sup>17</sup> that taken to extremes the highest performance would be expected using very small particles and high flow rates. In the case of liquid chromatography this has led to the current practice of "High Performance Liquid Chromatography" (HPLC) in

FIGURE 2.2

## Reduced Plate Height as a Function of Reduced Velocity.

This graph illustrates the Knox  $h, \nu$  relationship (equation 2.28). Typical values for the coefficients A, B and C of 1, 2 and 0.1 respectively, were assumed. The individual contributions from each term are indicated by the dotted lines.



which 3-5 $\mu$ m diameter particles and linear velocities of 1-2mm.s<sup>-1</sup> are used.

## 2.4 Limitations of Chromatographic Performance

The trend towards smaller particles, in liquid chromatography, is ultimately restricted by the fact that higher and higher pressure drops are required in order to maintain the required reduced velocity. For this reason the available pressure drop must be taken into account in the search for optimal conditions. The possibility of a kinetic optimisation in chromatography was first investigated by Knox and Saleem<sup>18</sup>.

The main conclusion of this study was that there exists an optimum particle diameter for a given plate number and available pressure drop. The mean linear velocity of the mobile phase in a chromatographic column is given by the following version of the Poiseuille equation,

$$u = \Delta P \cdot d_p^2 / \phi \cdot \eta \cdot L \quad 2.29$$

where  $\Delta P$  is the pressure drop, and  $\phi$  a dimensionless resistance parameter, which typically has a value of ca. 500 for spherical particles. If one substitutes  $u$  by  $L/t_m$  and subsequently  $L$  by  $N \cdot h \cdot d_p$ , following a minor rearrangement one obtains the following expression for  $t_m$ ,

$$t_m = N^2 \cdot h^2 \cdot \phi \cdot \eta / \Delta P \quad 2.30$$

The factors which depend on the nature of the column, namely  $h$  and  $\phi$ , can be



grouped together to give a parameter  $E = h^2 \cdot \phi$ . Since columns with a small value of  $E$  can produce an equivalent separation in a shorter time than those with larger values,  $E$  is referred to as the separation impedance. The best packed columns typically have a minimum  $E$  value of ca. 2000. It is evident from equation 2.30 that the shortest analysis time for a given pressure will be obtained by working at the reduced velocity for which  $h$  is a minimum. An expression for the particle size ( $d_{p(\text{opt})}$ ) necessary in order that this condition may be satisfied, can be obtained by substituting  $u$  in equation 2.29 by  $D_m \cdot v_{\text{min}} / d_p$  and  $N \cdot h_{\text{min}} \cdot d_p$  for  $L$  to give,

$$d_{p(\text{opt})} = (N \cdot h_{\text{min}} \cdot v_{\text{min}} \cdot \phi \cdot \eta \cdot D_m / \Delta P)^{1/2} \quad 2.31$$

where  $h_{\text{min}}$  represents the minimum reduced plate height value and  $v_{\text{min}}$  the reduced velocity at which this is obtained.

Currently in HPLC pressures of ca. 20MPa (200bar) together with particles of  $3\mu\text{m}$  and  $5\mu\text{m}$  in diameter are used. This enables the production of approximately ten thousand theoretical plates with an analysis time, for an unretained substance of about one minute. However, using typical values  $10^{-3}\text{Nm}^{-2}\text{s}$  for  $\eta$  and  $10^{-9}\text{m}^2\text{s}^{-1}$  for  $D_m$ , it can be shown that the realisation of one million plates would, in accordance with equation 2.30, require more than one day with the same pressure drop. In contrast, recent advances in the field of electrophoresis in free solution have shown that separations of ionic species, with efficiencies approaching one million theoretical plates are possible in less than one hour<sup>19</sup> (cf. chapter 4).



From the above discussion it can be concluded that the principal factor which restricts the performance of liquid chromatography is the limited pressure drop available. This is limited, not only because of instrumental factors, but also because of the physical strength of the porous packing material used to support the stationary phase.

The physical basis of electroosmosis is discussed in chapter 3. However, one of the properties of electroosmotic flow is that the mean linear flow velocity, is to a first approximation, independent of the size of the channel or pore network in which it occurs. In addition it is recognised that electroosmosis can be used to pump solvents through the pores of gel networks, which are apparently impermeable to pressure driven flow<sup>7</sup>. It is this aspect of electroosmosis which suggests that its use in liquid chromatography holds a great deal of promise.

## 2.5 Capillary Chromatography

Chromatography can also be carried out in open capillary columns, in which the stationary phase has been coated onto the capillary wall. In this case the plate height can be expressed by the Golay equation<sup>20</sup>. The predictable nature of the flow profile in an open tube allows an exact mathematical expression for the mobile phase mass transfer resistance. The Golay equation can be written in the form,

$$h = 2/\nu + C_m \nu + C_s \nu \quad 2.32$$

where  $C_m = (1 + 6k' + 11k'^2) / (96(1 + k')^2)$ , and  $\nu$  is defined as  $u \cdot d_c / D_m$  and  $h$  as  $H/d_c$  where  $d_c$  denotes the capillary diameter. The  $C_s$  term due to the

stationary phase mass transfer is normally very small, relative to  $C_m$ , and can justifiably be ignored.

Expressions analogous to equations 2.30 and 2.31 can be applied to capillary chromatography, as was demonstrated by Knox and Gilbert<sup>21</sup>, by using the above definitions for reduced plate height and reduced velocity and replacing  $\phi$  by its exact value for an open tube, which is 32.

Thus,

$$t_m = 32N^2 \cdot h^2 \cdot \eta / \Delta P \quad 2.33$$

and

$$d_{c(opt)} = (32N \cdot h_{min} \cdot v_{min} \cdot D_m \cdot \eta / \Delta P)^{1/2} \quad 2.34$$

For  $k' \simeq 1$ ,  $h_{min}$  has a value of 0.6 corresponding to a reduced velocity of 6.5. The separation impedance,  $E = h^2 \cdot \phi$ , in this situation, would have a value as low as 11.5 compared with ca. 4500 for a packed column, which suggests that equivalent separations could be carried out more than four hundred times faster, with the same available pressure. In fact equation 2.33 suggests that one million plates could be realised in approximately 10 minutes with a pressure of 200bar, if  $\eta = 10^{-3} \text{ Nm}^{-2} \text{ s}$  and  $D_m = 10^{-9} \text{ m}^2 \text{ s}^{-1}$ .

A problem arises however, when one calculates the capillary diameter required to give the optimum conditions with the full available pressure. In the above case, in order to obtain one million plates in the time quoted, one would require a capillary of only  $2.5 \mu\text{m}$  in diameter. Thus, the generation of very high plate

numbers in a short time in capillary liquid chromatography demands the use of capillaries which are far too small to be practical.

The situation for gas chromatography is somewhat different, where low viscosities mean that the same analysis times as in LC can be obtained with only about one fiftieth of the pressure drop, i.e. ca. 5bar. Inserting this value into equation 2.34, together with a typical value for  $D_m$  in gases of  $10^{-5} \text{ m}^2 \text{ s}^{-1}$ , shows that  $d_c$  may be 100 times larger than for LC, i.e. 250 $\mu\text{m}$  instead of 2.5 $\mu\text{m}$ . Practical conditions can therefore be found for GC, and as a result, capillary columns are widely used in gas chromatography.

## **CHAPTER 3**

### **ELECTROKINETIC PHENOMENA**



## Chapter 3

### ELECTROKINETIC PHENOMENA

#### 3.1 Introduction

Before discussing the theoretical aspects of electrophoresis, it is necessary to consider the physical nature of charges in an electrolyte medium, and the effect they have on their surroundings.

An ion or charged particle in an electrolyte exerts an influence on its immediate environment by virtue of its electric field. This electric field causes dipolar molecules in the immediate vicinity to orientate themselves according to the sign of the charge, like charged ions (co-ions) to be repelled from the area whereas oppositely charge ions (counter-ions) experience an attractive potential. As a consequence of the attractive potential counter ions would be expected to approach the charge until the smallest possible distance was achieved. However, the random thermal motion of ions in solution acts against this tendency. This combination of electrical potential energy and thermal energy gives rise to a locally organised region of electrolyte, whereby the ionic distribution in the vicinity of the charge results from the relative magnitudes of the two opposing factors. The resulting locally modified region is referred to, in the case of an ion, as the ionic atmosphere of the ion. Many solid surfaces, such as glass or most metals, acquire a charge through self ionisation when in contact with an electrolyte. In this case the surface together with its associated structured region of electrolyte is known as the electrical double layer. The latter is largely responsible for many of the observed electrokinetic effects and therefore merits



some consideration. Here, the term electrokinetic effects is used as a general term for four associated phenomena:

- **Electrophoresis** - As discussed in the previous chapter, electrophoresis is the migration of charged species in an electric field.
- **Sedimentation Potential** - This is the term given to the potential developed due to the sedimentation of charged particles in an electrolytic medium. This can be considered as the reverse process of electrophoresis.
- **Electroosmosis** - Electroosmosis is the bulk flow of electrolyte induced by an electric field.
- **Streaming Potential** - This effect can be regarded as the counterpart of electroosmosis, being the development of a potential difference (the streaming potential) resulting from the flow of electrolyte.

Rationalisation of the above effects, especially electroosmosis, owing to its particular relevance in this thesis, requires a suitable model of the electrical double layer.

### 3.2 The Electrical Double Layer

A theoretical model of the electrical double layer was first introduced by Helmholtz<sup>22</sup> in 1879 in which the liquid side of the layer was envisaged as consisting of an immobilised layer of adsorbed counter ions. This model was however inadequate in its explanation of observed electrokinetic effects. An alternative was developed by Gouy in 1910<sup>23</sup> and Chapman in 1913<sup>24</sup> in which the double layer was considered as a diffuse layer of counter ions, whose concentration decreases with increasing distance from the surface. This view was

also to some extent inadequate since, according to this model unrealistically high concentrations of counter ions were predicted at positions close to the surface.

The currently accepted model of the double layer combines the ideas of the above versions and is the result of work by Stern in 1924<sup>25</sup>.

### **3.2.1 Stern-Gouy-Chapman Model of the Electrical Double Layer**

In this model, which is depicted graphically by figure 3.1, the electrical double layer is viewed as consisting of two distinct regions, whereby the excess charges in the electrolyte are distributed between a layer of counter ions (the rigid layer) situated at the shortest possible distance from the charged surface and a diffuse layer.

### **3.2.2 Diffuse Layer**

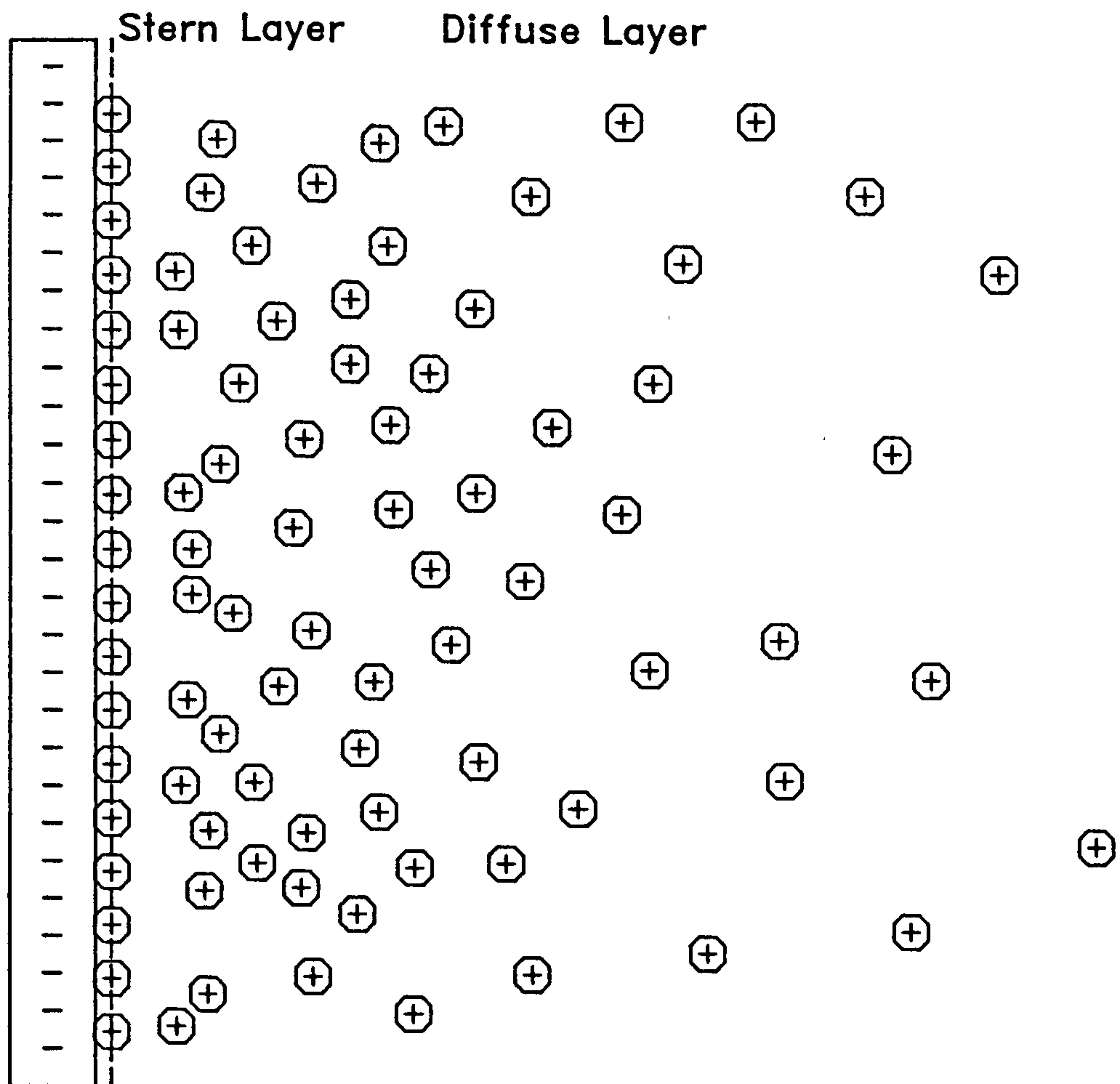
In this model of the diffuse part of the double layer the surface is considered to be flat and of infinite area. For such a hypothetical surface, in a vacuum, the electric field at any distance would be constant and thus the potential at any point would be infinite. Here, the potential is defined as the work done, per unit charge, in bringing a point charge  $dq$  from an infinite distance to its present position. In an electrolyte however, the presence of excess counter ions in the electrical double layer causes the field to drop with distance from the surface and thus the potential has a finite value.

The potential and the net charge density in the electrolyte can be related by the Poisson equation,

FIGURE 3.1

**Schematic view of the electrical double layer.**

The diagram below represents a schematic view of an electrical double layer composed of a negatively charged surface, e.g. glass or silica, and an excess of cations on the liquid side of the interface. In this representation only the *excess* cations are shown.



$$\nabla^2\psi = -\rho(x)/\epsilon_r\epsilon_0 \quad 3.1$$

where  $\rho(x)$  represents the net charge density at a distance  $x$  from the surface, and  $\epsilon_r$  and  $\epsilon_0$  the relative permittivity and the permittivity of free space respectively.

The simple geometry introduced by the assumption of a flat double layer of infinite area, allows the following simplified version to be used,

$$d^2\psi/dx^2 = -\rho(x)/\epsilon_r\epsilon_0 \quad 3.2$$

The solution of this equation would yield an expression for the variation of potential with distance from the surface, but before this is possible an expression for the net charge density is required.

The tendency for counter ions to remain close to the charged surface, brought about by the favourable potential is counteracted by the random thermal motion of the ions. A counter ion at a distance  $x$  from the surface where the potential is  $\psi$  will possess  $ze\psi$  less potential energy than an ion at infinite distance, where  $z$  refers to the charge number and  $e$  the charge on an electron, whereas the reverse is true for the co-ions. The populations of energy states with a known energy difference between them can be predicted by the Boltzmann distribution function,

$$n_1/n_0 = \exp(\Delta E/kT) \quad 3.3$$

This equation predicts the relative equilibrium populations of two energetic states



$E_0$  and  $E_1$  which are separated by an energy difference of  $\Delta E$  where  $n_1$  and  $n_0$  correspond to the populations of  $E_1$  and  $E_0$  respectively.

If the surface under consideration is positively charged, the number of anions per unit volume where the potential is  $\psi$  is given by equation 3.4.

$$n_- = n_0 \exp(z\psi/kT) \quad 3.4$$

Similarly the number of cations, per unit volume, is given by,

$$n_+ = n_0 \exp(-z\psi/kT) \quad 3.5$$

The number of excess negative charges ( $\rho$ ), per unit volume, at the plane where the potential is  $\psi$  is obtained by subtracting equation 3.5 from 3.4 and multiplying by the charge per ion ( $ze$ ) to give

$$\rho = (2ze n_0) \sinh(z\psi/kT) \quad 3.6$$

In this expression there are no unknown quantities other than  $\psi$  itself. Thus, substitution of equation 3.6 into the Poisson equation would permit a solution. However, the solution and the eventual expression are considerably simplified by making the following approximation which is valid if the argument for the hyperbolic sine function is considerably less than unity. In a later treatment of the ionic atmosphere Debye and Hückel made the same approximation, giving it the name of "the Debye-Hückel approximation".

$$\sinh(z\psi/kT) \simeq z\psi/kT \quad 3.7$$



The error introduced by the introduction of this approximation is less than 4% for a potential of 25mV at room temperature. For smaller values of  $\psi$  the error becomes negligibly small.

Using this approximation, the appropriate form of the Poisson equation is,

$$d^2\psi/dx^2 = -(2n_0 z^2 e^2 / \epsilon_r \epsilon_0 kT) \psi \quad 3.8$$

By gathering together the quantities which are, or are assumed to be, independent of  $x$  in the form of a constant  $\kappa^2$ , which is equivalent to the bracketed quantity in equation 3.8, the expression can be further simplified to,

$$d^2\psi/dx^2 = -\kappa^2 \psi \quad 3.9$$

The boundary conditions for the exact solution of this differential equation are,

- At infinite distance  $d\psi/dx = 0$  and  $\psi = 0$
- At zero distance ( $x=0$ )  $\psi$  is equivalent to the effective surface potential ( $\psi_d$ ) at the inner surface of the diffuse layer.

Solution of equation 3.9 under the above conditions yields the following simple expression for the potential, and thus also for the excess charge density, as a function of distance from the surface.

$$\psi = \psi_d \cdot \exp(-\kappa x) \quad 3.10$$

It follows that this part of the double layer is characterised by  $\kappa$  and by the

effective surface potential  $\psi_d$ . The constant  $\kappa$  which has reciprocal length units is generally referred to as the reciprocal thickness of the double layer or reciprocal Debye length.

The value of  $\kappa$  can be calculated from,

$$\kappa = (2n_0 z^2 e^2 / \epsilon_r \epsilon_0 kT)^{1/2} \quad 3.11$$

or more conveniently from,

$$\kappa = (2z^2 c F^2 / \epsilon_r \epsilon_0 RT)^{1/2} \quad 3.12$$

where  $c$  corresponds to the bulk concentration of electrolyte and  $F$  the Faraday constant.

Clearly when  $x = 1/\kappa$  the potential is only  $1/e$  of the surface potential. This distance is often referred to as the thickness of the electrical double layer. Typical values of  $1/\kappa$  range from 1nm to 1 $\mu$ m indicating that the double layer phenomenon is confined to a very narrow region adjacent to the surface. Bearing this in mind, it is not, even for large curved surfaces, entirely unreasonable to consider the double layer as being flat and of infinite extent.

### 3.2.3 The Rigid Layer or Stern Layer

In its simplest form the area bordering on the charged surface consists of an immobilised layer of adsorbed hydrated counter ions for which the attractive potential is sufficient to overcome the thermal motion of the ions. The plane defined by the centres of these ions is referred to as the Stern plane, or

sometimes the outer Helmholtz plane. The distance between this plane and the actual surface is denoted  $\delta$  and is equivalent to the radius of a hydrated counter ion.

This situation can be considered analogous to placing a sheet of charge parallel to the charged surface at a distance  $\delta$ . Here the potential could be expected to drop linearly within this region, exactly as it does between the plates of a charged capacitor. Thus, over the distance  $\delta$  the potential drops linearly from  $\psi_0$ , the actual surface potential to  $\psi_d$ , the potential at the Stern plane.

The behaviour of the potential throughout the double layer region is depicted by the graph in figure 3.2.

### 3.3 Debye - Hückel Theory

In order to provide a rational explanation for the departure from ideal behaviour, with respect to conductivity and chemical potential, of concentrated strong electrolytes, a similar treatment, as to that of the electrical double layer, was carried out for the ionic atmosphere by Debye and Hückel<sup>26</sup> in 1923.

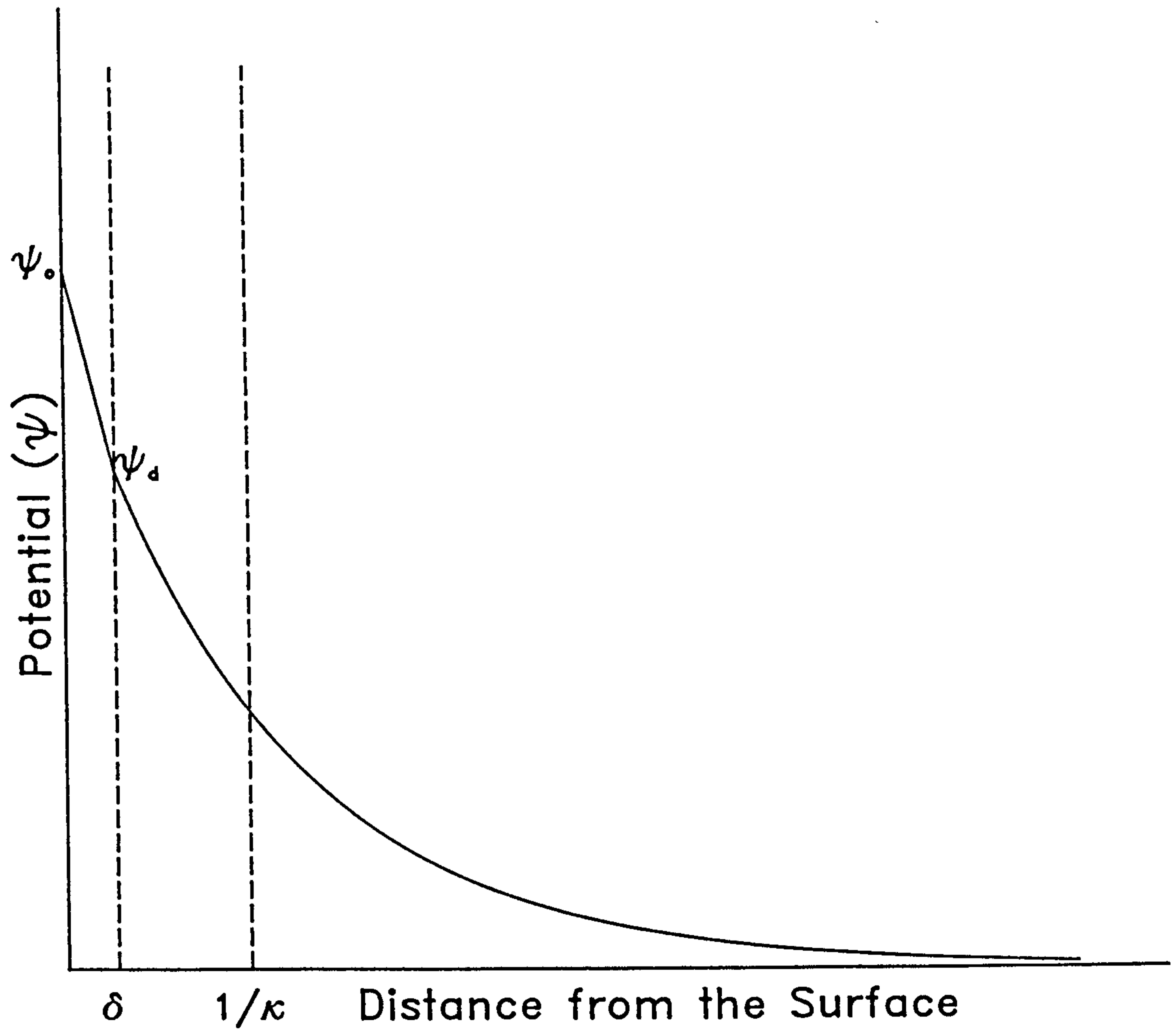
In this case the assumption is made that the central ion is small enough to be considered a point charge.

By applying the same considerations as for the diffuse part of the electrical double layer and making the Debye-Hückel approximation, but taking into account the spherical symmetry of the system, the appropriate form of equation 3.9 becomes,

FIGURE 3.2

## Variation of Potential within the Double Layer

Graph showing the variation of the electrical potential ( $\psi$ ) with distance from the charged surface.





$$d^2\psi/dx^2 + (2/x)d\psi/dx = -\kappa^2\psi \quad 3.13$$

If the same boundary conditions, as for the diffuse part of the double layer are applied one obtains,

$$\psi = \psi_d \cdot (a/x) \cdot \exp(-\kappa(a-x)) \quad 3.14$$

where  $\psi_d$  and  $a$  denote the potential at the inner boundary of the diffuse layer and the radius of the species respectively.

The assumption that the charge can be treated as a point charge is only valid if the radius of the charged species is small relative to the thickness of the electrical double layer. This condition is satisfied when  $a \ll 1/\kappa$  or  $\kappa a \ll 1$ .

The product  $\kappa a$  is an important factor which must be taken into consideration when deciding on the applicability of either of the above models. When  $\kappa a \gg 1$  the curvature of the charge surface is small relative to the double layer thickness and thus, the model of the flat double layer is appropriate.

Of the four electrokinetic phenomena mentioned in the introduction to this chapter, for which the electrical double layer is responsible, two, namely electroosmosis and electrophoresis, are relevant to this work and therefore merit further discussion.

The discussion of electrokinetic phenomena requires the definition of the term zeta potential which is of fundamental importance in the following arguments.

### 3.4 Zeta Potential ( $\zeta$ )

If the electrical double layer is caused to move parallel to the surface, either through the action of an applied pressure or electric field, there will be, in the case of a flat double layer, a plane of shear where the mobile diffuse double layer slips past the fixed rigid layer. The potential at this plane, which is situated a small but finite distance from the Stern plane, is termed the zeta potential and is denoted ( $\zeta$ ). It can be expected that the value of the zeta potential is very close to that of  $\psi_d$ . However, the importance of  $\zeta$  lies in the fact that experimental observations of electrokinetic phenomena can only yield values for  $\zeta$  and not for  $\psi_d$ . In other words the magnitude of observed effects depends on  $\zeta$  and not  $\psi_d$ .

The fact that the surface plus the double layer must be overall electrically neutral allows  $\psi_d$  to be related to the surface charge density  $\sigma_0$ . The integral of the charge density with respect to distance from the surface over the diffuse part of the double layer must be equivalent to the effective surface charge density ( $\sigma_d$ ) at the inner boundary of the diffuse layer. This leads to an expression for  $\psi_d$  as in equation 3.15.

$$\psi_d = \sigma_d / \epsilon_0 \cdot \epsilon_r \cdot \kappa \quad 3.15$$

Thus, the solution composition influences  $\psi_d$  and therefore  $\zeta$  through its effect on  $\kappa$  and  $\sigma_d$ . Increasing the electrolyte concentration increases  $\kappa$  causing a drop in  $\psi_d$  and consequently a lower value of the zeta potential results. For example, according to the 1942 data of Eversole and Boardman<sup>27</sup> for the case of a

Pyrex/aqueous KCl double layer, the zeta potential falls from 122mV for a KCl concentration of  $10^{-5}$  M to 69mV at  $10^{-3}$  M KCl.

### 3.5 Electroosmosis

If an electric field is applied parallel to the surface of a flat double layer, the ions in the diffuse part will move in the appropriate direction and in so doing will exert a force on the liquid, in accordance with their viscous drag. The magnitude of this force, per ion, is equivalent to  $zeE$  where  $E$  denotes the electric field strength. In the bulk liquid equal and oppositely directed forces are at work due to the migration of anions and cations in opposite directions and thus, no net force is applied to the liquid in the bulk region. In the electrical double layer however there exists an excess of counter ions over co-ions which means that in this region a net force is applied to the liquid in proportion to the excess charge density ( $\rho$ ).

The force which is applied within the electrical double layer will exert an influence on the rest of the liquid, in accordance with the definition of viscosity ( $\eta$ ),

$$F = \eta.A.(du/dx) \quad 3.16$$

This equation gives the magnitude of the force, acting in the flow direction, between two liquid planes with a velocity gradient ( $du/dx$ ), in the perpendicular direction, at the plane of contact, where  $A$  denotes the area of contact. This shows that the moving double layer will exert a force on the rest of the liquid



causing it to move and in so doing reduces ( $du/dx$ ).

The result of this can best be analysed by considering two large flat double layers separated by a distance which is large relative to the thickness of the double layers.

Immediately after application of the electric field only the liquid in the double layers will move. As a consequence of equation 3.16 force will be exerted on the adjoining layer causing it to move which will in turn induce movement in its neighbouring layer. This process will continue until, in the liquid area between the two double layers, the perpendicular velocity gradient ( $du/dx$ ) is zero. In other words the liquid between the two surfaces moves with a uniform velocity except in the double layer region. This development as a function of time is illustrated by figure 3.3. A mechanical analogy of this effect is that of a weight slipping on a moving conveyor belt. Here, whilst the weight is slipping an accelerating force will be applied to it depending on the coefficient of friction between the two surfaces and their velocity difference. The weight will accelerate until the velocity difference between it and the belt is zero and thereafter continue at the constant velocity of the belt.

The velocity of this uniform electroosmotic flow can be related to the zeta potential by the von Smoluchowski equation<sup>28</sup>.

### **3.5.1 The Smoluchowski Equation for Electroosmosis**

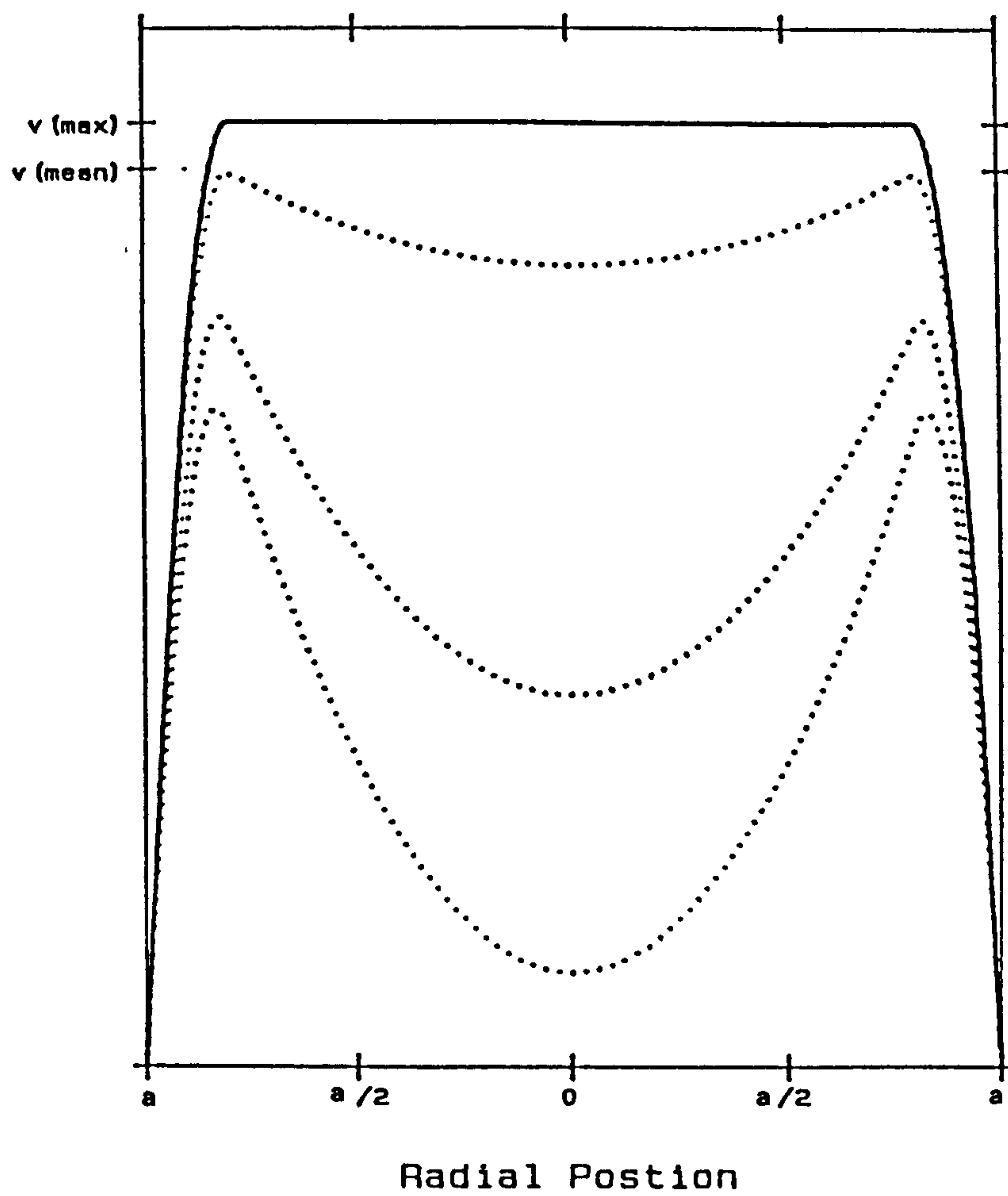
At equilibrium the electrical force applied in the double layer must be counteracted by an equal and oppositely directed viscous resistance.



FIGURE 3.3

## Velocity Profile for Electroosmotic Flow

The development of the flow profile in electroosmotic flow with time. The starting profiles are depicted by the dotted lines.



Consider the forces acting on a layer of width  $dx$  within the electrical double layer. The electrical force  $dF_E$  is given by  $E\rho dV$  where  $dV$  represents the volume of the layer.

Thus,

$$dF_E = E.A.\rho.dx \quad 3.17$$

where  $A$  is the area of the layer.

In accordance with equation 3.16, the viscous force  $dF_V$  acting on the layer is given by the product of the difference in velocity gradient from one side of the layer to the other, viscosity and area of contact.

Thus,

$$dF_V = \eta.A.d(du/dx) \quad 3.18$$

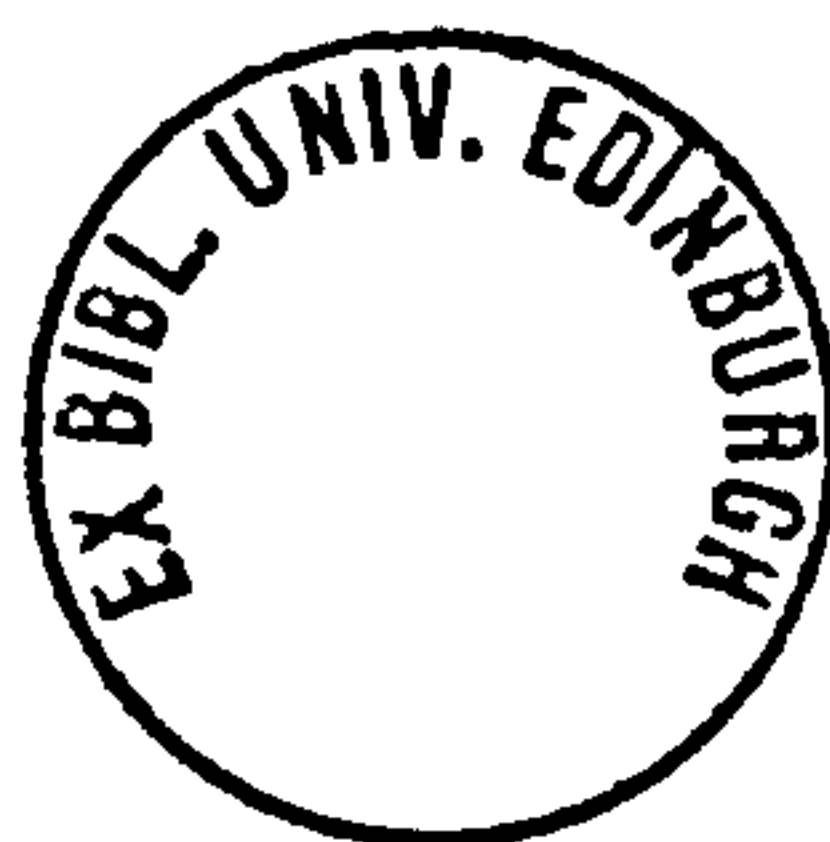
By equating 3.17 and 3.18 and making minor rearrangements one obtains,

$$d^2u/dx^2 = E\rho/\eta \quad 3.19$$

Eliminating  $\rho$  between equation 3.19 and the Poisson equation yields,

$$d^2u/dx^2 = -(E.\epsilon_r\epsilon_0/\eta)d^2\psi/dx^2 \quad 3.20$$

If the quantity in brackets is assumed to be constant throughout the double layer, this equation can be easily solved by integrating twice. The derivation therefore



makes the assumption that the relative permittivity and viscosity remain constant throughout the double layer.

Integrating once yields,

$$du/dx = -(E.\epsilon_r\epsilon_0/\eta)d\psi/dx + c \quad 3.21$$

From the previous arguments, at a significant distance relative to the double layer thickness  $du/dx$  and  $d\psi/dx$  are both equal to zero, which implies a value of zero for  $c$ . This expression is in agreement with the above qualitative model as it shows that  $du/dx$  has a non zero value only when  $d\psi/dx$  has a non zero value, i.e., within the double layer.

Following a second integration and applying the condition that at the plane of shear where  $\psi = \zeta$  the velocity must be zero, the expression becomes,

$$u = (E.\epsilon_r\epsilon_0/\eta).(\zeta - \psi) \quad 3.22$$

The velocity outwith the double layer where  $\psi = 0$  is clearly going to be very close to the overall mean velocity, provided that the distance between the surfaces is relatively large. Thus, the mean velocity of electroosmotic flow is expressed by equation 3.23 which is known as the von Smoluchowski equation,

$$u = (\epsilon_r\epsilon_0\zeta/\eta).E \quad 3.23$$

The bracketed quantity is analogous to electrophoretic mobility and is often written as  $\mu_{eo}$ , and referred to as the coefficient of electroosmotic flow.

Provided that the dimensions of the channels are not so small that the double layers on either side overlap, this equation would be valid for electroosmotic flow within any channel regardless of cross sectional shape and thus, also for capillary tubing. Bearing in mind that electrical double layer thicknesses may be as small as 1nm, it is clear that electroosmotic flow can occur in very narrow channels.

### 3.5.2 Comparison of Electroosmotic Flow and Pressure Induced Flow

The uniform velocity profile predicted for electroosmotic flow contrasts sharply to the situation for pressure induced flow. In the case of a cylindrical vessel, or capillary, the velocity of pressure induced laminar flow as a function of the radial position within the channel, can be expressed by the Poiseuille equation,

$$u(x) = \Delta P(a^2 - x^2)/4\eta.L \quad 3.24$$

where  $\Delta P$  represents the pressure drop,  $L$  the length of the tubing,  $a$  the radius of the channel and  $x$  the radial distance from the channel centre. A comparison of flow profiles in electroosmotic flow and pressure driven flow is given by figures 3.3 and 3.4.

The mean velocity of pressure driven flow in a capillary is given by,

$$u = \Delta P.a^2/8\eta.L \quad 3.25$$

or,

$$u = \Delta P.d_c^2/32\eta.L \quad 3.26$$

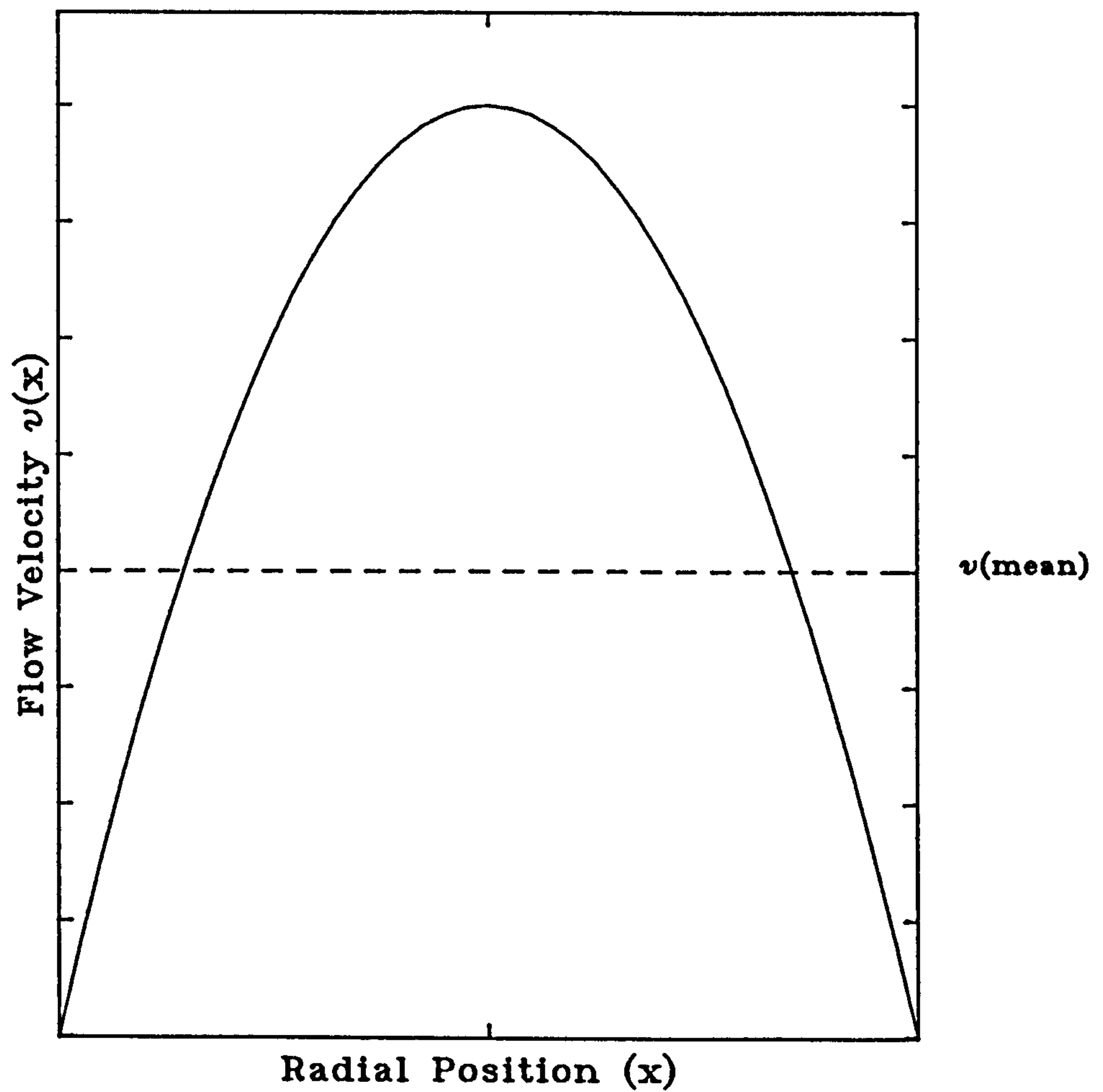
where  $d_c$  denotes the capillary diameter.



FIGURE 3.4

Velocity profile for pressure induced laminar flow.

The mean velocity, in the case of a cylindrical capillary, is equivalent to half the velocity in the central core.



Equations 3.24 and 3.25 show that the velocity of pressure driven flow has a parabolic dependence on the position within the channel and that the mean flow velocity is proportional to the square of the channel diameter. In contrast the velocity of electroosmotic flow, provided that the electrical double layers do not overlap, shows little dependence on the radial position within a channel. In addition, with the same condition, the mean velocity is not a function of the channel diameter.

### 3.5.3 Effect of Double Layer Overlap on Electroosmotic Flow

Where electroosmosis takes place in very narrow capillaries, for which the diameter is significant relative to the Debye length, or in porous beds of particles considered as networks of such capillaries, the possibility of double layer overlap must be taken into account. In such cases a departure from the classical von Smoluchowski equation would be expected.

Rice and Whitehead<sup>29</sup> have made a detailed theoretical study of the situation and have shown that the resulting velocity profile can be described by equation 3.27 where  $I_0$  represents the zero order modified Bessel function of the first kind, which arises from the solution of the Poisson equation for cylindrical geometry, and  $a$  the channel radius.

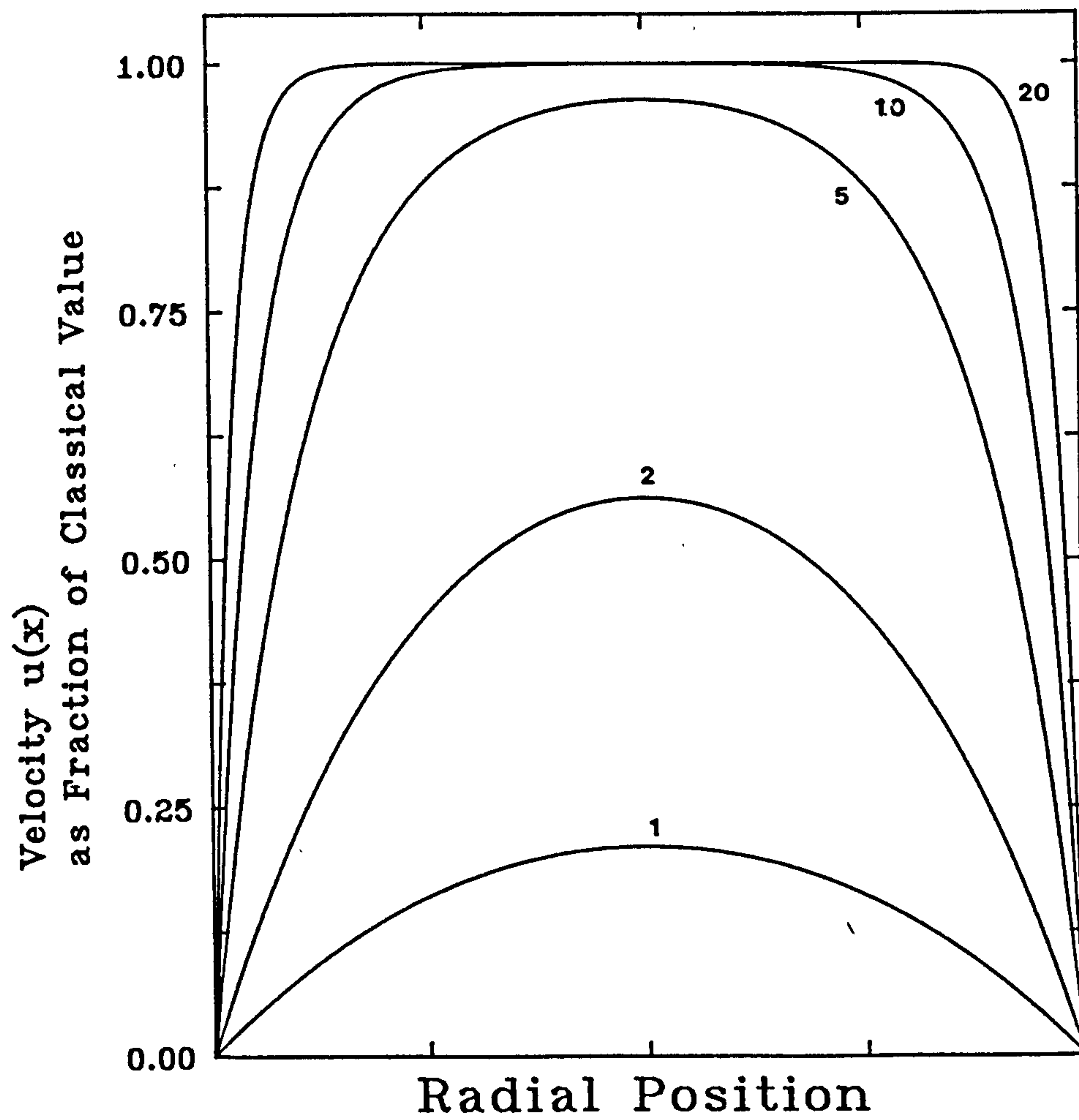
$$u(x) = (E \cdot \epsilon_r \epsilon_0 \cdot \zeta / \eta) \cdot (1 - I_0(\kappa x) / I_0(\kappa a)) \quad 3.27$$

Figure 3.5 shows the profiles according to this equation for several values of  $\kappa a$ , and clearly illustrates that the flat velocity profile of electroosmotic flow is lost in favour of a more parabolic like profile at small  $\kappa a$ , especially when  $\kappa a$  is less

FIGURE 3.5

Electroosmotic Flow Profiles for Various  $\kappa a$ 

Graph showing the flow profiles predicted by the equations of Rice and Whitehead for various values of  $\kappa a$ . The  $\kappa a$  is indicated next to each curve.



than 5. For large values of  $\kappa a$  the ratio of the two Bessel functions becomes negligible except for when  $x$  approaches  $a$ , i.e. within the double layer. Thus, for large values of  $\kappa a$  equation 3.27 reduces to the classical result of the von Smoluchowski equation.

Rice and Whitehead also derived an expression for the mean velocity of electroosmotic flow as a function of  $\kappa a$ ,

$$u = (E.\epsilon_r\epsilon_0\zeta/\eta).(1 - 2I_1(\kappa a)/\kappa a I_0(\kappa a)) \quad 3.28$$

where  $I_1$  represents a first order Bessel function, of the first kind.

A graph of this function is shown on figure 3.6. From this it is clear that for  $\kappa a$  values of greater than 10 the mean velocity is greater than 80% of the von Smoluchowski value. A greater than 50% deviation from the classical equation is only encountered when the  $\kappa a$  value is less than about 3.

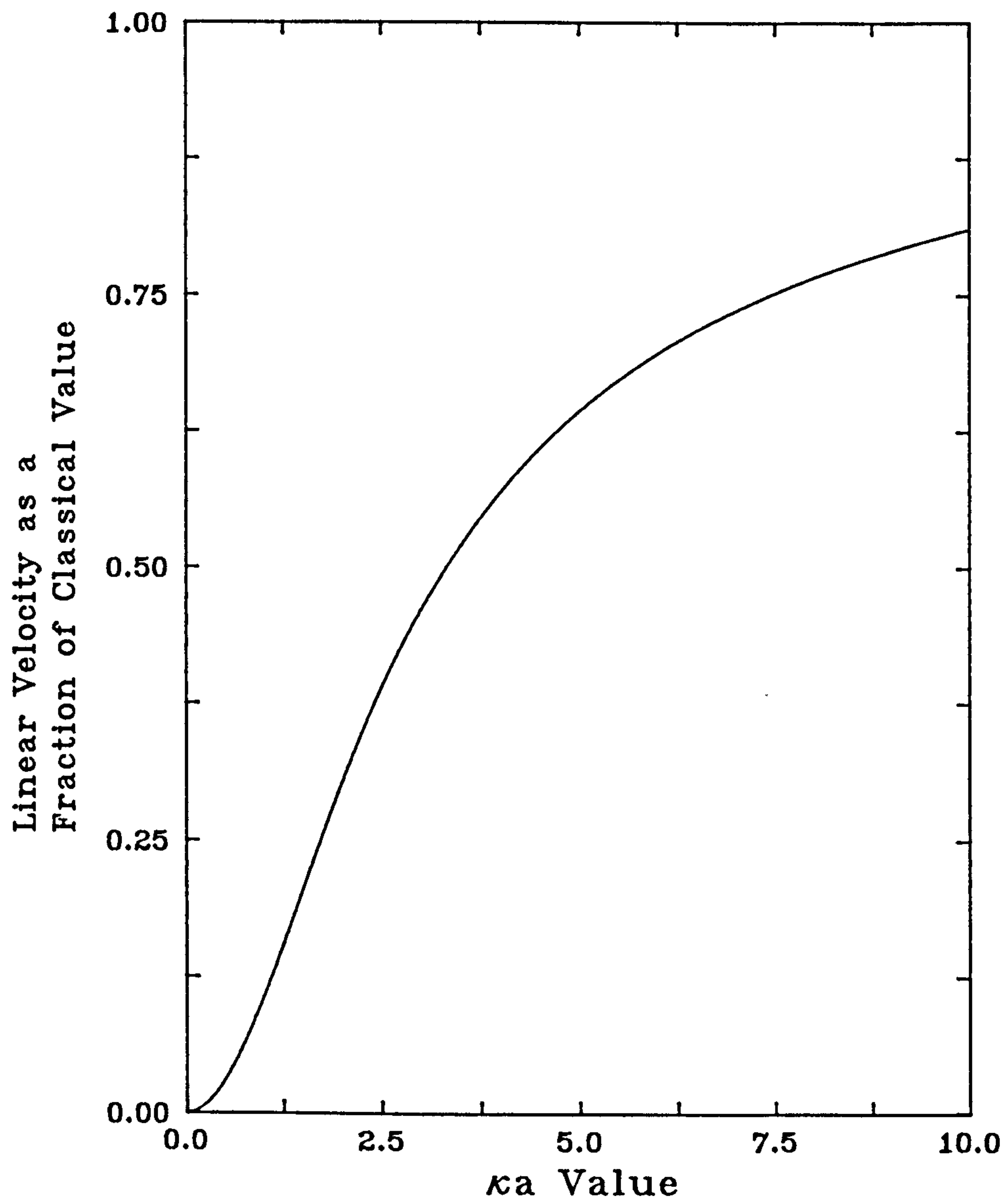
Equations 3.27 and 3.28 show that the desirable properties of electroosmotic flow namely, the flat profile and the lack of a dependence of velocity on channel diameter, are lost when operated under conditions of small  $\kappa a$ .



FIGURE 3.6

Linear Velocity as a Function of  $\kappa a$ .

Graph showing the mean linear velocity of electroosmotic flow, predicted by equation 3.28, in a cylindrical capillary as a function of  $\kappa a$ .



### 3.5.4 Electroosmosis in a Packed Capillary

The work of Rice and Whitehead has important consequences with regard to electrochromatography, where electroosmosis occurs within a packed bed of particles. If one makes the assumption that a chromatographic bed can be modelled as a network of capillary channels, the equations of Rice and Whitehead can be used to predict the mean flow velocity, and the nature of the flow profile, within such channels.

In order that these equations may be applied it is necessary to have an expression for the value of  $\kappa a$  in the interparticular channels of a packed bed.

By equating the Poiseuille equations for a packed and an open capillary one can obtain an expression for the mean radius of the internal channels ( $a$ ) in the packed bed, as in,

$$a = (8 / \phi)^{1/2} . d_p \quad 3.29$$

Thus, for a column packed with spherical particles, for which a typical  $\phi$  value of 500 could be expected, the mean radius of the channels between the particles is approximately one eighth of the particle diameter.

Taking into account the fact that for  $\kappa a$  values as low as 10 the flow velocity is still 80% of the von Smoluchowski value, it is clear that electroosmotic flow could be predicted to occur in beds packed with extremely small particles. The particle size at which overlap of electrical double layers becomes significant obviously depends on the value of  $\kappa$ , which is in turn a function of ionic

concentration. Thus, the value of  $\kappa a$  can always be increased by increasing the electrolyte concentration. However, the electrolyte concentration also influences the zeta potential (cf section 3.4) and in addition has an effect on band broadening in electrochromatography and electrophoresis, as discussed in section 3.7. The role of the electrolyte concentration in electrophoresis and electrochromatography is discussed further in the following chapters.

In a packed capillary the predicted electroosmotic flow velocities must be multiplied by a geometric constant  $\gamma$  (where  $0 < \gamma < 1$ ) in order to account for the tortuosity of the packed bed and in addition to allow for the fact that in a packed bed of porous particles mobile phase molecules spend only a fraction of their time in the actual mobile zone. Thus, the electroosmotic flow velocities in a packed bed of porous particles would be expected to be lower than for non-porous particles.

## 3.6 Electrophoresis

The equations describing the migration velocity of charged species can be treated as the limits of two extreme cases  $\kappa a \ll 1$  and  $\kappa a \gg 1$ .

### 3.6.1 Large $\kappa a$ - The von Smoluchowski Equation

In the case of a large  $\kappa a$  value where the particle diameter is large relative to the electrical double layer thickness, the situation is essentially the reverse of that discussed for electroosmosis. Thus, the velocity of migration for a charged particle in a large  $\kappa a$  situation is described by equation 3.23, the von Smoluchowski equation. The electrophoretic mobility of a particle in a situation where the zeta potential is  $\zeta$  is therefore given by,

$$\mu_{ep} = \epsilon_r \cdot \epsilon_0 \cdot \zeta / \eta \quad 3.30$$

### 3.6.2 Small $\kappa a$ - The Hückel Equation

In chapter 1 it was shown that the velocity of ions in an electric field could be described by equation 1.13 where  $u = Eq/6\pi\eta a$ . However, if an expression in terms of zeta potential is required, an expression for  $q$  in terms of  $\zeta$  must be found.

Since the solution must be overall neutral the sum of the charge in the ionic atmosphere must be equivalent to the charge on the central ion, but of opposite sign. Thus, the volume integral of the charge density from the charged surface to infinite distance must be equivalent to  $-q$ .



Hence,

$$q = -4\pi \cdot \int_a^\infty (x^2 \cdot \rho(x)) \cdot dx \quad 3.31$$

Substituting  $\kappa^2 \psi \cdot \epsilon_r \epsilon_0$  for  $\rho$  and equation 3.14 for  $\psi$  yields,

$$q = 4\pi \cdot \epsilon_r \epsilon_0 \cdot \psi_d \cdot a(1 + \kappa a) \quad 3.32$$

If  $\zeta \simeq \psi_d$  and, since  $(1 + \kappa a) \simeq 1$ , the electrophoretic mobility is described by,

$$\mu_{ep} = 2\epsilon_r \epsilon_0 \cdot \zeta / 3\eta \quad 3.33$$

This result is referred to as the Hückel equation<sup>30</sup>.

The equations for the migration velocity for a large  $\kappa a$  (where the double layer is considered large and flat) and for a small  $\kappa a$  (where the species is considered as a point charge with a spherical double layer) differ by a factor of 2/3. The apparent discrepancy between these two results was resolved by Henry<sup>31</sup> following a more rigorous treatment resulting in a general equation for all values of  $\kappa a$ . The resulting Henry equation is,

$$u = (E \cdot \epsilon_r \epsilon_0 \cdot \zeta / \eta) \cdot f(\kappa a) \quad 3.34$$

where  $f(\kappa a)$  ranges from 2/3 for  $\kappa a \ll 1$  to close to unity for a large  $\kappa a$  ( $\kappa a > 1000$ ).

### 3.7 Band Broadening in Electrophoresis and Electrochromatography

The application of chromatographic concepts, such as  $H$  and  $N$ , to define the separating ability of electrophoretic systems was first carried out by Giddings in 1969<sup>32</sup>. The result of this treatment led to an expression for  $N$  in terms of the change in electrical potential energy of the species over the course of the separation.

In ideal electrophoresis there are no sources of band broadening other than that due to longitudinal diffusion. Thus, the plate height can be expressed as,

$$H = 2D_m/u \quad 3.35$$

The diffusion coefficient  $D_m$ , of a solute in a fluid of viscosity  $\eta$  can be expressed by the Einstein-Stokes equation as,

$$D_m = kT / (6\pi.\eta.a) \quad 3.36$$

where  $a$  denotes the Stokes radius of the solute and  $k$  the Boltzmann constant.

Equation 1.13 (cf section 1.5) for  $u$  can also be written in the form,

$$u = (q / 6\pi.\eta.a).(V / L) \quad 3.37$$

where  $E$  has been substituted by the potential difference  $V$  divided by the distance ( $L$ ) between the electrodes. Substitution of equations 3.36 and 3.37 into equation 3.35 yields the following expressions for  $L/H$ , i.e.,  $N$ .

$$N = q.V / 2k.T \quad 3.38a$$

or

$$N = -\Delta G_0 / 2RT \quad 3.38b$$

Here  $-\Delta G_0$  represents the drop in electrical potential energy per mole of species, i.e.,  $q.V$  multiplied by Avogadro's number. From the above Giddings predicted in 1969 that the ultimate performance would be obtained by using a very high voltage drop, as  $\Delta G_0 \propto V$ . More recently an equivalent expression for  $N$  was derived independently by Jorgenson and Lukacs<sup>33</sup>, as in equation 3.39.

$$N = V.\mu_{ep} / 2D_m \quad 3.39$$

Equations 3.38 and 3.39 are particularly interesting since they show no dependence of  $N$  on the length migrated. In addition large molecules with small diffusion coefficients would, given similar mobilities, be expected to show larger values of  $N$ . However, the use of an electrolyte in which  $D_m$  is small would not increase  $N$ , as both  $\mu_{ep}$  and  $D_m$  are linked to the viscosity of the medium.

Both equations point towards a very favourable situation in which the number of plates can be increased by increasing the voltage, resulting in a greater efficiency in less time, since, for a given migration distance,  $t \propto 1/V$ . This line of reasoning, when carried to its logical conclusion, would imply that the application of very high voltages would enable the realisation of extremely high plate numbers with the analysis times tending towards zero. Inserting values of voltage within easy reach together with typical values for  $\mu_{ep}$  and  $D_m$  show that plate numbers in



excess of one million should be accessible.

However, it should be emphasized that equations 3.38 and 3.39 represent the efficiency only in ideal cases where no other factors contributing to band spreading are at work. Additional band broadening is principally due to the effects of the heat liberated during the analysis. The medium in which electrophoresis is carried out must be electrically conducting to such an extent that the conductivity of the migrating zone is not significantly increased due the presence of the analytes. If this were not the case the electric field within the zone would vary with the analyte concentration in accordance with Ohms law, and thus, the migration velocity would be a function of the position within the zone which would lead to distorted peaks<sup>34</sup>. This requirement for a conducting medium means that the production of heat is unavoidable. This ohmic heat has a deleterious effect in two ways. The heating of the medium causes convection currents within it which prevent the formation of sharp bands. This effect can be minimised, in the case of an aqueous medium, by operating at a temperature of 4°C where the variation of density with temperature is a minimum<sup>35</sup>, or by carrying out the analysis in a rotating cylindrical vessel<sup>36</sup>. However, the most convenient solution to this problem has been the introduction of stabilising gels<sup>5</sup>. The second consequence of ohmic heating is the formation of a temperature gradient within the medium. The heat is produced uniformly throughout the medium, but can, ultimately, only be lost to the surroundings via the walls of the vessel. This leads to a higher temperature in the centre of the vessel and, as a consequence of the effect temperature has on the viscosity of the medium, a higher migration velocity. Clearly both of the above effects will be exacerbated by



increasing the voltage in an attempt to increase the efficiency.

### 3.7.1 Band Broadening due to Self-Heating

In order to quantify the detrimental effect of the trans-column temperature variation, it is necessary to estimate the magnitude and the functional form of the temperature distribution across the column axis and its subsequent effect on the velocity profile. A theoretical analysis of this was first carried out for electrophoresis in capillary columns in 1974 by R. Virtanen<sup>37</sup>.

### 3.7.2 Trans-Column Temperature Profile

For a planar surface where there exists a temperature gradient ( $dT/dx$ ) perpendicular to the surface, the rate of heat transfer ( $Q$ ) by conduction across this surface will be given by the heat diffusion equation,

$$Q = -K.A.(dT/dx) \quad 3.40$$

where  $A$  is the surface area,  $K$  the thermal conductivity of the material and  $dT/dx$  the temperature gradient.

Making the assumption that the majority of heat energy liberated is lost by conduction, the rate of heat energy liberation due to ohmic heating of the medium must be equivalent to rate of heat loss by conduction.

In a column of radius  $a$  with an imaginary cylindrical surface at radius ( $x$ ), where  $x < a$ , the total power generated will be  $i^2R$  or  $V^2/R$ , and that generated within the surface defined by a radius of  $x$  can be expressed by equation 3.41.

$$Q_x = x^2 V^2 / a^2 . R \quad 3.41$$

The electrical resistance of the medium can be related to the electrical conductivity of the medium by,

$$1/R = c . A_C \Lambda / L \quad 3.42$$

where  $c$  is the ionic concentration,  $\Lambda$  the molar conductance of the electrolyte,  $A_C$  the cross sectional area of the conducting medium and  $L$  the column length. Combination of equations 3.41 and 3.42 gives,

$$Q_x = c . \pi \Lambda . x^2 . V^2 / L \quad 3.43$$

where  $A_C$  has been replaced by  $\pi . a^2$ .

The heat lost by conduction through this hypothetical cylindrical surface is given by,

$$Q_x = -K . 2\pi . x . L . (dT/dx) \quad 3.44$$

where the surface area in equation 3.40 has been replaced by  $2\pi . x . L$ .

Since rate of heat lost must be equivalent to the power generated one can equate equations 3.43 and 3.44 which then gives an expression for the temperature gradient at any point at radius  $x$ .

$$dT/dx = x . c \Lambda . E^2 / 2K. \quad 3.45$$

From this it can be seen that the temperature will exhibit a parabolic profile on moving across the column axis.

By integrating this expression from the column centre to the column\_wall one obtains the difference between the two extremes of temperature.

Thus, the maximum temperature difference is given by,

$$\Delta T = d_c^2 \cdot c \Lambda \cdot E^2 / 16K \quad 3.46$$

where  $d_c$  denotes the capillary diameter.

### 3.7.3 Correlation of $\Delta T$ with H

Equation 3.26 shows that the electrophoretic mobility of a species is dependent on the relative permittivity of the eluent and on the viscosity of the medium. The effect on the migration velocity as a result of changes in these parameters can be expressed as,

$$du/u = d\epsilon/\epsilon - d\eta/\eta \quad 3.47$$

The effect of temperature on both of these properties can be expressed by an equation of the form  $di/i = -\alpha_i \cdot dT$ , where  $i$  represents the property concerned and  $\alpha_i$  a constant with units of  $K^{-1}$ . Thus the variation of  $u$  with temperature can be expressed by,

$$du/u = (\alpha_v - \alpha_e) \cdot dT \quad 3.48$$

where  $\alpha_e$  and  $\alpha_v$  are the coefficients relating to permittivity and viscosity respectively. For water, in the liquid range,  $\alpha_v$  has a value of approximately  $0.026\text{K}^{-1}$  whereas  $\alpha_e$  has a value of only  $0.006\text{K}^{-1}$ , and therefore the variation in dielectric constant plays a fairly minor role and can justifiably be ignored.

Thus,

$$du/u \simeq \alpha_v \cdot dT \quad 3.49$$

If the difference in velocity between the capillary centre and the wall is defined as  $2\Delta u$ , the following can be written, provided that the relative changes are small,

$$2\Delta u/u = \alpha_v \cdot \Delta T \quad 3.50$$

where  $\Delta T$  represents the temperature difference between the electrolyte at the wall and in the centre of the tube. Thus, the velocity profile has the same form as the cross column temperature profile.

The resultant velocity profile is the sum of a parabolic velocity profile with a mean velocity of  $\Delta u$  (as the mean velocity of a parabolic profile is half the central maximum ) and a flat profile with a velocity equivalent to the velocity at the wall region.

For a capillary of diameter  $d_c$  the dispersion of an initially narrow sample zone as a result of the parabolic laminar flow profile with a mean velocity ( $u$ ), can be quantified by the second term in the Taylor equation<sup>38</sup>,

$$\sigma_L^2 = (d_c^2 \cdot u / 96D_m) \cdot L \quad 3.51$$



where  $L$  represents the distance migrated.

If one considers the progress of the dispersion from a moving frame of reference moving at the wall velocity (i.e.  $u - \Delta u$ ) the profile is then equivalent to a Poiseuille parabolic profile of mean velocity  $\Delta u$ . The dispersion after a time  $t$  is therefore given by,

$$\sigma_L^2 = (\Delta u \cdot d_c^2 / 96D_m) \Delta u \cdot t \quad 3.52$$

However, during this time the total migration distance relative to the wall is  $u \cdot t$  and thus the value of  $H$  can be obtained by dividing by this distance to give,

$$H = (u \cdot d_c^2 / 96D_m) \cdot (\Delta u / u)^2 \quad 3.53$$

From equation 3.50  $\Delta u / u$  can be expressed as  $\alpha_V \cdot \Delta T / 2$ . Substituting this together with the value of  $\Delta T$  from equation 3.46 into the above and replacing  $u$  by  $E \cdot \mu_{ep}$  yields the following expression for the plate height due to self heating.

$$H = (\mu_{ep} \cdot E^5 \cdot d_c^6 / 98304D_m) \cdot (\alpha_V \cdot \Lambda \cdot c / K)^2 \quad 3.54$$

Equation 3.54 is equivalent to the expression derived by Virtanen, although here it is expressed in terms of chromatographic plate height as opposed to the conventional psuedo-diffusion coefficients in electrophoresis literature.

This expression shows clearly that the effect of self heating grows extremely rapidly with increasing velocity, since  $u \propto E$ , but can nevertheless be kept to within acceptable levels by decreasing the capillary diameter, due to the strong

dependence on  $d_c$ . It therefore implies that efficient electrophoresis must be carried out in narrow capillaries. It is clear from the work of Virtanen that the total plate height, for a given capillary diameter, will exhibit a minimum at a certain field strength, as discussed by Bocek et al<sup>39</sup>, leading to a maximum value of  $N$  for a fixed length of capillary.

In principle the efficiency predicted by equations 3.38 and 3.39 can always be achieved regardless of the column diameter, provided that the capillary length is great enough, i.e.  $E$  small enough, for the value of the self heating plate height to become negligible. However, for large values of  $d_c$  this would require a very long analysis time since  $t \propto 1/L^2$ . It is however possible to optimise the column length for a specified column diameter, and thus, the analysis time, for a given plate number provided that this is smaller than the maximum allowed by equation 3.39.

### 3.8 Optimisation of Analysis Time in Electrophoresis

The term performance in chromatography is often used to denote the number of plates obtained per unit time. For pressure driven chromatography, with a given particle diameter, the number of plates generated per unit time increases to a limit asymptotically as the flow velocity is increased. However, in electrophoresis, owing to the dependence of the heat term on  $u^5$  the performance will exhibit a maximum at a certain velocity. Clearly the best method of achieving a specified number of theoretical plates is to work at the field strength corresponding to this maximum in performance and to modify the capillary length until the desired number of plates is obtained, provided that sufficient

voltage is available to sustain the field at the optimum.

In the absence of any additional broadening effects the total plate height for electrophoresis can be expressed by,

$$H = 2D_m/u + (\alpha_V \Lambda.c/K)^2 \cdot \mu_{ep} \cdot E^5 \cdot d_c^6 / 98304 D_m \quad 3.55$$

As the performance =  $N/t$ , which is equivalent to  $u/H$ , dividing both sides by  $u$  yields an expression for the reciprocal of the performance,

$$H/u = 2D_m/E^2 \cdot \mu_{ep}^2 + (E^4 \cdot d_c^6 / 98304 D_m) \cdot (\alpha_V \Lambda.c/K)^2 \quad 3.56$$

where  $u$  in equation 3.55 has been replaced by  $\mu_{ep}E$ .

Differentiation of the above, with respect to  $E$ , allows the determination of the value of  $E$  for which the performance  $u/H$  is a maximum.

This leads to,

$$E_{OPT} = (D_m \cdot K / \mu_{ep} \Lambda \cdot c \cdot \alpha_V)^{1/3} \cdot (6.8 / d_c) \quad 3.57$$

The field predicted by the above equation gives rise to a larger plate height, than the minimum implied by equation 3.55 and therefore, for a given length of capillary a smaller plate number. However, it would always be possible to obtain a given plate number, in a shorter time, by working at  $E_{OPT}$  and with the appropriate length of capillary.

Inserting this value into the total plate height equation (3.55) gives the plate

height at the optimum field strength, as in,

$$H_{Eopt} = 3D_m / E_{OPT} \cdot \mu_{ep} \quad 3.58$$

Substitution of  $V/L$  for  $E$  and  $L/N$  for  $H$  yields the following expression for the number of plates obtained at this optimum field.

$$N_{Eopt} = V \cdot \mu_{ep} / 3D_m \quad 3.59$$

The value of this expression is only 67% of the maximum value  $N_{max}$  obtainable predicted by equation 3.39. However, consideration of equation 3.55 shows that in order to obtain values of  $N$  predicted by equation 3.39 it would require an infinite analysis time. Higher values of  $N$ , approaching that of the maximum, can indeed be obtained by the use of a longer capillary and the same voltage however, as  $N \rightarrow N_{max}$ ;  $t \rightarrow \infty$ .

The required analysis time can be expressed as,

$$t = L / \mu_{ep} \cdot E \quad 3.60$$

If  $L$  is eliminated through substitution by  $V/E$  one obtains,

$$t = V / \mu_{ep} \cdot E^2 \quad 3.61$$

Substitution of  $E_{OPT}$  for  $E$  gives,

$$t = (V / 46\mu_{ep}^{1/3}) \cdot (\Lambda \cdot c \cdot \alpha_V / D_m \cdot K)^{2/3} \cdot d_c^2 \quad 3.62$$



Or in terms of  $N$ , where  $V$  is substituted via equation 3.59, as,

$$t = ( 3N.D_m^{1/3} / 46\mu_{ep}^{4/3} ).( \Lambda.c.\alpha_V / K )^{2/3}.d_c^2 \quad 3.63$$

The above expression represents the shortest possible analysis time for an efficiency of  $N$  plates provided that sufficient voltage is available to satisfy equation 3.59, i.e.  $N$  is not greater than 67% of  $N_{max}$ . For an efficiency of 95% of  $N_{max}$  a doubling of the time would be required, whereas for 99% of  $N_{max}$  the analysis time would increase by a factor of four, for a capillary of the same diameter.

The above argument shows that the number of plates which can be obtained depends on the available voltage and that the tube diameter determines the time in which this can be realised. In short  $N_{max} \propto V$  and  $t \propto d_c^2$ . The viscosity of the medium influences  $D_m$  and  $\mu_{ep}$  since both are inversely proportional to  $\eta$ . Consideration of equation 3.63, in this respect, shows that the analysis time is directly proportional to  $\eta$ , exactly as in the case of chromatography (cf equation 2.32).

Inserting typical values for the terms involved into equation 3.63 shows that for  $N=10^6$  within 15mins one would require a tube diameter of less than 200 $\mu$ m. Typical values used here are;  $D_m=10^{-9}\text{m}^2\text{s}^{-1}$ ,  $\mu_{ep}=5\times10^{-8}\text{m}^2\text{s}^{-1}\text{V}^{-1}$ ,  $K=0.4\text{Wm}^{-1}\text{K}^{-1}$ ,  $V=60\text{kV}$ ,  $\Lambda=0.015\text{m}^2\text{mol}^{-1}\Omega^{-1}$ ,  $\alpha_V=0.026\text{K}^{-1}$  and  $c=0.03\text{mol.dm}^{-3}$ .

The analysis times, according to equation 3.63, together with the column lengths required for  $N=10^6$  are shown for several capillary diameters in table 3.1.

TABLE 3.1

Theoretical Minimum Analysis Times for  $N = 10^6$ 

Theoretical minimum analysis times for  $10^6$  theoretical plates for several diameters of capillary. The times are calculated according to equation 3.63 using the following values for the parameters involved:  $\mu_{ep} = 5 \times 10^{-8} \text{ m}^2 \text{ s}^{-1} \text{ V}^{-1}$ ,  $\eta = 10^{-3} \text{ Nm}^{-2} \text{ s}$ ,  $c = 30 \text{ mol.m}^{-3}$ ,  $D_m = 10^{-9} \text{ m}^2 \text{ s}^{-1}$ ,  $\Lambda = 0.015 \text{ m}^2 \text{ mol}^{-1} \Omega^{-1}$  and  $V = 60 \text{ kV}$ .

$d_c/\mu\text{m}$	$L/\text{m}$	$E_{\text{OPT}}/\text{kVm}^{-1}$	$t_m/\text{s}$
500	5.0	12	8330
200	2.0	30	1350
100	1.0	60	340

Column 3 shows the field strength,  $E_{\text{OPT}}$  at which the number of plates generated per unit time is a maximum.

In contrast to the case in chromatography it is reasonable with electrophoresis to expect very large plate numbers within an acceptable time. HPLC limited to a pressure drop of 200bar would require an analysis time in excess of one day, even with the use of the optimal particle size, for an efficiency of one million plates.

Although equation 3.63 represents an ideal hypothetical case, where no additional band broadening processes are at work, the expression nevertheless shows the types of dimensions for the separation compartment (capillary or otherwise) which must be used in electrophoresis. In practice, at least for free solution electrophoresis, the performance predicted by equations 3.55 and 3.63 is never achieved, and thus, at best, should be regarded as a theoretical maximum.

### 3.9 Self Heating in Electrochromatography

A similar deleterious effect on efficiency to that described above for electrophoresis must also be expected in a packed capillary in which the flow of mobile phase, in a chromatographic system, is the result of electroosmosis. Owing to the variation of viscosity across the axis of the capillary the electroosmotic flow velocity will exhibit the same type of parabolic profile as that shown by a charged species migrating in electrophoresis. The conductivity of a packed capillary will be less than that of an open tube of the same internal diameter because the cross sectional area of the current carrying mobile phase will be smaller in the former. For this reason the appropriate version of equation 3.46 for a packed capillary is,

$$\Delta T = d_c^2 \cdot \epsilon \cdot c \cdot \Lambda \cdot E^2 / 16K \quad 3.64$$

where  $\epsilon$  represents the porosity of the packed bed.

The variation in  $k'$  with temperature must also be considered here. The coefficient ( $\alpha_k$ ) for the variation of  $k'$  with temperature can be related to  $(\Delta H_A / RT^2) \cdot (k' / (1 + k'))$  where  $\Delta H_A$  is the enthalpy of adsorption, from the liquid onto the solid phase, per mole of solute. For a typical  $\Delta H_A$  value of  $5 \text{ kJ mol}^{-1}$  the value of  $\alpha_k$  is approximately  $0.003 \text{ K}^{-1}$  for a  $k'$  of unity. The variation of  $k'$  with temperature is therefore small when compared with the variation of viscosity ( $\alpha_v \approx 0.03 \text{ K}^{-1}$ ) and thus, as was the case with electrophoresis, only the effect of viscosity need be considered. Thus, the additional plate height due to self heating, for a neutral species, in electrochromatography is given by an expression similar to equation 3.54 where  $\mu_{ep}$  is replaced by  $\epsilon_r \epsilon_0 \cdot \gamma \zeta / \eta$  to give.



$$H = ( \epsilon_r \epsilon_0 . \gamma \zeta . E^5 . d_c^6 / 98304 \eta . D_m ) . ( \epsilon . \alpha_V . \Lambda . c / K )^2 \quad 3.65$$

This equation can also be expressed in reduced terms as,

$$h = ( \epsilon . \Lambda . c . \alpha_V / K )^2 . ( D_m . \eta / \epsilon_r . \epsilon_0 . \gamma \zeta )^4 . ( d_c / d_p )^6 . v^5 / 98304 \quad 3.66a$$

or,

$$h = D . \chi^6 . v^5 \quad 3.66b$$

where D represents  $( \epsilon . \Lambda . c . \alpha_V / K )^2 . ( D_m . \eta / \epsilon_r . \epsilon_0 . \gamma \zeta )^4 / 98304$  and  $\chi$  denotes  $d_c / d_p$ .

For this reason electrochromatography is subject to the same limitations on the column diameter as in electrophoresis. Equation 3.66b shows that in order to maintain a constant relative contribution to the overall plate height a reduction in the particle diameter must be accompanied by the same relative reduction in column diameter, since  $h \propto \chi^6$ . Thus, if high efficiencies are to be achieved in electrochromatography miniaturisation is mandatory.

## **CHAPTER 4**

# **MODES OF CHROMATOGRAPHY AND ELECTROPHORESIS**

## Chapter 4

# MODES OF CHROMATOGRAPHY AND ELECTROPHORESIS

### 4.1 Introduction

Since their beginnings in the early part of this century liquid chromatography and electrophoresis have developed into an enormous range of specialised techniques. This chapter aims to present an overview of the most important of these with particular emphasis on the techniques relevant to this work namely capillary zone electrophoresis (CZE) and related techniques, and electrochromatography.

### 4.2 Traditional Electrophoretic Methods

#### 4.2.1 Moving Boundary Electrophoresis

The earliest form of electrophoresis used for analytical purposes was moving boundary electrophoresis<sup>40</sup>. In this form of electrophoresis the sample is not introduced to the separation compartment as a narrow zone, as is the case in zone electrophoresis or elution chromatography. Rather, a boundary is formed, at one end of the separation compartment, between a solution of the sample in the electrolyte and the pure electrolyte. On the application of the field the boundaries for substances of different electrophoretic mobilities migrate at different rates. Although the substances cannot actually be separated by this method, the position of a boundary after a given time provides the

electrophoretic mobility of that substance. This form of electrophoresis is no longer widely used.

#### 4.2.2 Slab Gel Electrophoresis

One of the most common forms of electrophoresis is that carried out in polymer gels, of which the best known is polyacrylamide gel electrophoresis (PAGE)<sup>41</sup>. In this method gels of the appropriate pH are prepared and polymerised to form thin slabs with a thickness of ca. 1mm. The polymer network acts as an additional selection mechanism since small molecules will migrate through the pore structure faster than larger ones. After the separation is complete the resultant bands are detected, usually by means of a staining reagent which causes them to become visible.

This method is particularly useful for proteins especially when used in the form of SDS-PAGE<sup>42</sup> (sodium dodecylsulphate - polyacrylamide gel electrophoresis), in which proteins can be separated according to molecular weight.

#### 4.2.3 Isoelectric Focusing

Another method which is routinely carried out in polymer gels is isoelectric focusing<sup>43</sup>. For this purpose gels are prepared in which the value of the pH varies along the migration path.

The sample, which must show zwitterionic character, can be introduced at any position along the migration path. If a component of the sample is at a position where the local pH is greater than its isoelectric point, it will bear a negative charge and therefore migrate towards the anode and vice versa if the pH is lower.



Provided that the electrodes are arranged such that anions migrate towards lower pH and cations towards a region of higher pH, each substance will migrate until it reaches a position where the pH is equivalent to its isoelectric point (PI). In this position its net charge is zero and it therefore ceases to migrate. Given sufficient time, each component of the sample mixture builds a narrow band at the location where the pH corresponds to its PI value, thereby providing the PI values of the sample components. As with PAGE it is particularly useful for the separation of proteins.

Isoelectric focusing and SDS-PAGE can be combined to give two dimensional slab gel electrophoresis<sup>44</sup>, in which SDS-PAGE and isoelectric focusing are carried out consecutively in orthogonal directions. This represents a very powerful technique since the effective efficiency of the technique becomes the product of the efficiencies for the individual methods.

Common to all forms of electrophoresis in polymer slabs is the fact that the slabs can only be used once and that quantitation of the separated species is difficult.

#### 4.2.4 Isotachophoresis

In isotachophoresis<sup>45</sup>, which literally means "same speed transportation", ionic substances are separated into adjacent bands migrating with identical velocities, with sharp boundaries between them. Selectivity is simply on the basis of differing electrophoretic mobilities. This is normally carried out in Teflon capillaries ranging from 200 $\mu$ m to 1mm in bore.

The system is arranged such that the capillary contains two different electrolytes

sharing one ion in common. The sample is located at the interface between these two solutions. The solution ahead of the sample (the leading electrolyte) contains ions of the same sign as that of the analytes, but with a greater ionic mobility than any of these. Conversely the solution following the sample, or the trailing electrolyte, contains ions of a lower electrophoretic mobility than any of the sample ions.

The boundary between electrolytes containing like charged ions of different mobility remains sharp during the course of electrophoretic migration. Less mobile ions which stray across the interface into the electrolyte of higher conductivity will experience a lower field and consequently, migrate at a smaller velocity allowing the interface to catch up. The reverse is true for ions of the more mobile species wandering in the opposite direction across the boundary.

In isotachophoresis, provided that sufficient time has elapsed for equilibrium to become established, a series of such boundaries are formed in which the zones between the boundaries contain ions of only one type, in addition to the common counter ion. The end result is a series of adjacent zones, whose order is determined by the electrophoretic mobilities of the ions they contain.

## **4.3 Column Liquid Chromatographic Techniques**

### **4.3.1 Frontal Chromatography**

The chromatographic analogue of moving boundary electrophoresis is frontal chromatography. With this technique, as was the case with the moving boundary method, the sample, dissolved in the eluent, is continually fed into the column, and the resulting chromatogram is a series of fronts. In most forms of chromatography however, the sample is applied as a narrow zone, as in zone electrophoresis. The latter method is termed elution chromatography.

### **4.3.2 High Performance Liquid Chromatography (HPLC)**

The most advanced form of column liquid chromatography, and by far the most common, is "high performance liquid chromatography" or HPLC.

In HPLC the mobile phase is forced through a column (normally 4.6mm i.d.) of fine porous particles, typically 3-5 $\mu$ m in diameter, under pressures of ca. 200bar. Efficiencies of ten to twenty thousand theoretical plates can normally be obtained, with an analysis time of ca. two minutes for the first eluted peak. The separated components are detected as they are eluted from the column by means of a suitable detector, the most common being an UV absorbance detector. The chromatogram obtained consists of an absorbance verses time graph, which allows quantitation of the peak areas.

HPLC exists in a great variety of forms, all of which can not be adequately described here. However, the most common form of HPLC is the so-called



reverse phase HPLC. The term "reverse phase" is used because of the fact that, in contrast to earlier forms of chromatography, a non-polar stationary phase and a polar mobile phase are used. Usually the non-polar stationary phase consists of a porous silica support, whose surface has been derivatised by reaction with an alkylating agent, to give a hydrophobic surface. The most commonly used material is silica gel which has been derivatised using an octadecyldimethylsilyl (ODS) reagent. The mobile phase, in the simplest cases, is usually aqueous and contains varying percentages of an organic modifier such as acetonitrile or methanol. In addition to the use of derivatised silicas, reverse phase chromatography can also be carried out on non-polar adsorbants, such as graphite<sup>46</sup>. Reverse phase HPLC can be used for substances with a wide range of polarity, including many ionic species.

An alternative method for the separation of ionic species is ion exchange chromatography<sup>47</sup>, in which the stationary phase has fixed ionised groups, which can interact with analytes of the opposite charge. Ion pair chromatography<sup>48,49</sup> can also be used, for ionisable species. The addition of an ion pairing agent, such as cetyltrimethylammonium bromide, to the mobile phase, promotes the formation of neutral ion pairs with the analytes, which are then separated, usually under normal phase conditions.

The separation of macromolecules can be achieved by the use of gel permeation or exclusion chromatography<sup>50</sup>. In this form of chromatography the separation mechanism is based on the fact that small molecules can gain better access to the pores of a porous material than larger ones, provided that the pore diameter is of the same order as the molecular dimensions. Large molecules which are fully or



partially excluded from the pores migrate faster through the column than smaller molecules which have full access to the pores. The chemical nature of the analytes or the support material plays no part in the separation mechanism, and the separation is purely on the basis of size. In this respect exclusion chromatography bears some resemblance to polyacrylamide gel electrophoresis, although the separation according to molecular size is in the opposite direction.

#### **4.3.3 Displacement Chromatography**

Displacement chromatography<sup>51</sup> is a chromatographic method, which is in some respects similar to isotachophoresis. Like isotachophoresis the mobile phase following the sample is different from the eluent already in the column, and after establishing a steady state, the analytes migrate through the column as a series of adjacent bands moving at the same velocity. This situation arises because a substance which has a strong affinity for the stationary phase can displace those with a less strong affinity. The same substance can itself be displaced by a substance exhibiting an even stronger interaction with the phase. After the introduction of the sample the displacer solution, which contains a substance with an affinity for the phase, which is greater than that of any of the sample components, is pumped into the column, in order to bring about the series of displacements.

Because the sample concentrations involved are normally higher than in elution chromatography, displacement chromatography is often used as a preparative method.

## 4.4 Capillary Electroseparation Methods

In the previous chapter it was shown from theoretical considerations that short analysis times together with high efficiencies are possible in electrophoresis provided that narrow capillaries are used for the separation compartment. The last decade has seen the realisation of the high plate numbers predicted in chapter 3, in the form of capillary zone electrophoresis or CZE.

In 1978 Everaerts et al.<sup>34</sup> achieved electrophoretic separations of several organic anions with an efficiency of up to 36,000 theoretical plates, while working with 200 $\mu$ m i.d. Teflon capillaries. The decisive step, however, was taken by Jorgenson and Lukacs<sup>33</sup> who introduced the use of glass capillaries as small as 75 $\mu$ m i.d.. Using such capillaries the separation of several dansylated amino acids, induced by the application of a potential difference of 30kV over a 1m length of capillary was described. The separation of twelve compounds shows a plate number of approximately 200,000 plates and was complete within ca. twenty minutes, a performance which is typical of the most efficient form of chromatography, capillary gas chromatography. This notable development has led to a renaissance of the use of electrophoretic methods, and following, this pioneering work four distinct capillary electroseparation methods have been developed:

1. Capillary Zone Electrophoresis
2. Complexation Electrophoresis
3. Capillary Gel Electrophoresis
4. Micellar Electrokinetic Capillary Chromatography

#### 4.4.1 Capillary Zone Electrophoresis (CZE)

In capillary zone electrophoresis glass or fused silica capillaries of 25 $\mu$ m to 75 $\mu$ m i.d. are normally used. The detection is usually carried out close to the capillary outlet, although still within the capillary, by means of fluorescence<sup>52,53</sup>, or UV absorbance<sup>54</sup>, giving rise to the term "on-column" detection. The need for such a detection method is discussed in chapter 5. Typically a voltage of 30kV is used with capillaries ranging from 0.25-1.0m in length. The same basic apparatus can be used for all the above mentioned capillary electroseparation methods.

In glass or fused silica capillaries, because of the presence of an electrical double layer at the capillary wall, the electrophoresis is usually accompanied by electroosmosis. The presence of electroosmosis would not be expected to introduce any additional band broadening thanks to its extremely flat velocity profile (see section 3.5). One effect of electroosmosis is to add a constant velocity ( $u_{eo}$ ) onto the migration velocity of each species. The result can be considered similar to that achieved by physically moving a chromatographic column in the flow direction while the separation is in progress. For this reason the plate numbers quoted in capillary zone electrophoresis must be interpreted with this in mind. The electroosmotic migration velocity is often faster than the electrophoretic velocity of ionic species migrating in the opposing direction. For this reason electroosmosis allows the simultaneous electrophoretic separation of cations and anions. Several separations of this type have been reported<sup>55</sup>.

In many cases the high efficiencies predicted for CZE electrophoresis are not realised especially for peptides and proteins. One of the main reasons for this is



interaction of the analytes with the walls of the capillary, giving rise to a chromatographic effect. If this were the case, mass transfer across the capillary axis would be required in order to establish an equilibrium. Thus, even for a perfectly flat profile, resistance to mass transfer in the mobile phase plays a role in determining the overall plate height.

This effect has been quantified by Aris<sup>56</sup>, and also for electroosmotic flow profiles of varying  $\kappa a$  by Martin and Guiochon<sup>57</sup>. For a plug profile, i.e., large  $\kappa a$ , the plate height ( $H_{mt}$ ) due to resistance to mass transfer in the mobile phase is given by,

$$H_{mt} = (k'^2 / (16(1+k')^2)) \cdot (d_c^2 / D_m) \cdot u \quad 4.1$$

For  $k'=0$  the contribution is of course zero. For very large values of  $k'$ , where  $k' \gg 1$ , the contribution to the plate height is equivalent to 6/11 of that for mobile phase mass transfer resistance in the Golay equation for large  $k'$  (cf section 2.5).

Even very small values of  $k'$  can have a very serious effect on the observed overall plate height in capillary electrophoresis.

For a 75 $\mu$ m bore capillary operated under optimal conditions, in accordance with equation 3.56 (cf section 3.8), the total plate height as a result of axial diffusion and self heating is 0.75 $\mu$ m at  $u=4 \times 10^{-3} \text{ ms}^{-1}$ , for  $c=30 \text{ mM}$ ,  $\mu_{ep}=5 \times 10^{-8} \text{ m}^2 \text{ s}^{-1} \text{ V}^{-1}$  and  $V=30 \text{ kV}$ . If interaction with the wall leads to an effective  $k'$  value of 0.1, then according to equation 4.1 the plate height as a result of mass transfer resistance is equivalent to 14 $\mu$ m, using the above values for  $u$  and  $D_m$ . In this case the result would be a twenty fold increase in plate



height over that predicted from diffusion and self heating alone. Thus, it is clear that slightest interaction with the wall must be avoided, if high efficiencies are to be achieved, particularly for large biomolecules for which  $D_m$  is likely to be very small.

In the case of proteins and peptides Lauer and McMannigil<sup>58</sup> have shown that the interaction with the wall can be suppressed by the use of high pH buffers. If the electrolyte pH is greater than the isoelectric point of the analyte, the wall and the analyte bear the same charge (negative) and therefore repel each other. This technique has made possible the separation of very large species with a high efficiency. The interaction with the wall can also be diminished by the use of additives, such as organic zwitterions, in the electrolyte to saturate the active sites on the wall<sup>59</sup>, or by the use of high concentration salts<sup>60</sup> in order to saturate any ion exchange sites.

Hjerten<sup>61</sup> has shown that the wall adsorption can be significantly reduced by coating the wall of the capillary with a layer of polyacrylamide. In addition this method eliminates electroosmotic flow, which may, or may not, be an advantage depending on the nature of the separation.

The range of application for CZE stretches from simple pharmaceutical ionic species<sup>62</sup> to proteins<sup>63</sup> and nucleotides<sup>64</sup> and others.

#### **4.4.2 Complexation Electrophoresis**

An obvious prerequisite for a separation by electrophoresis is that the analytes must exist in an ionic state. An attempt to overcome this limitation has been the

introduction of complexation electrophoresis. In this method the separation mechanism is based on the complexation of neutral species with a charged additive in the electrolyte. An example of this technique is the use of large quaternary ammonium ions, which are hydrophobic, dissolved in the electrolyte. These ions may form complexes with neutral species in the sample, thereby imparting a finite electrophoretic mobility on them. The capillary electrophoretic separation of neutral hydrocarbons has been demonstrated using this technique<sup>65</sup>.

#### 4.4.3 Capillary Gel electrophoresis

A capillary version of polyacrylamide gel electrophoresis was introduced in 1987 by co-workers of B.L.Karger<sup>66</sup>. Like the slab form, the presence of the gel modifies the selectivity of the separation by the introduction of a molecular sieving effect, in addition to the separation on the basis of electrophoretic mobility. Furthermore the gel eliminates any residual convective effect which may be present in open capillaries, and also prevents electroosmotic flow.

The SDS-PAGE technique (cf section 4.2) has also been demonstrated in capillaries<sup>67</sup>, giving high performance separations purely on the basis of molecular weight.

The selectivity of gel-filled columns can be further modified by the inclusion of complex-forming agents in the gel matrix. One such example is the use of cyclodextrin in a polyacrylamide matrix<sup>68</sup>. Using this method high resolution chiral separations of dansylated amino acid enantiomers has been reported.

Capillary gel electrophoresis shows efficiencies similar to those observed in open tubular capillary zone electrophoresis.

#### 4.4.4 Micellar Electrokinetic Capillary Chromatography

The possibilities of capillary electrophoresis were expanded still further by Terabe et al.<sup>69,70</sup> through the introduction of micellar electrokinetic capillary chromatography. This technique is essentially chromatographic in nature, for it involves the partition between two moving phases: a micellar phase and the electrolyte. Surfactants, such as sodium dodecylsulphate (SDS), are added to the aqueous electrophoresis buffer, at a concentration which is greater than the critical micelle concentration, and thus, leads to the presence of micelles in the electrolyte. In the case of SDS the micelles bear a negative charge and therefore migrate at a velocity  $u_m$ , against the electroosmotic flow, which is usually directed towards the cathode. The net migration velocity of the micelles is therefore  $u_{eo} + u_m$ . In this situation the separation of neutral species is possible via a partition between the electrolyte and the micelles. The net migration velocity ( $u_s$ ) of each component of the sample will be the electroosmotic velocity ( $u_{eo}$ ) plus the product of the micellar velocity and the fraction of that component in the micellar phase at any time.

Thus,

$$u_s = u_{eo} + (k'/(1+k')) \cdot u_m \quad 4.2$$

The migration velocities of all neutral species must lie between  $u_{eo}$  for  $k'=0$  and  $(u_{eo} + u_m)$  for  $k'=\infty$ . Thus, all peaks must elute between the elution time for an



unretained species and the time for a species fully incorporated in the micelles. Since all peaks must appear between these times the total number of components which can, in principle, be separated (the peak capacity) is limited, except where  $u_m = -u_{eo}$ .

Although the presence of micelles should bring about a contribution to the plate height due to resistance to mass transfer in the micellar phase, the small dimensions of the micelles ensure that this is negligibly small. For this reason the high efficiency of capillary zone electrophoresis is maintained in MECC.

In the original experiment of Terabe et al.<sup>69</sup>, at a buffer pH of ca. 9.0, the electroosmotic flow is strong enough to carry the micelles towards the cathode. The separation of five aromatic hydrocarbons, is demonstrated, in approximately ten minutes with an apparent plate number, where the distance migrated is considered as relative to the capillary walls and not to the micelles, of ca. 300,000.

The utility of MECC is not only in the separation of neutral species. In the case of ionic species the migration velocity will be the sum of that given by equation 4.2 and the electrophoretic velocity. In this way the selectivity of CZE can be modified by the addition of surfactants, thereby enabling the separation of species with identical mobilities, but different  $k'$ . The separations of ionic compounds of pharmaceutical interest by MECC have been reported<sup>71</sup>.

MECC is undoubtedly an extremely useful technique in that it achieves separations of a chromatographic nature, but preserves the efficiency of capillary electrophoresis. It is nevertheless not an ideal separation method since the



compounds to be separated must be sufficiently soluble in an aqueous surfactant solution. The poor detection capability for capillary methods, especially where UV absorbance is the detection method (cf section 5.3) prohibits the dilution of the sample in order to ensure complete dissolution. The addition of an organic modifier to the electrolyte would naturally improve the solubility of neutral species, but would raise the required surfactant concentration for micelles to form (CMC), and would also reduce the distribution coefficient between the micelles and electrolyte.

The problem with solubility and the limited peak capacity of the method are the main drawbacks of this otherwise excellent technique.

#### 4.5 Electrochromatography

As mentioned in the introduction reports concerning of the use of electrochromatography are few. The earliest papers, which could be considered as dealing with the subject, made use of the fact that a different selectivity could be obtained for ionic species by superimposition of an electrophoretic mobility onto the chromatographic migration in the standard columns used for column liquid chromatography. In the 1939 work of H.H.Strain<sup>6</sup> the application of ca. 200V across clay filled columns, 13cm and 20cm in length, was reported. Using this method the separation of ionic dyes was obtained by a combination of differences in electrophoretic mobility and differences in  $k'$ . As the compounds involved were all charged, the presence of electroosmosis was not essential to the separation. The effect of electroosmotic flow was indeed suppressed by Strain through the use of back pressure, in which case the migration velocity could be

described by,

$$u_s = \mu_{ep} \cdot E / (1 + k') \quad 4.3$$

The term electrochromatography has also been used recently by Tsuda<sup>72,73</sup>, for the description of a separation method which is essentially an HPLC equivalent of the experiment described by Strain. In this case narrow bore columns (ca. 500 $\mu$ m i.d.) packed with 3 $\mu$ m diameter particles were used. The application of 5kV across a 7.4cm length of column enabled the separation of two components which were observed to co-elute without the presence of the electric field. Here the flow was provided by means of a conventional HPLC pump and not as a result of electroosmosis. High efficiencies could not be expected however due to the column diameter used, which is large in comparison with the capillaries used in CZE.

The first reported separation in which electroosmosis was an essential agent, was the work of Synge and Tiselius<sup>7</sup>, as discussed in chapter 1. The technique which they called *electrokinetic ultrafiltration*, was demonstrated by the apparent electrophoretic separation of electrically neutral amylose hydrolysis products in a column of agar gel. The mechanism was judged to be as a result of the molecular sieving action of the gel. Since the separation mechanism is based on kinetics and not on partition, it cannot be regarded as a genuine chromatographic technique. Nevertheless, it did show that electroosmosis can be used to transport substances through the pores of a gel matrix.

The use of electroosmosis specifically as a means of driving eluent through a

chromatographic column was first proposed by Pretorius et al<sup>74</sup> in 1974. Although no actual separations, in columns, were described, the dispersion of an unretained species, in a column packed with 100 $\mu$ m diameter particles of silica gel, was investigated using both pressure driven flow and electroosmotic flow. In the electrically driven case a lower plate height was observed at all mobile phase linear velocities, thus, providing evidence for a smaller flow dispersion term (A-term). From the data, it appears that typical reduced plate heights of ca. 14.5 were obtained for pressure driven flow, whereas for the electroosmotic flow plate heights of approximately 6 particle diameters were obtained, both at a reduced velocity of ca. 40. The particles used however are far larger than those currently used in high performance liquid chromatographic columns.

Jorgenson and Lukacs<sup>75</sup> as part of an early paper on CZE described the use of a capillary column (170 $\mu$ m i.d.) packed with 10 $\mu$ m diameter ODS-derivatised spherical silica particles. Using the same apparatus which they had described for CZE, the column was used to perform electrochromatography with an eluent of pure acetonitrile. Although no detailed measurements were reported, reduced plate heights of ca. 2 were obtained for the separation of aromatic hydrocarbons.

True separations using electroosmotic flow have also been described by Tsuda et al<sup>76</sup> using open tubular capillary columns. In contrast to the case with CZE, where action is often taken to avoid the possibility of analytes interacting with the capillary wall, the adsorption onto the wall is, in this case, actively encouraged. The capillary walls are etched by the action of sodium hydroxide solution in order to increase the area, and are then derivatised with a silanising reagent. For capillaries of 130 $\mu$ m i.d. plate heights, for an unretained species, of



ca.  $6\mu\text{m}$  were reported.

The interaction with the wall introduces a mobile phase mass transfer resistance term in the observed plate height. In this situation the plate height due to resistance to mass transfer in the mobile phase can be described by equation 4.1, provided that the flow profile is fairly close to a plug profile. Thus, for  $k'=0$  only axial diffusion should contribute to the plate height. However, for a  $k'$  of unity a plate height of ca.  $500\mu\text{m}$  would be predicted at the flow velocity quoted ( $2 \times 10^{-3} \text{ms}^{-1}$ ). The performance of open tubular columns in electrochromatography is better than the pressure driven case, but for large  $k'$  the improvement is not significant, since as  $k'$  becomes significant the plate height tends towards its maximum value of ca. 55% of its value predicted by the Golay equation (cf. section 2.5) for a parabolic profile. Hence, the need to use extremely narrow capillaries, in order to obtain high efficiencies in open tubular LC, cannot be overcome by the use of electroosmosis, although provided that  $k'$  is small, the diameter may be a little larger than for pressure driven flow.



**PAGE**

**NUMBERING**

**AS ORIGINAL**

## **CHAPTER 5**

### **EXPERIMENTAL METHODOLOGY**

## **Chapter 5**

### **EXPERIMENTAL METHODOLOGY**

#### **5.1 Introduction**

This chapter describes the experimental methods and apparatus used in the experimental work carried out in capillary electrochromatography and capillary chromatography. The obligatory miniaturisation of the chromatographic system, in order to avoid ohmic heating problems, has made necessary the solution of considerable practical problems, not only in the areas of detection and sample introduction, but also in the production of suitable packed capillaries.

The work concerns the construction of the apparatus, which was a prerequisite for the carrying out of experimental work with electrically driven chromatography. In order that the capillaries to be used could also be characterised under conventional pressure driven flow, thereby allowing the direct comparison of the data obtained from identical columns, the construction of a suitably miniaturised liquid chromatograph was also necessary. The commercial chromatographic equipment, available at present, is designed principally for use with conventional columns (usually 4.6mm internal diameter), and as a result requires considerable modification if it is to be used successfully with capillary columns.

#### **5.2 Production of Packed Capillary Columns**

During the last decade many reports of liquid chromatography in capillary

columns of 200 $\mu$ m in diameter, have emerged, notably by Ishii<sup>77</sup> and by Novotny. The columns described were packed with standard 3 $\mu$ m and 5 $\mu$ m reversed phase packing materials. These columns were reported to exhibit reduced plates heights of ca. 3, and with long capillaries, approximately 1m in length, efficiencies in excess of 100,000 theoretical plates were obtained<sup>78</sup>. The packed capillaries described in these reports were produced by the same means as conventional 4.6mm ID HPLC columns, which means that the packing material, in the form of a thick colloidal suspension or "slurry" is forced into the column under high pressure. In order to differentiate packed capillaries produced in this way from those produced by other methods, they shall be referred to as "slurry-packed capillaries".

The use of a glass drawing machine for drawing pre-packed glass rods down to the desired capillary diameter, as a means of producing packed capillary columns, was demonstrated by Novotny et al.<sup>79</sup>. The columns, described as packed microcapillaries, had diameters of ca. 3 particle diameters, and were produced using particles ranging from 30-100 $\mu$ m in diameter. The capillaries described were rather sparsely packed by comparison with HPLC columns. The production of similar columns, but with a higher packing density, using 10 $\mu$ m diameter particles, where the column diameter is up to ten times the particle diameter has been described by Tsuda and co-workers<sup>80</sup>. The capillaries produced in this way were reported to show a reduced plate height of ca. 3 and a value for  $\phi$  of only 100, and as a result a separation impedance (cf section 2.4) of only 900, compared with ca. 4500 for conventional packed columns. In this work columns of this type shall be referred to as "drawn packed capillaries".



In order to produce capillary columns with the dimensions required for use in electrochromatography, experimental procedures for the production of both types of columns were developed.

### **5.2.1 Production of Drawn Packed Capillaries**

Using the method outlined below drawn packed capillaries were produced with diameters as small as 30 $\mu$ m packed with particles down to 3 $\mu$ m in diameter.

During the drawing phase in the initial experiments it was noted that gas bubbles formed within the emerging capillaries, which subsequently led to irregularly packed columns and eventually to the failure of the drawing process. This observation was attributed to residual water being driven off the silica at the glass drawing temperature of ca. 650° C. Thus, it was apparent that effort must be made to exclude water from the system.

Prior to the packing stage the silica gel was dried overnight at 400° C and allowed to cool, to room temperature, in an evacuated desiccator. To facilitate the dry packing stage, a small funnel was formed at one end of the glass tube by sealing one end in an oxygen/methane flame and gently blowing from the other end. After sealing the open end in the flame the dry silica was introduced to the funnel and transferred to the tube by repeated tapping and vibration, using an engraving tool. This process was repeated until ca. 30cm of the tube was packed. Following this the material was secured in place by inserting a glass wool plug into the open end of the tube and pushing this hard down onto the silica with a glass rod. The final step makes possible the evacuation of the tube without disturbing the packing.

In order to remove any additional moisture accumulated during the packing procedure the packed tube was heated to 500°C for a period of ca. 1 hour. During this time the tube was evacuated by attaching a rotary oil pump to the open end. After cooling the tube was placed in the glass drawing machine (Shimadzu GDM-1B) with continued evacuation. Figure 5.1 shows a schematic diagram of the apparatus.

The drawing process was initiated at 650°C and the temperature subsequently lowered to between 560°C and 600°C. The actual temperature used varied depending on the final diameter of the capillary being produced. It was found that the best packed capillaries were produced by operating at the lowest temperature at which the glass would still draw without breaking. At some point within the furnace, the packing material must undergo a considerable rearrangement. The force required to bring about this process can only be supplied by the converging glass walls of the capillary within the furnace. For this reason the viscosity of the glass must be high enough, i.e. temperature low enough, for the glass walls to be able to exert this force.

The continual evacuation of the system during drawing serves to remove any residual gas issuing from the silica, and also provides an additional pressure of one atmosphere on the glass walls.

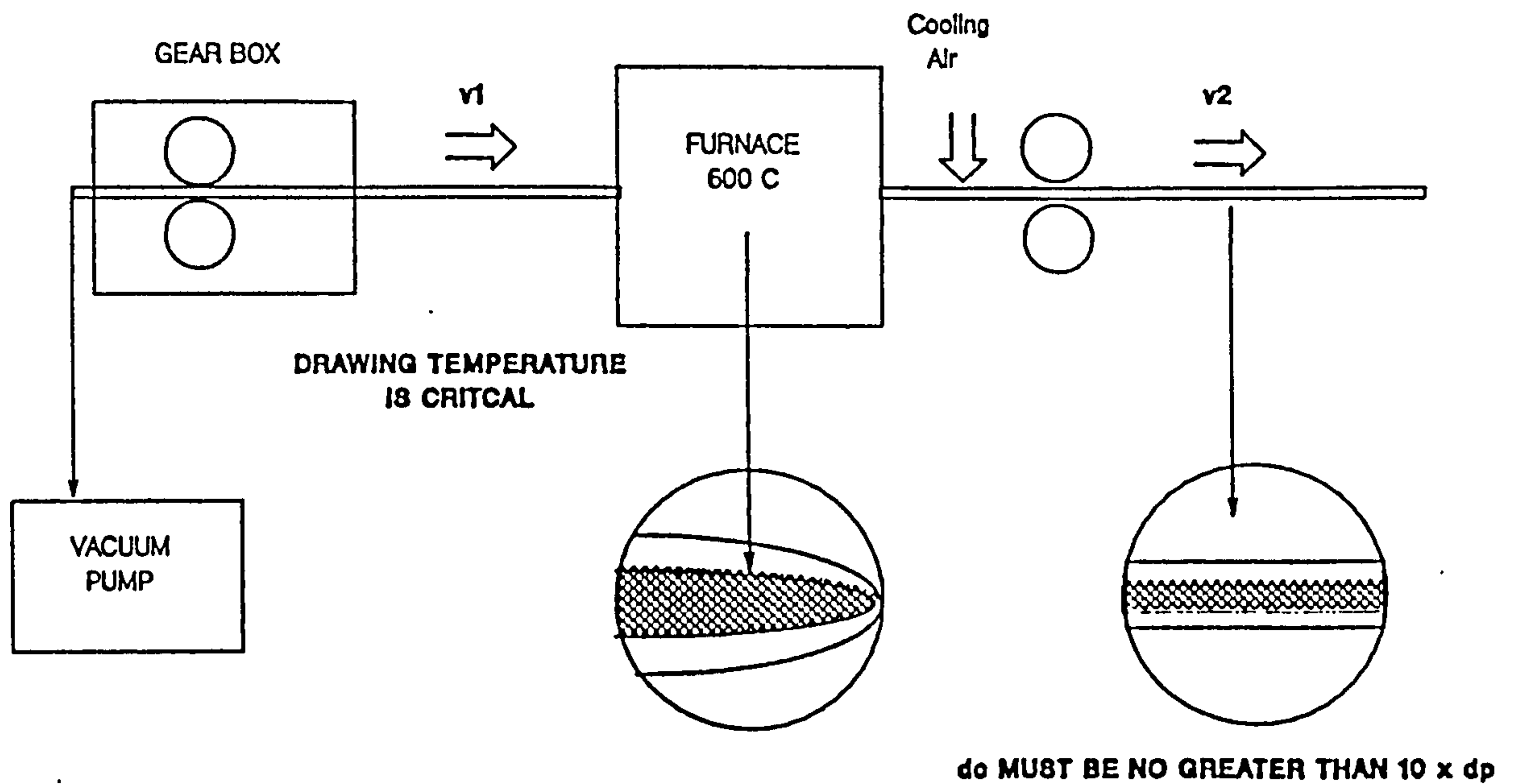
Removal of the vacuum pump during drawing was observed to cause an immediate deterioration of the packing uniformity.

The capillaries packed in this manner were tested for stability to solvent flow. In accordance with the findings of Tsuda<sup>80</sup>, for 10µm diameter particles, it was

FIGURE 5.1

## Schematic View of Glass Drawing Process

Glass is drawn at a constant velocity  $v_2$ . The feed velocity  $v_1$  can be varied. The final diameter is given by the product of the initial diameter and  $(v_1/v_2)^{1/2}$ .





found that the particles could not be washed out even with pressure gradients of 300bar per metre, provided that  $d_c/d_p$  was less than about 10. Some experiments with capillaries packed with 5 $\mu$ m particles, for which  $d_c/d_p$  was ca. 15 have shown that the stability to solvent flow is lost for wider capillaries. Thus, for particles of 3 $\mu$ m diameter it is essential that the internal diameter of the capillary does not exceed 30 $\mu$ m.

The stability to flow, without need of a retaining frit, is due to the fact that some of the particles become partially embedded in the glass walls during drawing. Provided that the internal diameter is not too great these partially embedded particles prevent the others from moving. Evidence for this is shown in figures 5.2 and 5.3 which show photomicrographs of 40 $\mu$ m i.d. capillaries packed with 5 $\mu$ m diameter particles.

In order to produce capillaries of 50 $\mu$ m i.d. or less, it was found to be more convenient to use two consecutive drawing processes. The following describes the procedure for 40 $\mu$ m i.d. capillaries packed with 5 $\mu$ m particles. Typically the initial dimensions of the Pyrex tube are 1mm i.d. 8mm o.d.. After filling this is drawn down to ca. 2mm o.d., 250 $\mu$ m i.d. using a drawing ratio of 32:1. In order to achieve the correct diameter at this stage it is necessary to allow a controlled slipping at the feeding side of the furnace, to give an effective drawing ratio of ca. 12:1. The capillaries produced in this way are drawn down again to produce columns of ca. 40 $\mu$ m i.d. 120 $\mu$ m o.d., using drawing ratios of 80-100. Capillaries of 30 $\mu$ m i.d. are produced in a similar manner, but with a higher drawing ratio in the second stage.



## FIGURE 5.2

**Photomicrograph of Drawn Packed Capillary**

The photomicrograph below shows a 300 $\mu\text{m}$  long section of a drawn packed capillary packed with 5 $\mu\text{m}$  diameter Hypersil. At several points along the inner wall partially embedded particles can be seen.

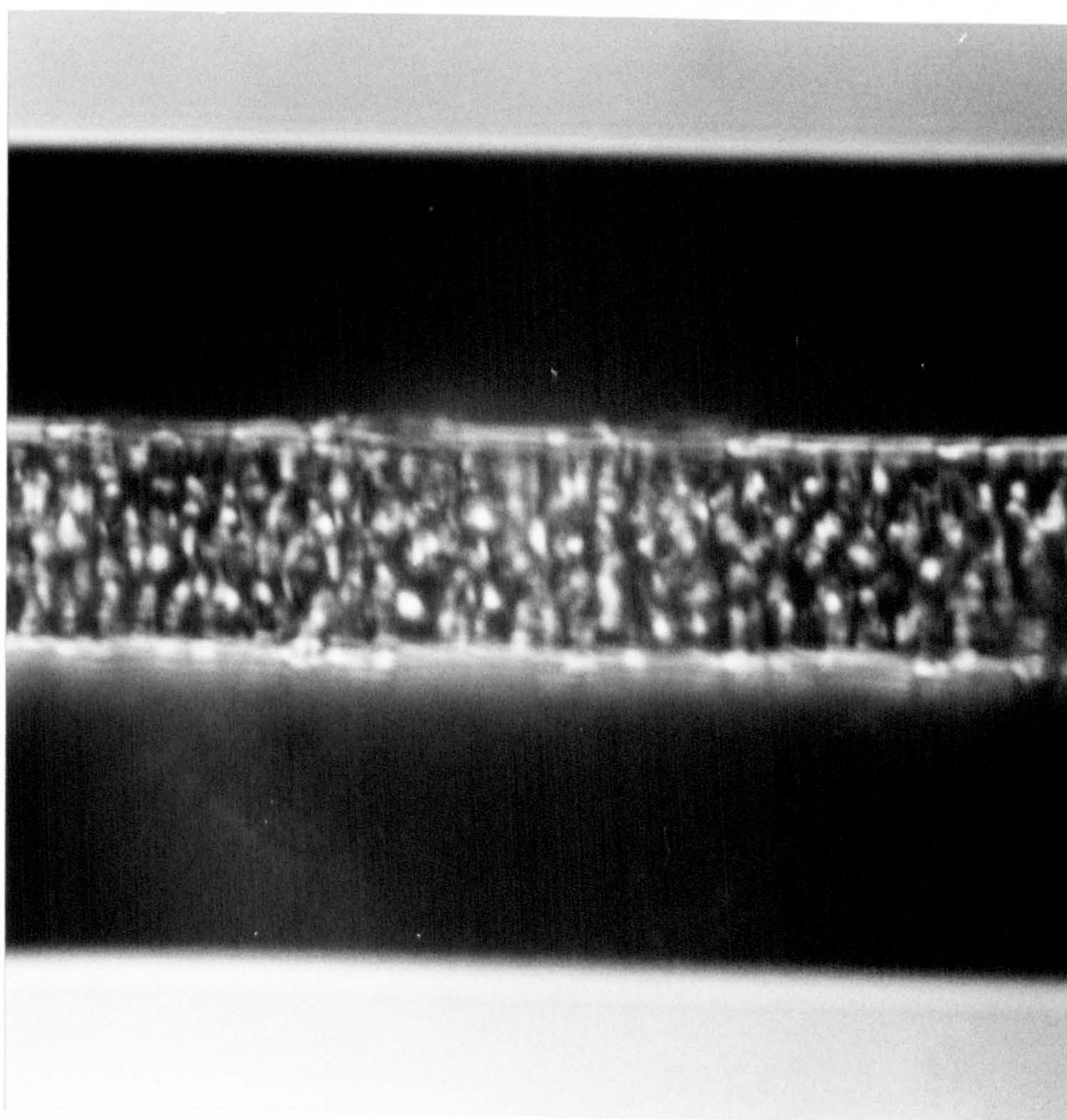
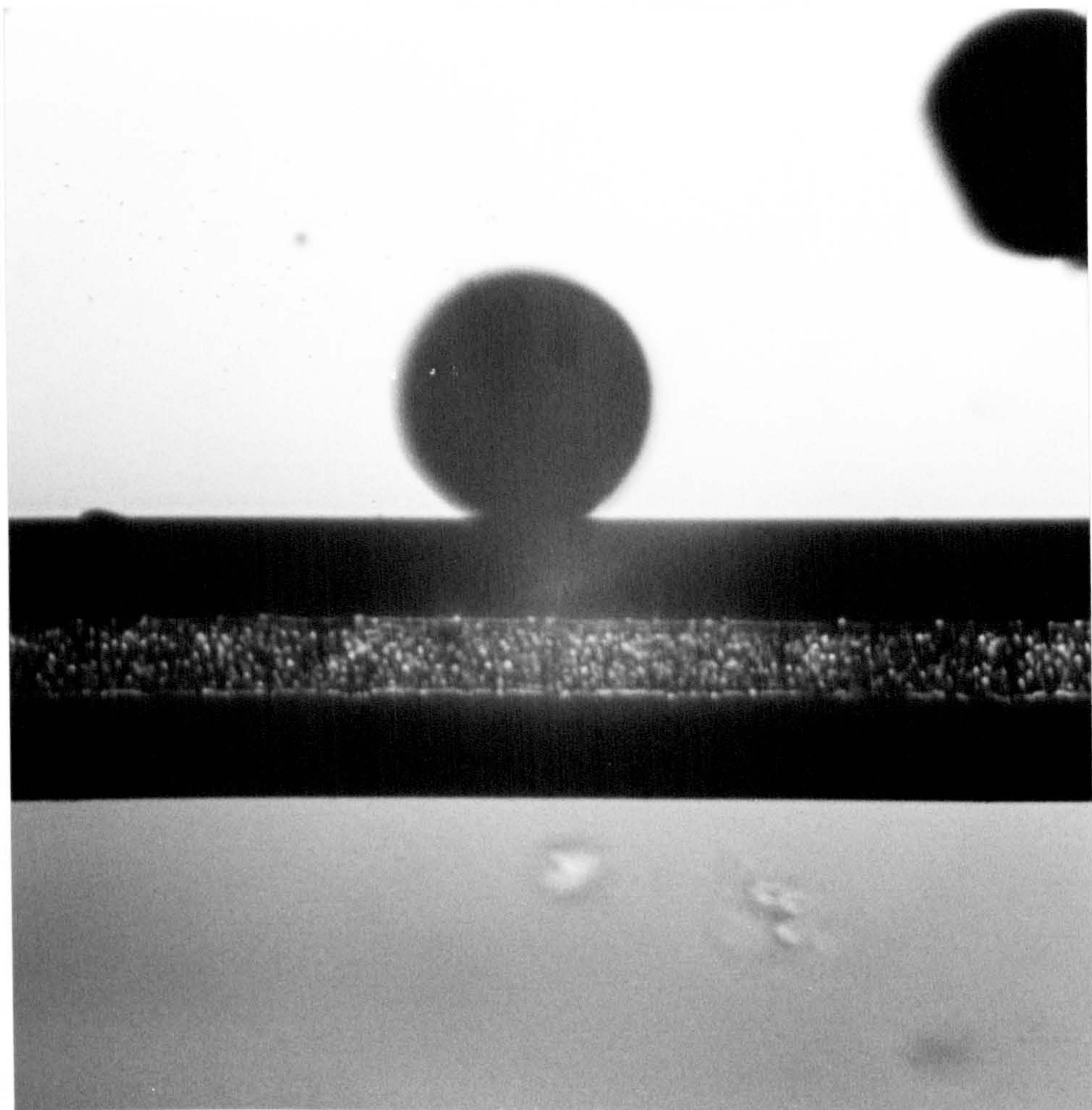




FIGURE 5.3

**Photomicrograph of Drawn Packed Capillary**

The high degree of packing uniformity, in comparison to drawn capillaries described by Novotny et al (reference 79) is illustrated below. The dark sphere next to the capillary has an approximate diameter of  $150\mu\text{m}$ .





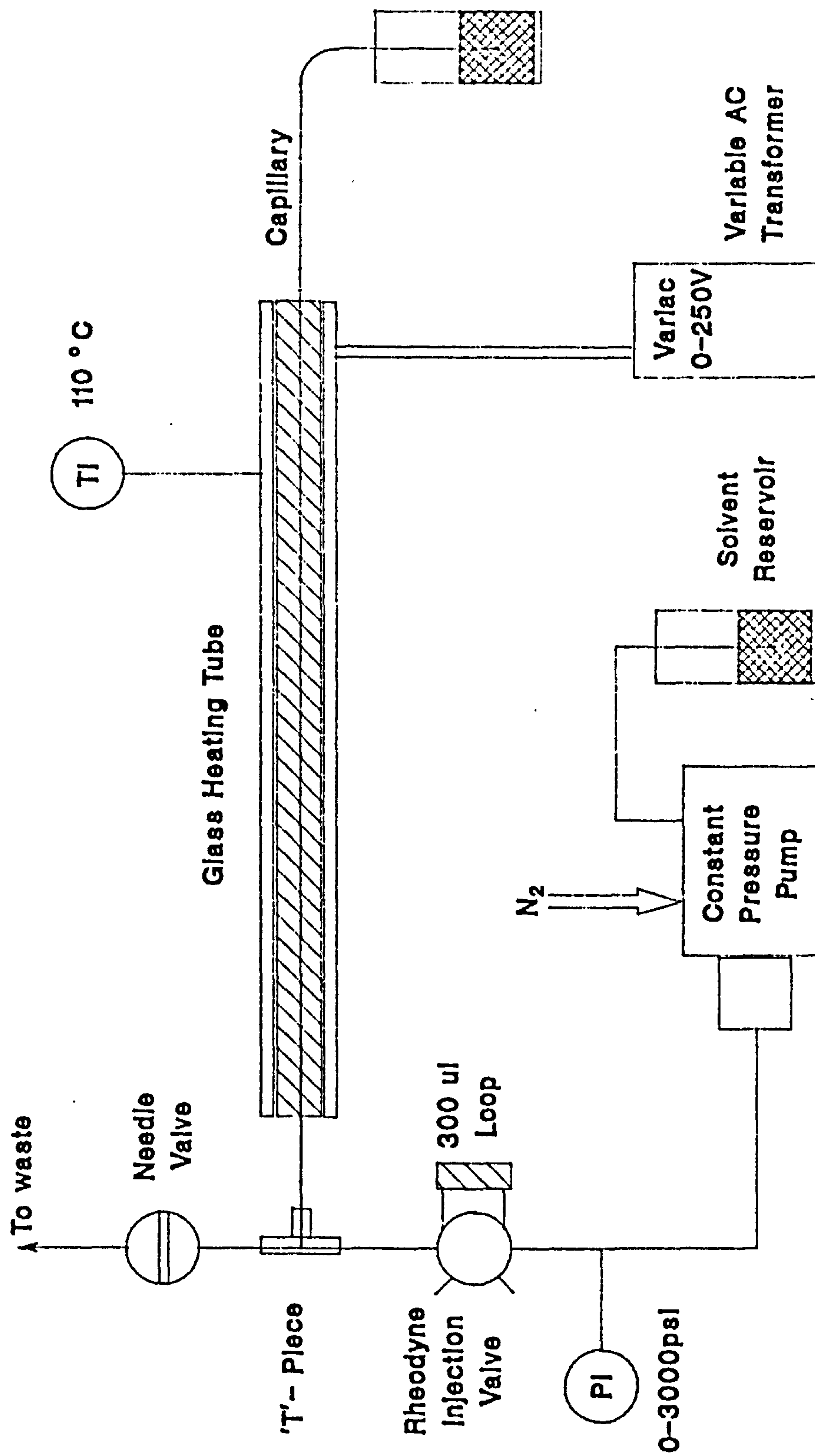
### 5.2.2 Derivatisation of Drawn Capillaries

The high temperatures involved in the drawing process preclude the use of any pre-derivatised silica gels, such as ODS-silica. Thus, if drawn packed capillaries are to be used in reversed phase chromatography it is necessary to carry out the derivatisation step in-situ after the column has been drawn. This was carried out to produce trimethylsilyl (TMS) and octadecyldimethylsilyl (ODS) derivatised silicas, using a method based on that described by Tanaka et al.<sup>81</sup> for the derivatisation of similar capillaries packed with 10 $\mu$ m material. The actual method used is described below.

A schematic diagram of the apparatus used for in-situ silanisation is shown in figure 5.4. Prior to derivatisation the column was washed at room temperature with dry tetrahydrofuran followed by toluene at 110°C. The capillary was maintained at this temperature by leading it through a 2cm bore glass tube, which had been wound with nichrome wire. Since only very small volumes were required, the silanising solution was injected into the system by means of a standard HPLC injection valve with a loop volume of 300 $\mu$ l (typical column volumes being less than 2 $\mu$ l). This was introduced to the column by operating the injection valve at a low pressure, and with most of the effluent going to a split line. After sufficient time for the reagent solution to have reached the column inlet the split line was closed diverting the solution into the column. The inlet pressure, supplied by a pneumatic intensifier, was then increased to ca. 150bar. This procedure is necessary because the time taken otherwise to flush out the volume of the connecting tubing between the injector and the column inlet would be quite considerable especially at the low flow rates obtained for 30 $\mu$ m and

FIGURE 5.4

Schematic View of Apparatus used for 'In-Situ' Silanisation





50µm i.d. capillaries.

In order to produce ODS-derivatised capillaries the silanising reagent used was octadecyldimethyl-N,N-diethylaminosilane prepared by the reaction of octadecyldimethylchlorosilane (Fluka A.G., Switzerland) with diethylamine (Fisons Ltd., UK), in HPLC grade n-hexane (Rathburn Chemicals Ltd., UK). The mixture was stirred for one hour at 50°C before the precipitate of diethylamine hydrochloride was filtered off. The silanising reagent was isolated simply by distilling off the n-hexane, and was used without further purification. The same procedure was used to prepare trimethyl-N,N-diethylaminosilane by substituting trimethylchlorosilane for ODS-chlorosilane.

The reagent was used as a 20% (by volume) solution in toluene. The reaction temperature was held at 110°C and the reaction was allowed to proceed for 2 hours. In order to prevent boiling of the toluene at this temperature the capillary length was chosen such that it extended 30-50cm beyond the heated area. This was done to ensure that the pressure within the column was always greater than the vapour pressure of toluene at the reaction temperature. This section was discarded before use. The reaction procedure was repeated twice, each time washing with toluene between reagent introductions. The column was then flushed with toluene for several hours and finally with HPLC grade acetonitrile prior to use.

### 5.2.3 Slurry Packing of Capillaries

The method described for the production of slurry packed capillaries was used for packing capillaries ranging from 50-200 $\mu$ m i.d. with reversed phase and normal phase particles ranging from 1.5-5 $\mu$ m in diameter. Polyimide coated fused silica capillaries (SGE Ltd., Australia) were used for this purpose.

The first problem which must be solved prior to packing capillaries using the slurry packing method, is the formation of a suitable porous frit to retain the packing material being forced into the capillary under high pressure. This can be accomplished by drawing the column end in a flame to form a cone and packing the first few millimetres with fairly coarse material<sup>82</sup>. However, for this work the method described below was used.

A small amount of 5 $\mu$ m diameter silica gel (Hypersil) is moistened with a dilute solution of sodium silicate (BDH Ltd., UK.), until it forms a paste which only just appears moist. The paste is then lightly compacted into a small sample vial to a depth of 1-2cm, using a glass rod. This paste is then introduced to the empty capillary by repeatedly forcing one end into the compacted paste, until a length 200-500 $\mu$ m from the capillary end is packed. The particles are then fused together by heating, with rotation, in a small Bunsen flame, until the particles just begin to glow. Prior to use, the sodium silicate solution is diluted to five times its original volume as received from the supplier. This concentration appears to produce a plug strong enough to withstand the pressures used in packing.

Before packing the capillary a short length of the polyimide protective coating is removed to facilitate detection. This is achieved by heating the capillary in a

small flame, whilst rotating it between thumb and forefinger, at a point ca.15cm from the end, in order to remove approximately 1cm of the protective coating. Care must be taken not to deform the capillary by overheating.

Several slurring media have been investigated including balanced density slurries using 1,2 dibromoethane, with the addition of small amounts of methylene chloride to achieve balance. However, the most practical, for reversed phase materials, has proved to be acetonitrile, partly because the difference in refractive indices of silica and acetonitrile makes visual observation of the packing progress possible. For underivatized materials a 1:1 acetonitrile:water mixture is used.

The slurry is produced by adding 1.5ml of acetonitrile, or acetonitrile/water to ca. 100mg of the packing material. The mixture is then shaken followed by ultrasonication for 15 minutes. Following dispersion the slurry is removed using a syringe and quickly transferred to the slurry chamber, being careful to exclude any air bubbles.

The slurry chamber consists of a 300mm x 2mm i.d., 6.4mm o.d. stainless steel tube. The capillary is connected to the lower end of the slurry chamber using a 1/4" to 1/16" Swagelok reducing union, to which the capillary is connected by means of a 300 $\mu$ m i.d. graphitised Vespel ferrule. Before tightening, the capillary is arranged such that the inlet protrudes approximately 10mm into the slurry chamber. This ensures that the inlet will not be buried in the particles collecting at the bottom of the chamber as a result of sedimentation. The upper end of the slurry chamber is connected to a standard HPLC column packing pump



(Shandon Southern Products Ltd., UK). After switching on the pump, the pressure is raised slowly from zero to 500bar over a period of a few minutes. The packing may take a few minutes to several hours depending on the particle diameter.

With such columns it is important to avoid sudden pressure drops. For this reason after visual observation of the capillary confirms that it is fully packed, the pump is then switched off and the pressure allowed to dissipate overnight before removing the packed capillary.

### 5.3 Instrumentation

The principal instrumental concern with the use of very narrow capillaries is the avoidance of extra-column broadening, which is the term used to describe zone broadening which occurs outwith the actual separation media and not as a result of the processes described in section 2.3. The factors which contribute to extra-column zone broadening are listed below:

- **Dead volume:** This includes the connecting tubing prior to the column inlet and that following the column prior to the detection system. Dispersion due to the parabolic profile (for pressure driven flow) within these areas and also the complex flow patterns at connecting unions broaden the sample before introduction to the separation medium and broaden the separated zones en route to the detection area.
- **Finite Sample Width:** Clearly the separated zones can never be narrower than the initial sample zone. Accordingly, if the sample width is large relative to



the expected peak widths, the former becomes the dominant factor contributing to the overall width.

- **Detection Volume:** The volume of space, in which the presence of an analyte gives rise to a signal, must also be small relative to the peak volumes, if this is not to contribute significantly to the width of the final signal.

### 5.3.1 Sample Introduction Techniques

An ideal sample introduction procedure would result in a sample concentration profile having an infinitesimal thickness in the direction of the separation path. In practice however, the best which can be achieved is a plug profile of a finite length. The actual width of the sample zone must be kept within strict limits so as not to cause unacceptable broadening of the resultant separated zones. The maximum acceptable width of the sample zone can be calculated by defining a maximum permissible fractional loss of the potential plate number (N). For example, one can impose the condition that no more than 10% of the potential plate number should be lost to extra column effects. Calculations of this type have been carried out for open tubular capillary columns by Knox and Gilbert<sup>21</sup>.

The effective standard deviation of a plug profile, of length (l), is given by equation 5.1.

$$\sigma_i = l / (12)^{1/2} \quad 5.1$$

where the subscript i denotes that this is due to the injection procedure. This expression can be arrived at by evaluating the second moment of a sharp edged plug profile of length l. If the condition is imposed that the extra-column

broadening should amount to no more than 10% of the potential plate number being lost, the standard deviation of the sample plug should not exceed one third of that expected of the final zone. The peak standard deviation ( $\sigma_c$ ) resulting from the migration through a distance  $L$  of the separation medium is given by,

$$\sigma_c = L / (N)^{1/2} \quad 5.2$$

where  $N$  is the number of theoretical plates within a length  $L$  of the column. If one applies the above condition limiting the standard deviation of the injection zone, one obtains,

$$l_{\max} = (L / 3) \cdot (12 / N)^{1/2} \quad 5.3$$

where  $l_{\max}$  denotes the maximum permitted width of the sample. If typical values for capillary zone electrophoresis are inserted into equation 5.3, such as  $L=1\text{m}$  and  $N=10^6$ , the maximum permitted sample length is 1.2mm. This implies that for a 50 $\mu\text{m}$  bore capillary column the total injected volume should not exceed 3nl. In the case of a chromatographic column, retained components will form a narrower injection profile than an unretained species, for equivalent injection volumes. Thus, the effect is most severe for early eluting species.

### 5.3.2 Sample Introduction in Capillary Chromatography

Previous published work in the field of packed capillary chromatography has involved two methods of low volume sample introduction, namely the dynamic split and the heart-cut methods. In the case of a dynamic split the capillary is connected, through a T-piece, to a conventional injection valve. To the other arm

of the T-piece a system with a relatively low resistance to hydraulic flow is connected. In this way the majority of the sample is lost to the low resistance part of the system and only a small proportion, which can be varied by choosing the appropriate resistance, is introduced to the capillary. The heart-cut method<sup>83</sup> employs a similar system, except that the side arm of the T-piece is connected to a valve which can either be fully closed or opened to atmospheric pressure. Closure of the valve for a predetermined time interval, as the sample passes over the inlet in the capillary, results in a small volume of sample being diverted into the column, which would otherwise pass through the open valve. A version of the latter method was used, in this work, for the characterisation of the packed capillaries.

### **5.3.3 Sample Introduction in Capillary Electrophoresis**

Research papers in capillary zone electrophoresis (CZE) have also described two different methods of sample introduction. The most common method involves the sample being introduced electrophoretically by placing the inlet of the capillary in the sample solution and applying a potential difference for a time sufficient to introduce a sample plug of appropriate length. After the sample introduction is complete the capillary inlet is transferred to the vessel containing the electrolyte. A problem associated with this technique arises from the fact the species of varying electrophoretic mobilities migrate at different rates into the capillary during sampling. As a result the relative amounts of each species in the sample plug are not truly representative of the relative concentrations present in the solution to be analysed<sup>84</sup>. This must be taken into account, and corrected for, in the analysis of data obtained using this method.



An alternative to the above method is to create a slight pressure drop across the capillary, either by the application of a sub-atmospheric pressure to the column outlet or by raising the column inlet above the level of the outlet, whilst the inlet is surrounded by the sample solution. After sufficient time has elapsed the pressure drop is removed and the sample solution replaced by the electrolyte. This method avoids the bias effect which accompanies the electrophoretic injection method.

#### **5.3.4 Experimental - Capillary Chromatography Injection Method**

The basis of the "heart-cut" injection system used in the experimental work is illustrated by figure 5.5. The sample is introduced using a conventional HPLC injection valve (Negretti-Zambra Ltd., UK) fitted with a 100 $\mu$ l sample loop. The inlet of the capillary column is fed through a 1/16" T-piece (Swagelok Ltd., UK) into a short length of 1mm i.d. stainless steel tubing, which is subsequently connected to the stainless steel capillary leading from the valve outlet by means of a drilled through 1/16" union. The capillary is secured at the other side of the T-piece using a graphitised Vespel ferrule (SGE. Ltd., Australia). The branch of the T-piece is connected to a stainless steel ball valve (Whitey Corp., USA), which opens to atmospheric pressure.

During the injection phase the solvent delivery is achieved using a glass reservoir pressurised, using nitrogen from a cylinder, to a pressure of 2bar above atmospheric pressure. The variables which control the volume of the sample introduced are, the injection pressure and the time for which the ball valve is closed. The pressure of 2bar was chosen in order to produce injection times of



several seconds. Thus, precise valve timings are not necessary. The procedure carried out in performing an injection is outlined below.

1. The eluent reservoir is pressurised to 2bar.
2. The 100 $\mu$ l sample loop is filled and the valve turned to the inject position.
3. After a short time (the time required for the sample mixture to fill the area surrounding the column inlet) the ball valve is closed for a predetermined time interval.
4. The excess sample is washed out from the system, by allowing the passage of eluent through the ball valve for five minutes.
5. Elution is started by the closure of the valve and increasing the pressure to that required.

The required elution pressures for capillary chromatography are obtained using a pneumatic intensifier pump. The complete solvent delivery system is illustrated in figure 5.6.

FIGURE 5.5

**Principle of the Heart-Cut Injection Method**

In the diagram below the arrow represents the flow from the outlet of the sample valve.

1. The injection valve is operated with the ball valve open.
2. When the approximate centre of the sample pulse reaches the area surrounding the capillary inlet, the ball valve is closed.
3. After a predetermined time interval, the ball valve is opened and the excess sample washed out.

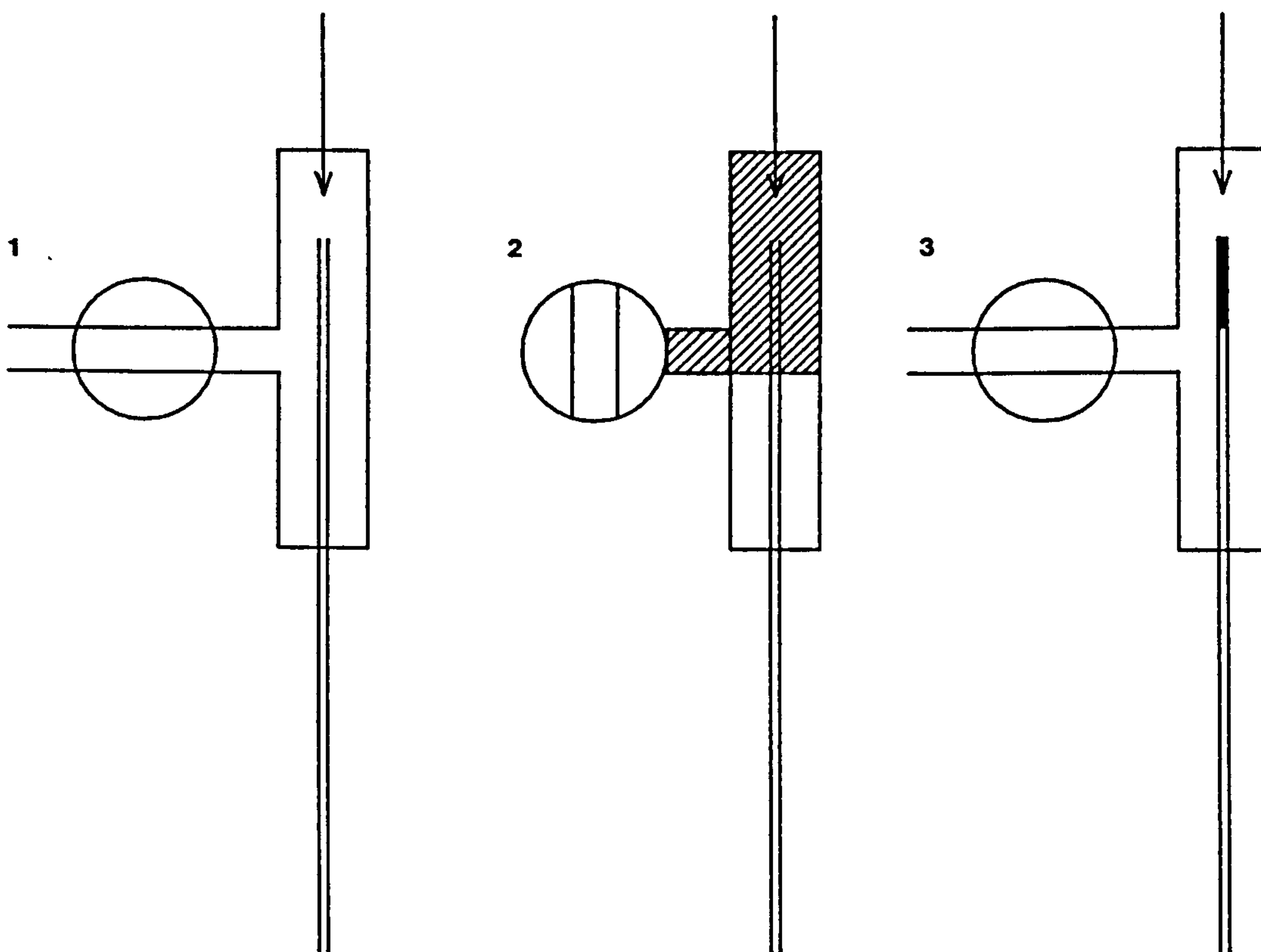
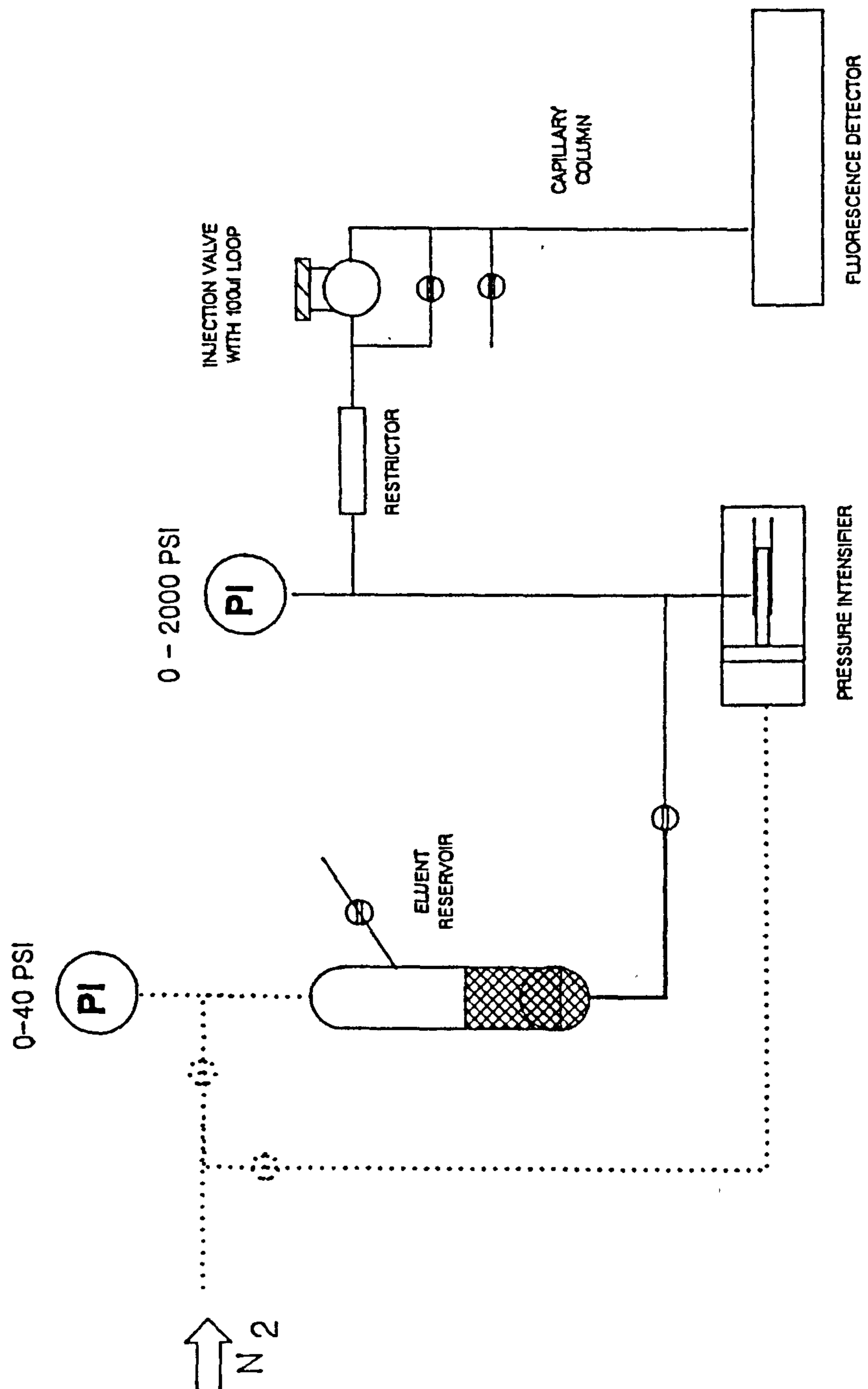


FIGURE 5.6

## Injection and Solvent Delivery System for Capillary LC



### 5.3.5 Experimental - Electrochromatography Injection Method

For the experiments in electrochromatography an electrophoretic analogue of the "heart-cut" method was developed. The construction of the injection system is depicted by figure 5.7. As the diagram shows this consists of two three-way valves (Hamilton A.G., Switzerland) connected at right angles by means of a 1/16" T-piece (Swagelok Ltd., USA). Valve A, as indicated in the diagram, is connected to the T-piece via a length of 1mm i.d. stainless steel capillary tubing. The capillary column is led into this connecting tube, through the opposite port of the T-piece, and secured, using a 300µm ID graphitised Vespel ferrule, with the inlet approximately halfway between valve A and the T-piece. At one of the other ports of valve A a needle port was formed to facilitate filling from a syringe. The operating procedure of this system is described below.

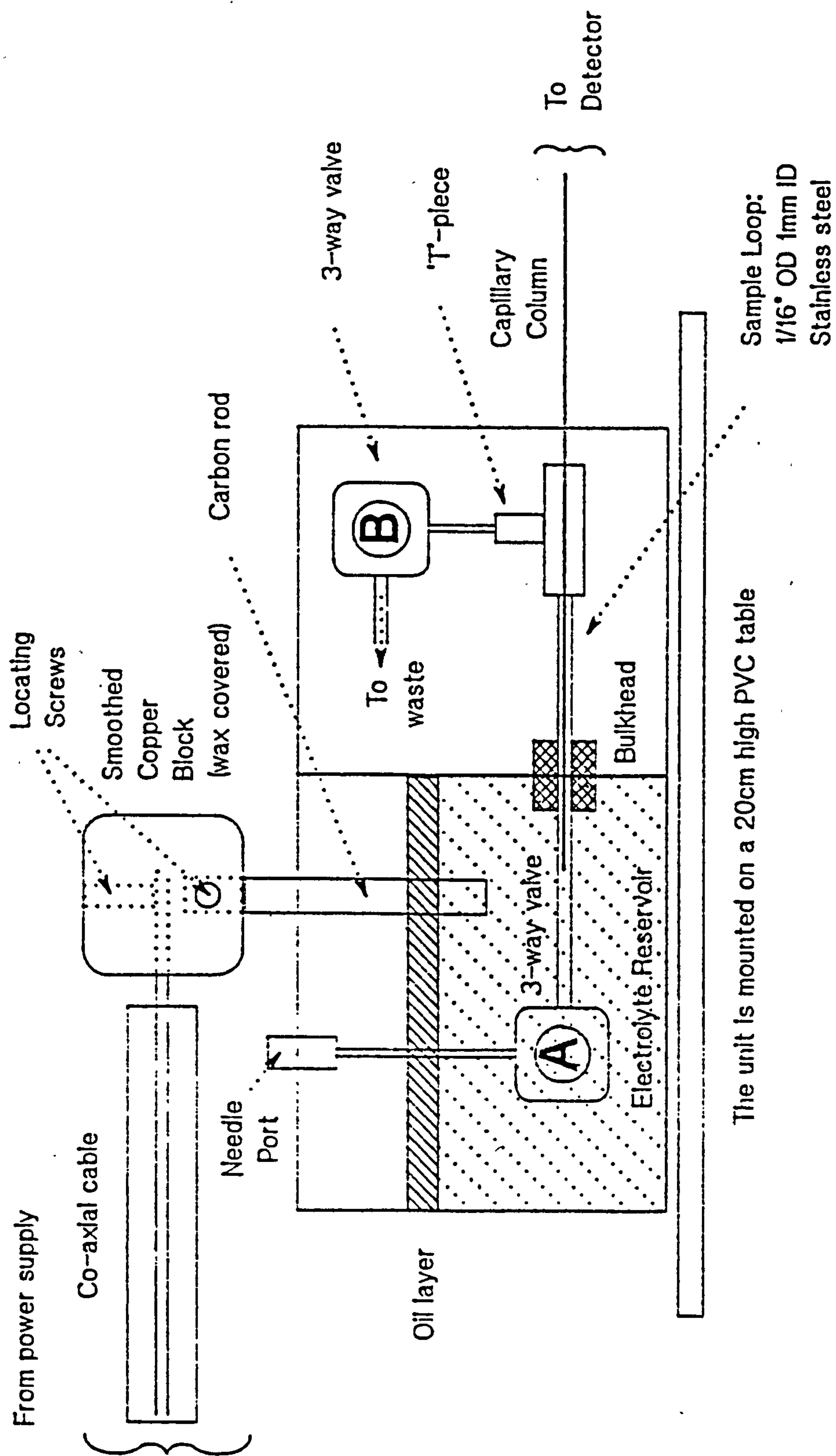
1. The sample is introduced through valve A filling the connecting tubing completely.
2. A potential difference, which is small relative to that used for the analysis, is applied to the capillary, causing a small portion of the sample to migrate into the column. Typically a potential of 5kV is applied for 5 to 15 seconds.
3. The connecting tubing is washed out thoroughly with the desired eluent before reapplying the potential to begin elution. Because of the small amount of eluent required, the electrolyte contained within the connecting tubing is sufficient for the complete analysis.

This system is also suitable for carrying out frontal chromatography. This can be achieved simply by applying the potential required for elution directly after the first step.



FIGURE 5.7

## Injection Components for Electrochromatography



### 5.3.6 Detection in Capillaries

A second major experimental problem with capillary methods is the provision of adequate detection. As discussed above the region of space in which detection takes place must be strictly limited. If the detector provides a uniform response within this area, the maximum acceptable detector volume can be estimated in the same manner as in the calculation of the permissible injection volume. As was the case with the injection, the volume must be less than a few nanolitres. This represents a volume smaller by a factor of ca.  $10^4$  than that of the detection cell in a conventional UV-absorbance detector for use in HPLC.

The most practical means of achieving low volume detection is to carry out detection actually within the column, which has been the preferred means of detection in capillary zone electrophoresis. This technique, referred to as "on-column" detection, makes use of UV-absorbance<sup>54</sup> or fluorescence<sup>52</sup> within the separation capillary. In addition to the forementioned spectroscopic means, conductivity<sup>85</sup> and electrochemical detection<sup>86</sup> have been demonstrated with sufficiently small detection volumes.

In on-column UV absorbance, the capillary is illuminated using a beam perpendicular to the capillary axis. The optical path length available for absorbance is therefore, in principle, no greater than the capillary diameter, and as a result only a very poor sensitivity (in terms of concentration) can be expected. Mass sensitivities of a few picograms are often quoted, but are deceptive since several picograms in a volume of only a few nanolitres is by no means a dilute sample. The method chosen for this work, however, was

on-column fluorescence, which had been demonstrated for capillary zone electrophoresis by Jorgenson<sup>33</sup>. The choice of fluorescence as a means of detection was dictated by the superior sensitivity of this technique in comparison to UV absorbance.

### **5.3.7 Experimental - Detection System for Electrochromatography**

In this work the detection is accomplished using a modified fluorescence detector, designed primarily for use in HPLC (Perkin Elmer Model LS4, USA.). The modifications carried out are as follows. The original cell supports were removed and replaced by two stainless steel capillary tubes lined with 300 $\mu$ m i.d. Teflon tubing. These were arranged in such a way, that they were separated by a gap of approximately 1cm at the position of the original cell. The LS4 cell assembly is such that, the incident monochromatic light is focused onto the cell by a parabolic mirror, the fluorescence is then collected at right angles to the incoming light by a similar mirror. The separation capillary is fed through the Teflon lined supports, leaving a small region exposed at the focal point of the two mirrors. The illuminated volume is limited by painting the capillary with matt black enamel in order to leave a length of only ca. 1mm exposed to the excitation beam. This gives rise to an additional peak standard deviation, in length terms, of ca. 300 $\mu$ m. Fine adjustments to the mirrors can be made by filling the capillary with a solution of fluorene in acetonitrile, and making corrections to the mirror supports until an adequate signal is obtained. In the case of polyimide coated fused silica capillaries the protective coating, at the point of detection, must be removed before use, as described in section 5.2.



### 5.3.8 Experimental - Dispersion due to Injection and Detection

In order to determine whether or not the dispersion caused by the injection and detection systems was small enough not to cause severe extra column broadening, the following test was carried out. For pressure induced laminar flow, the variance (in length units) resulting from the the dispersion of an initially narrow zone can be predicted by the following version of the Taylor equation<sup>38</sup>,

$$\sigma^2 = ( 2D_m/u + u.d_C^2/96D_m ).L \quad 5.4$$

Any additional observed dispersion is therefore due to the injection procedure or the detection system or both. Peaks significantly wider than the width predicted by the Taylor equation would indicate that an unacceptable level of extra-column dispersion was present.

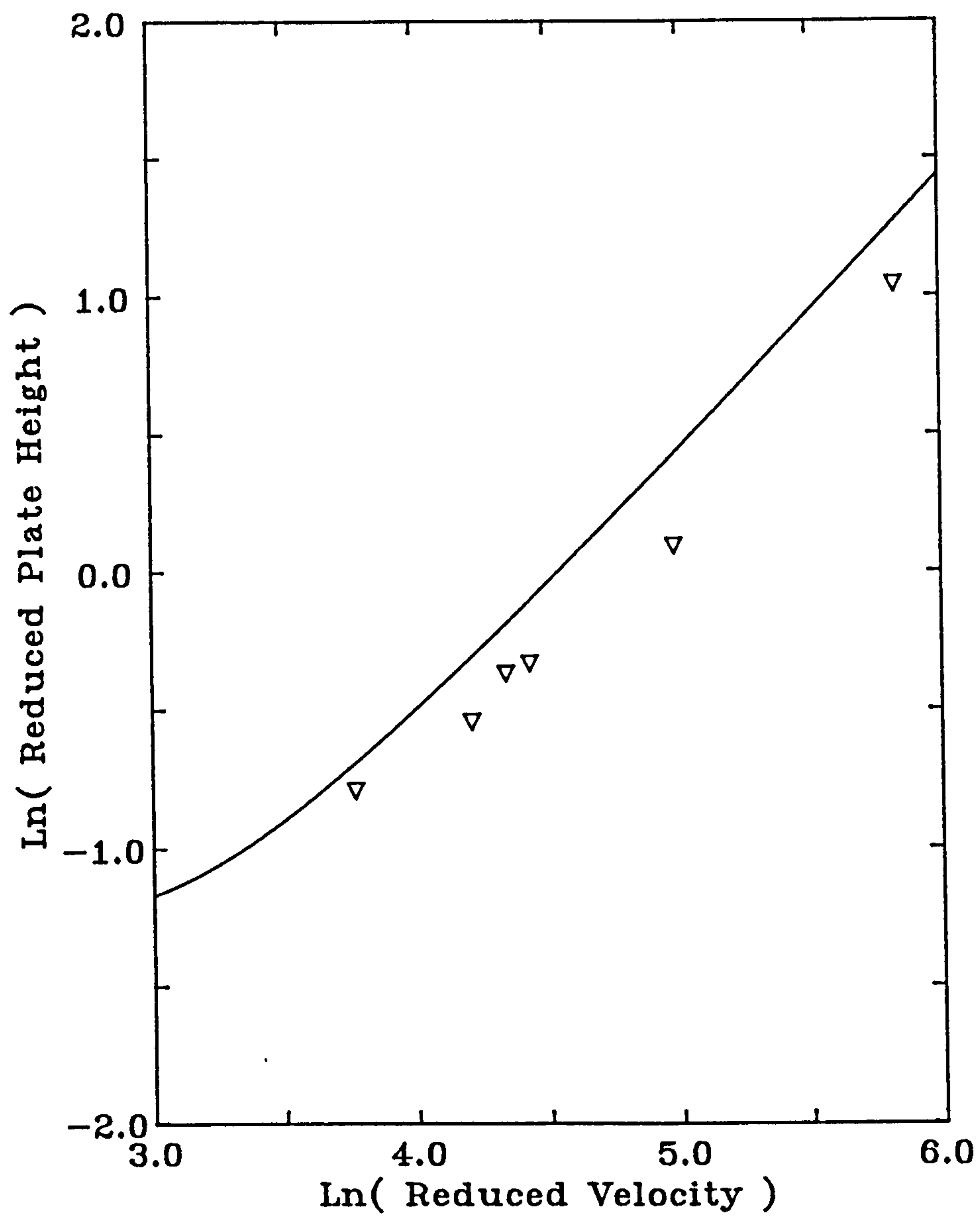
Figure 5.8 shows the plate heights measured at several solvent velocities for a series of injections of fluorene in acetonitrile. The capillary internal diameter and length to the point of detection were 100 $\mu$ m and 1.8m respectively. From this it can be seen that all experiment points lie close to, although slightly below the value predicted by the Taylor equation, indicated by the solid line, confirming that the apparatus produces negligible dispersion, and is therefore suitable for the characterisation of packed capillary columns.



FIGURE 5.8

## Taylor Plot for Dispersion in a Capillary due to Laminar Flow

$d_c = 100\mu\text{m}$ ,  $L = 1.8\text{m}$ . The solid line represents the value predicted from the Taylor equation.



### 5.3.9 Apparatus for Electrochromatography

A schematic diagram of the complete experimental assembly for experiments in electrochromatography is shown in figure 5.9.

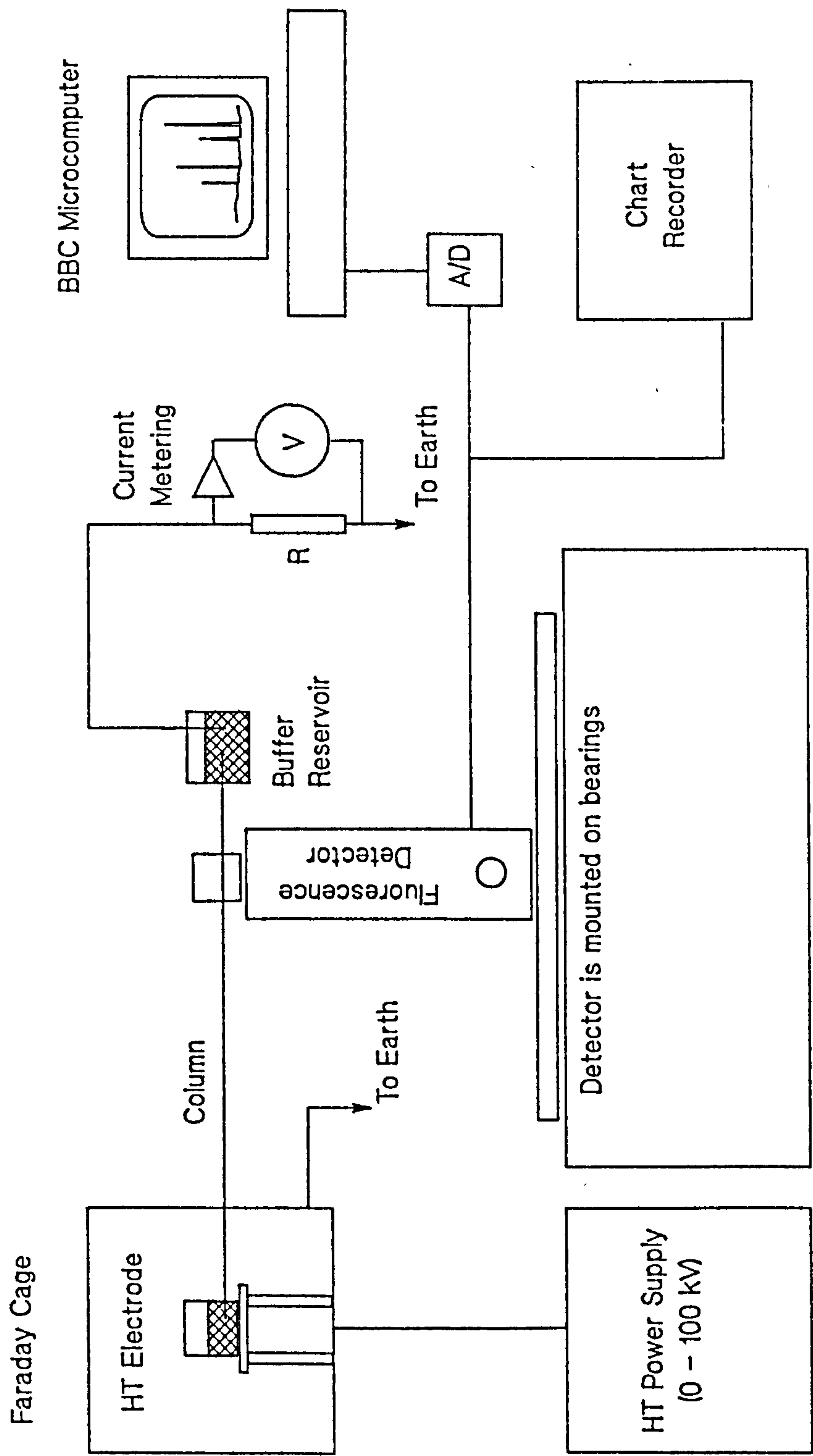
The generation of the electroosmotic flow velocities required for electrochromatography makes necessary the use of high electric fields, typically  $50\text{kVm}^{-1}$ . Therefore, if capillaries of up to 1m in length are to be used a potential difference of up to 50kV must be available.

The use of such a high electrical potential requires considerable planning if electrical discharges to nearby earthed objects are to be avoided and the safety of the operator ensured. For this reason the parts of the apparatus to be raised to the high potential were housed in an earthed Faraday cage. This not only prevents physical contact with the electrode, but also prevents disturbances of sensitive electronics in the vicinity such as the detector or microcomputer. Prior to operation the Faraday cage is locked by a shunt lock, activating a relay which in turn enables the high voltage supply. Opening of the cage results in the power supply being immediately disabled. A second microswitch on the floor of the cage ensures that the power supply can only be enabled when the cage is closed, thereby preventing the operation of the power supply by merely operating the shunt lock with the cage in the open position.

A Brandenburg high tension power supply, model 2829P (Brandenburg Ltd., UK) capable of providing a positive high voltage of up to 100kV, at a maximum load of 1mA, was used. The output can be varied continuously between zero and the maximum. The possible use of voltages up to 100kV means that objects at the

FIGURE 5.9

Schematic View of Electrochromatographic System



high potential must be kept at a distance of greater than 10cm from any earthed object, such as the wall of the Faraday cage. In order to provide a safety margin the Faraday cage was constructed so that the electrode and injection components were at least 20cm from the extremities of the cage. The injection components were supported in the approximate centre of the cage by a PVC table.

The Faraday cage was formed from angle iron and covered with a wire mesh. The floor and one wall of the cage consisted of a 1/2" thick aluminium plate. The heavily insulated cable was passed through a hole in the aluminium wall and firmly secured using a brass plumbing union fixed to the wall. The cable was arranged such that the exposed copper core was in the approximate centre of the cage.

Contact between the injection system and the central core of the high voltage power supply co-axial cable was achieved by means of a carbon electrode, dipping into the electrolyte contained within the box, which was connected at right angles, in a carefully rounded copper block, as illustrated by figure 5.7. Only a small length(ca. 20mm) of the insulation surrounding the central core was removed in order to allow the connection to the copper block without leaving a length of the core exposed to the atmosphere.

Initially it was found that raising the potential to greater than 30kV resulted in violent ionisation of the air in the vicinity of the electrode, which could be seen as a violet glow in the darkened laboratory. By covering the copper block with a smooth layer of paraffin wax several millimetres thick, the voltage limit before the onset of excessive ionisation was increased to greater than 50kV. A further



improvement was obtained by covering the surface on the electrolyte, contained within the Perspex box, with a layer of paraffin oil, thereby reducing the atmospheric humidity in the cage. It was never possible to operate routinely at more than 60kV.

In order to permit the use of straight rigid glass capillaries, it was necessary to mount the fluorimeter on its side. In addition it was also necessary for the fluorimeter to be supported on a moving carriage, so that the distance between the injector and the detector could be varied. For this reason the fluorimeter support was mounted on cylindrical bearings running on two 1" diameter steel rods. The arrangement, shown in figure 5.9, allows the use of rigid capillaries ranging from 0.5-1.5m in length.

After passing through the detector the capillary is led into the electrolyte reservoir at earth potential. This contains a stainless steel electrode connected to earth via a load resistor, as shown in figure 5.9. By measuring the voltage across the resistor the current flowing within the capillary can be determined.

## 5.4 Data Handling

The fluorescence output was digitised and stored for further analysis using a BBC model B microcomputer fitted with a 6502 second processor (Acorn Computers Ltd., UK.). The maximum possible sampling rate, using the built-in analogue to digital convertor, is one sample every 30ms, i.e., approximately 30Hz, with a resolution of one part per thousand. Only the fluorescence values are stored since for a constant sampling rate the time axis is already defined. The actual time can always be calculated from the serial number of the sampled point multiplied by the sampling interval. The BBC BASIC routine used for data collection and storage was based on a program called Labmaster by Dr. A.G. Rowley.

### 5.4.1 Calculation of Plate Numbers from Fronts and Gaussian Peaks

The BBC BASIC routines for processing the fluorescence data in order to evaluate plate numbers from chromatographic fronts and Gaussian peaks were developed specifically for this work, and are listed in Appendix II.

#### 5.4.1.1 Analysis of Fronts

In order to extract the required information from error function sample fronts, both rising and falling, the program uses the following simple algorithm. The serial numbers of two sample points  $t_b$  and  $t_e$ , which define the beginning and end of the front respectively, are chosen using an "on-screen" moving cursor. Provided  $t_b$  and  $t_e$  respectively represent times before and after the elution of the

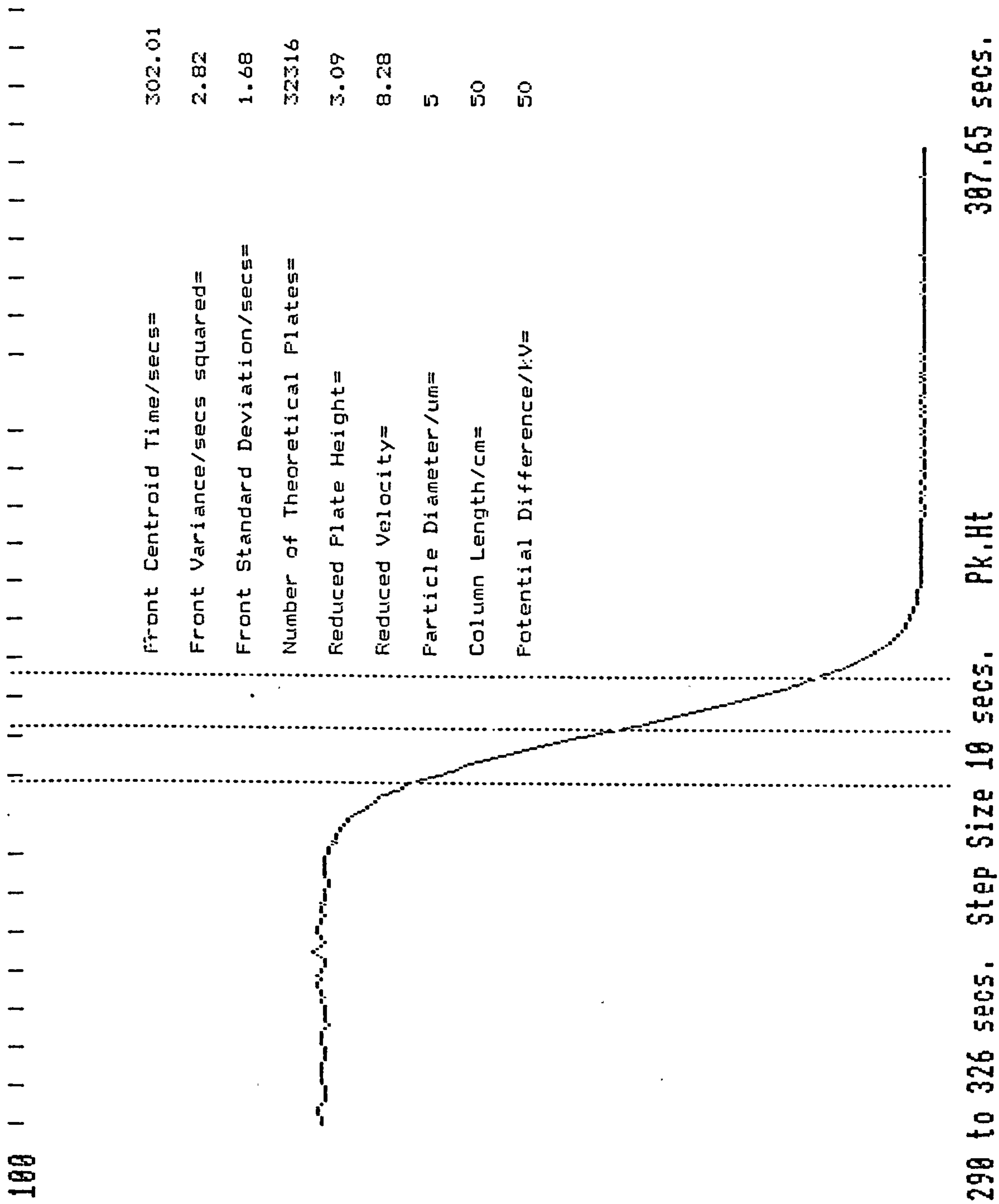
front, the exact values are not important since they serve only to define the region of the data to be processed. The fluorescence signal can be defined as  $c(t)$ . If  $c(t_e)$  is greater than  $c(t_b)$  then the front is rising, and vice versa if  $c(t_e)$  is smaller. After establishing whether the front is rising or falling, the maximum height is determined from the absolute value of  $c(t_e)-c(t_b)$ . In the case of a rising front, each sampled point is examined in turn, starting with  $t_b$ , until  $c(t)$  is only just greater than 16% of the maximum height. The serial number of the sample at which this occurs is denoted  $t_l$ . Similarly, by starting at  $t_e$  the program examines each previous point until  $c(t)$  falls just below 84% of the maximum height, and the corresponding sample serial number is recorded as  $t_r$ . The value of  $(t_r-t_l)+1$  corresponds to twice the standard deviation of the front, accurate to plus or minus one sampling interval. The mid-point of the front( $t_m$ ) is determined in a similar manner by determining the serial numbers corresponding to the half height. The standard deviation and the mid-point are then converted to absolute times, by multiplying by the time interval between samples. Before beginning each run the column length and particle diameter are entered, thereby allowing the program to calculate relevant chromatographic parameters.

An example datasystem report for a falling front eluted by electroosmotic flow in a capillary packed with 5 $\mu$ m diameter particles is shown in figure 5.10.

FIGURE 5.10

Example Datasystem Report for a Chromatographic Front

The vertical dotted lines, from left to right, denote  $t_l$ ,  $t_m$  and  $t_r$  respectively.  $t_b$  and  $t_e$  can be anywhere on the approximately flat areas to the left and to the right of the front. The example is from an unretained front in a 75 $\mu$ m i.d. slurry packed capillary ( $d_p = 5\mu$ m) eluted by electroosmosis.





### 5.4.1.2 Analysis of Gaussian Peaks

For Gaussian peaks the peak variance is determined by calculating the second statistical moment of the profile. As with the previous case the beginning and end of the data region to be analysed are defined by estimating the beginning and end of the peak using the cursor. The determination of the variance by the statistical second moment method requires the evaluation of the following three integrals.

$$I_0 = \int_{t_b}^{t_e} c(t).dt \quad 5.5$$

$$I_1 = \int_{t_b}^{t_e} (t.c(t)).dt \quad 5.6$$

$$I_2 = \int_{t_b}^{t_e} (t_m - t)^2 .c(t).dt \quad 5.7$$

where  $t_b$  and  $t_e$  represent the effective beginning and end of the peak respectively.

The program first evaluates  $I_0$  and  $I_1$  using the trapezium rule. The centre of gravity of the profile, i.e., the first statistical moment, corresponds to  $t_m$  and is given by  $I_1/I_0$ . Determination of  $t_m$  enables the evaluation of  $I_2$ . The variance of the profile is given by  $I_2/I_0$ .

In contrast to the situation with error function fronts, the times  $t_b$  and  $t_e$  defining the beginning and the end of the peak must be chosen carefully, as the value of the second moment is sensitive to the exact values of these. Before use with

chromatographic peaks the procedure was tested using synthetic data files containing tabulated Gaussian functions of known variance. The values obtained for chromatographic peaks were also shown to be in agreement with those calculated from a chart recorder running at a very high chart speed.

By determining the maximum value of  $c(t)$  in the region being analysed, the width at half height is also determined. Each point is examined in turn starting from  $t_b$  until  $c(t)$  is just above half height, to give  $t_l$ , and similarly by starting from  $t_e$  and working backwards, to give  $t_r$ . The width at half height ( $w_{1/2}$ ), to the nearest sampling interval, is given by  $(t_r - t_l + 1)/2$ . The plate number is then evaluated from,

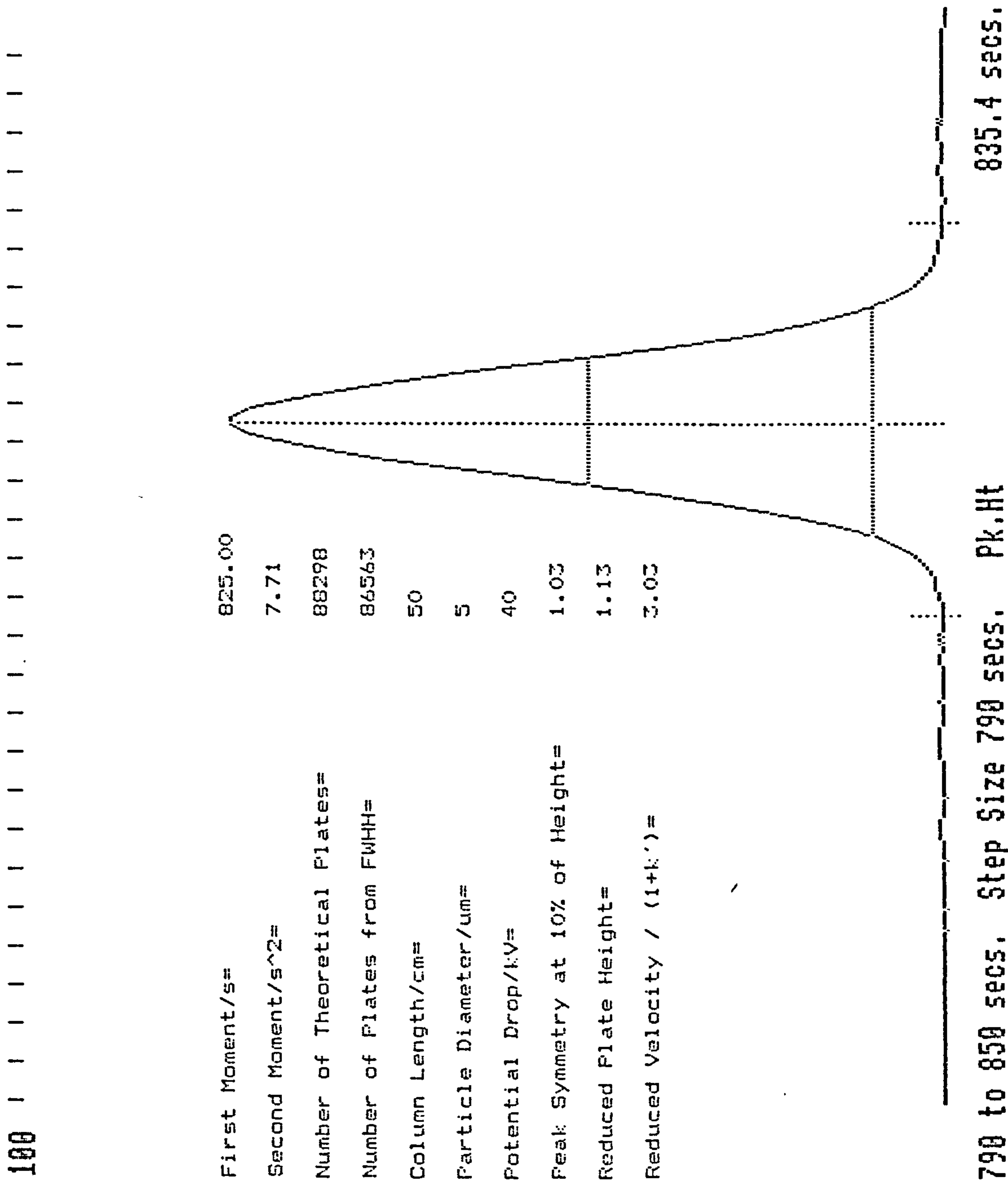
$$N = 8 \ln(2) \cdot (t_m / w_{1/2})^2 \quad 5.8$$

The evaluation of  $N$  using this method is not sensitive to the choice of times defining the beginning and the end of the peak. The numbers of plates determined using both methods are reported in the output. In addition to  $N$ , the program calculates the peak symmetry at 10% of the height, reduced plate height and reduced velocity. Figure 5.11 shows the output from the data system for a typical run.

FIGURE 5.11

Example Datasystem Analysis of a Chromatographic Peak

The values of  $t_b$  and  $t_e$  are indicated by the dotted vertical lines on the baseline either side of the peak. The example is taken from the separation of aromatic hydrocarbons by electrochromatography (cf. chapter 6).



## **CHAPTER 6**

### **EXPERIMENTAL MEASUREMENTS**



## Chapter 6

### EXPERIMENTAL MEASUREMENTS

#### 6.1 Introduction

The apparatus described in the previous chapter was used to determine the chromatographic performance of the packed capillaries in both the pressure driven and electrically driven modes of operation.

The majority of the plate height measurements were made using capillaries packed with normal phase, i.e. non-derivatised, silica gel. The plate heights were determined from the elution of an unretained species. For this purpose an eluent of 70% acetonitrile (Rathburn Chemicals Ltd., UK.), by volume, in double distilled water was used. The unretained species was the polycyclic hydrocarbon fluorene, which shows a strong fluorescence signal at a wavelength of 305nm induced by excitation at 265nm. Under such conditions no significant retention of fluorene is observed. This allows the mean linear velocity of the mobile phase, and thus, the reduced velocity to be determined from the elution time of the fluorene peak. The acetonitrile/water mixture (70:30 v/v) has a viscosity of  $0.6 \times 10^{-3} \text{ Nm}^{-2} \text{ s}$  and a relative permittivity of 43, at room temperature. These values were used in the calculation of the flow resistance parameter ( $\phi$ ) and the zeta potential, from experimental data. For the calculation of reduced velocity the diffusion coefficient for fluorene in this medium was assumed to be  $1.0 \times 10^{-9} \text{ m}^2 \text{ s}^{-1}$ .

## 6.2 Pressure Driven Experiments

### 6.2.1 Drawn Packed Capillaries

Table 6.1 shows the plate heights determined for various reduced velocities from a typical section of a 40 $\mu$ m i.d. drawn packed capillary packed with 5 $\mu$ m diameter Hypersil (Shandon Southern Products Ltd., UK.) for various elution pressures. These data are also presented in the form of a graph in figure 6.1 showing the measured plate height against the reduced velocity. From the graph it is clear that the reduced plate height exhibits a minimum value of ca. 2.7 which is fairly typical for conventional 4.6mm i.d. packed columns. In some cases reduced plate heights as small as 2.2 were recorded, as shown by table 6.2 which tabulates the data obtained from a particularly efficient batch. The results compare favourably with the data of Tsuda<sup>80</sup> for drawn packed capillaries packed with 10 $\mu$ m particles which show a minimum value of ca. 3 for the reduced plate height. The capillary used in figure 6.1 typically produced ca. 50,000 plates in approximately 10 minutes.

In addition to the acceptable plate heights, the capillaries were found to have a permeability superior to that of conventional columns. This was also reported by Tsuda. Using the Poiseuille equation (eqn. 2.29) the dimensionless flow resistance factor  $\phi$  can be evaluated. In contrast to conventional slurry packed columns used in HPLC, which usually show a value of between 500 and 1000 for  $\phi$ , the value measured for the drawn capillaries, with 5 $\mu$ m diameter particles, is approximately 150, based on the data listed in table 6.2.

TABLE 6.1

**Drawn Packed Capillary - Pressure Driven Mode.**

Stationary Phase	Hypersil ( $d_p = 5\mu\text{m}$ )
Mobile Phase	70:30 $\text{CH}_3\text{CN}:\text{H}_2\text{O}$ (v/v)
Capillary i.d.	$= 40\mu\text{m}$
Total Length	$= 0.98\text{m}$
Length to Detector	$= 0.79\text{m}$

$t_m/\text{s}$	$u/\text{mm.s}^{-1}$	$v$	$h$
3804	0.21	1.05	3.65
3603	0.22	1.11	3.50
2339	0.34	1.71	3.30
1428	0.56	2.80	3.61
1277	0.63	3.13	2.84
663	1.21	6.03	3.00
514	1.56	7.78	3.06
505	1.58	7.91	3.18
449	1.78	8.90	2.73
425	1.88	9.41	3.48
360	2.22	11.09	3.19
349	2.29	11.46	3.61
346	2.31	11.53	3.75
269	2.96	14.82	3.86
259	3.08	15.42	4.18

FIGURE 6.1

Reduced Velocity versus Reduced Plate Height for  
a 40 $\mu$ m i.d. Drawn Packed Capillary

Eluent: Acetonitrile:Water 70:30 (v/v), Sample: Fluorene,  
Packing Material: Hypersil ( $d_p = 5\mu$ m).

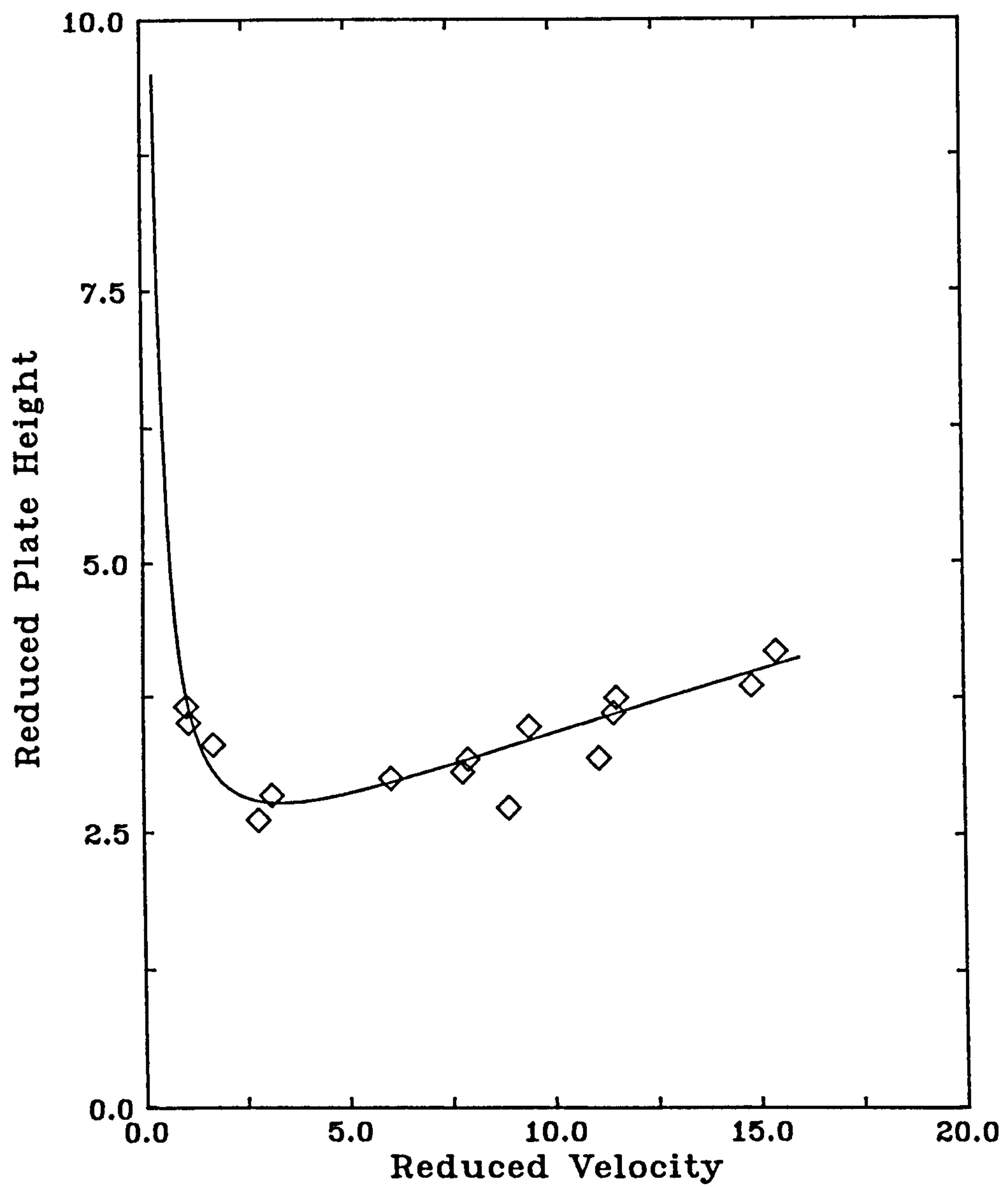




TABLE 6.2

Drawn Packed Capillary - Pressure Driven Mode.

Stationary Phase	Hypersil ( $d_p = 5\mu\text{m}$ )
Mobile Phase	70:30 $\text{CH}_3\text{CN}:\text{H}_2\text{O}$ (v/v)
Capillary i.d.	$= 40\mu\text{m}$
Total Length	$= 0.77\text{m}$
Length to Detection	$= 0.60\text{m}$

$\Delta P/\text{bar}$	$t_m/\text{s}$	$u/\text{mm.s}^{-1}$	$v$	$h$
30	557	1.08	5.38	2.17
40	409	1.46	7.32	2.55
40	388	1.55	7.73	2.76
40	381	1.57	7.86	2.62
60	269	2.23	11.16	2.57

Estimated value of  $\phi = 150$

The minimum separation impedance ( $h^2 \cdot \phi$ ) for these columns is approximately 700, which compares favourably with the value for conventional columns, the latter often being ca. 4500. The very low value of separation impedance for these capillaries suggests that high efficiency separations can be obtained with drawn capillaries faster than with conventional packed columns. Using a good conventional column, for which  $E_{\min}$  is 3500, 100,000 plates could be obtained, at optimal conditions, in 25 minutes with a pressure drop of 200bar, for  $\eta = 10^{-3} \text{ Nm}^{-2} \text{ s}$  and  $D_m = 10^{-9} \text{ m}^2 \text{ s}$ . With the drawn capillaries packed with  $5\mu\text{m}$  particles this efficiency could be achieved using the same pressure drop, even at a reduced velocity of greater than the optimum, in only 12 minutes<sup>a</sup>, assuming typical values of A, B and  $C_s$  in the plate height equation. The latter would require a capillary of 1.9m in length which would present no practical difficulties, since the drawn capillaries can be made to any desired length.

Table 6.3 shows the data obtained from a  $30\mu\text{m}$  i.d. drawn packed capillary packed with  $3\mu\text{m}$  diameter Hypersil. In this case the minimum reduced plates heights are approximately 2.0, which is significantly lower than for the  $5\mu\text{m}$  material. For these capillaries the estimated value of  $\phi$  was 110, which gives rise to a separation impedance of only 440. The column, from which the data in table 6.3 were obtained, exhibited plate numbers of up to 80,000. If a pressure drop of 200bar were used with an 84cm length of such a capillary, 100,000 plates would be obtained in only 6.5 minutes. To achieve this performance, in terms of number of plates per unit time, in open tubular chromatography, would require a

---

<sup>a</sup> Calculated using an iterative method, see Appendix III

capillary diameter of less than  $19\mu\text{m}$ , for the same  $D_m$  and  $\eta$ .

The relatively high performance of the drawn packed capillaries is illustrated by figure 6.2 which shows the separation of several polycyclic aromatic hydrocarbons on an ODS derivatised capillary packed with  $5\mu\text{m}$  Hypersil. The column was derivatised, after drawing, using the "in situ" derivatisation process outlined in the previous chapter. Using a 1.5m length of the capillary a plate number of ca. 80,000 was achieved.

FIGURE 6.2

**Separation of Polycyclic Aromatic Hydrocarbons in an  
'In-Situ' Derivatised Drawn Packed Capillary**

Eluent: Acetonitrile:Water 70:30 (v/v), Packing Material: Hypersil ( $d_p = 5\mu\text{m}$ ),  
Column Length = 1.5m,  $d_p = 5\mu\text{m}$ ,  $\Delta P = 150\text{bar}$ . Detection:  $\lambda_{\text{ex}} = 265\text{nm}$ ,  
 $\lambda_{\text{em}} = 330\text{nm}$  (for  $0 < t < 35\text{mins}$ )  $\lambda_{\text{ex}} = 238\text{nm}$ ,  $\lambda_{\text{em}} = 390\text{nm}$  (for  $t > 35\text{mins}$ ).  
 $N \approx 80,000$ .

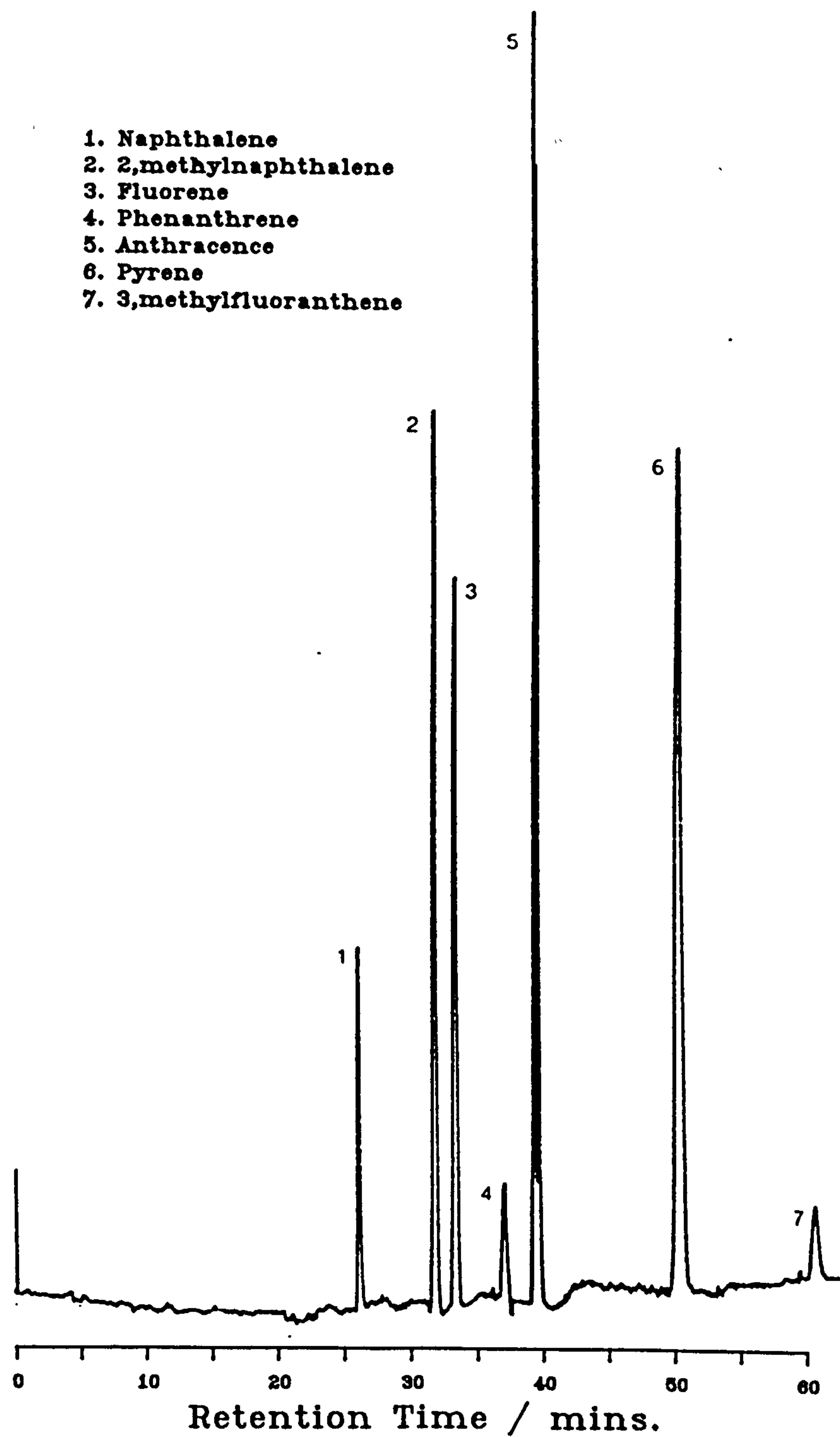




TABLE 6.3

Drawn Packed Capillary - Pressure Driven

Stationary Phase

Mobile Phase

Capillary i.d.

Total Length

Length to Detector

Hypersil ( $d_p = 3\mu\text{m}$ )

70:30  $\text{CH}_3\text{CN}:\text{H}_2\text{O}$  (v/v)

= 30 $\mu\text{m}$

= 0.65m

= 0.50m

$\Delta P/\text{bar}$	$t_m/\text{s}$	$u/\text{mm.s}^{-1}$	$v$	$h$
20	1381	0.36	1.09	3.03
25	1173	0.43	1.28	2.92
30	931	0.54	1.61	2.35
50	451	1.11	3.33	2.25
60	378	1.32	3.97	2.16
70	345	1.45	4.34	2.14
70	346	1.45	4.43	2.06
75	313	1.60	4.81	2.08
75	308	1.62	4.86	2.14
80	292	1.71	5.14	2.14
90	262	1.91	5.72	2.22
100	239	2.09	6.28	2.53
120	205	2.44	7.31	2.42

Estimated value of  $\phi = 110$   
( $\eta$  is taken to be  $0.6 \times 10^{-3} \text{Nm}^{-2}\text{s}$ )

### 6.2.2 Slurry Packed Capillaries

Experiments were carried out using capillaries ranging from 50 $\mu$ m to 200 $\mu$ m in internal diameter packed with 3 $\mu$ m and 5 $\mu$ m diameter particles. Tables 6.4 and 6.5 show the reduced plate heights measured for slurry packed capillaries packed with 5 $\mu$ m and 3 $\mu$ m diameter particles, respectively. In both cases the material is underivatized Hypersil (Shandon Ltd., U.K.).

The results obtained are typical of the data previously published on wider bore slurry packed capillaries<sup>78</sup>. The  $\phi$  values of 380 and 800 for the 5 $\mu$ m and 3 $\mu$ m diameter particles, respectively are, as expected, considerably greater than those of the drawn packed capillaries. This results in a longer analysis time for a given separation in cases where the pressure drop is limited. The chromatogram in figure 6.3 shows a separation similar to that shown in figure 6.2, but using a slurry packed capillary, and clearly demonstrates this point. The 200 $\mu$ m i.d. capillary was packed with ODS-Hypersil ( $d_p = 5\mu$ m). Both separations were carried out using the same mobile phase and approximately the same pressure drop. The slurry packed capillary shows a smaller plate number ( $N \approx 40,000$ ), and, in addition, requires a considerably longer analysis time, due to the higher  $\phi$  value.

TABLE 6.4

Slurry Packed Capillary - Pressure Driven Mode

Stationary Phase	Hypersil ( $d_p = 5\mu\text{m}$ )
Mobile Phase	70:30 $\text{CH}_3\text{CN}:\text{H}_2\text{O}$ (v/v)
Capillary i.d.	$= 75\mu\text{m}$
Total Length	$= 0.69\text{m}$
Length to Detector	$= 0.50\text{m}$

$\Delta P/\text{bar}$	$t_m/\text{s}$	$u/\text{mm.s}^{-1}$	$v$	$h$
60	590	0.85	4.24	2.52
70	461	1.09	5.43	2.99
100	310	1.61	8.06	3.03

The above data imply a value of 380 for  $\phi$ .

TABLE 6.5

Slurry Packed Capillary - Pressure Driven Mode.

Stationary Phase	Hypersil ( $d_p = 3\mu\text{m}$ )
Mobile Phase	70:30 $\text{CH}_3\text{CN}:\text{H}_2\text{O}$ (v/v)
Capillary i.d.	= $50\mu\text{m}$
Total Length	= 0.72m
Length to Detector	= 0.55m

$\Delta P/\text{bar}$	$t_m/\text{s}$	$u/\text{mm.s}^{-1}$	$v$	$h$
80	2598	0.21	0.64	5.20
100	1892	0.29	0.87	4.00
120	1671	0.33	0.99	3.94

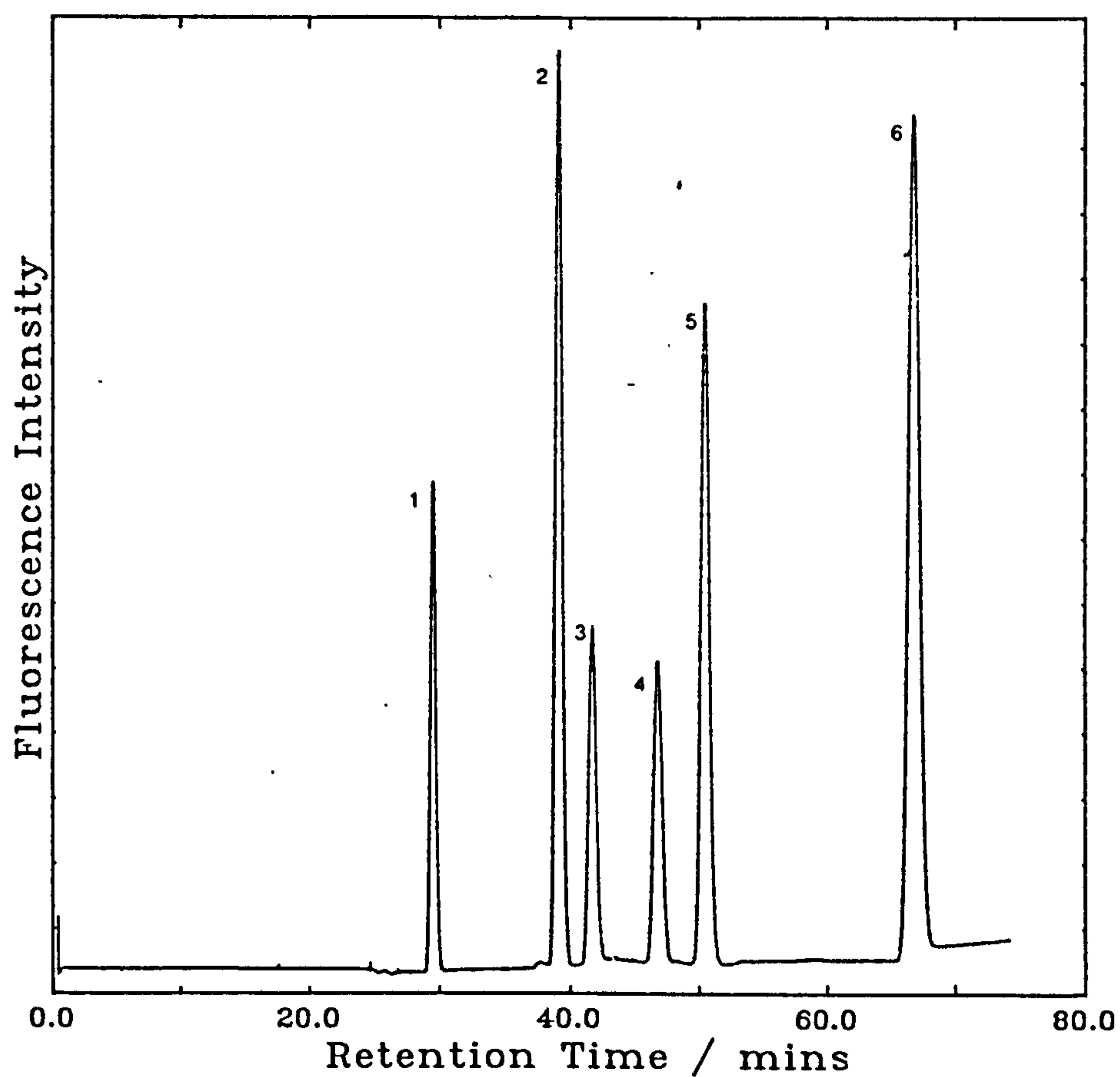
The above data imply a value of 800 for  $\phi$ .



FIGURE 6.3

**Separation of Polycyclic Aromatic Hydrocarbons in  
200 $\mu$ m i.d. Slurry Packed Capillary**

Eluent: Acetonitrile:Water 70:30 (v/v), Packing Material: ODS-Hypersil  
( $d_p = 5\mu\text{m}$ ) Column Length = 0.85m,  $d_p = 5\mu\text{m}$ ,  $\Delta P = 110\text{bar}$ . Detection:  
 $\lambda_{\text{ex}} = 265\text{nm}$ ,  $\lambda_{\text{em}} = 330\text{nm}$  (for  $0 < t < 45\text{mins}$ )  $\lambda_{\text{ex}} = 238\text{nm}$ ,  $\lambda_{\text{em}} = 390\text{nm}$  (for  
 $t > 45\text{mins}$ ).  $N \approx 40,000$ . Elution order as for figure 6.2.



### 6.3 Measurements in Electrochromatography

Measurements were carried out using both types of packed capillary columns. Packing materials with particle diameters ranging from 1.5 $\mu$ m to 50 $\mu$ m were used.

#### 6.3.1 Experimental Procedure

The general experimental procedure for carrying out electrochromatography was as follows. The capillary to be used was filled with the desired electrolyte under high pressure using a conventional pumping system. After connecting the capillary to the injection system, the latter was flooded with the chosen mobile phase. In order to establish whether or not electroosmotic flow was present a potential of 30kV was applied and the outlet of the capillary, which was immersed in the earthed electrolyte reservoir, was inspected. The presence of electroosmosis was confirmed by the observation of a noticeable schlieren effect resulting from the difference in refractive index between the electrolyte issuing from the end of the capillary and that contained in the reservoir.

In early experiments the flow was often observed to stop after some minutes accompanied by a drop in the measured current. Visual inspection of such capillaries revealed the presence of lighter, partially dried out areas of packing. Steps were therefore taken to ensure that the column was completely saturated with the mobile phase prior to connection. In the case of drawn packed capillaries a short length (ca. 1cm) of the capillary was removed from each end immediately before connection to the apparatus, in order to eliminate the

possibility of a dry section at each end as a result of evaporation. This procedure was only possible with the drawn capillaries since they require no retaining frit at the column ends. In the case of slurry packed capillaries the column ends were immersed in electrolyte after filling until the final connection to the injector was made. The mobile phase to be used was thoroughly degassed by ultrasonication before use. However, despite thorough degassing, electroosmotic flow could not be routinely obtained in slurry packed capillaries of greater than 75 $\mu$ m i.d., without the formation of dry areas leading to the breakdown of the flow. This was attributed to residual dissolved oxygen coming out of solution at the elevated temperatures in the capillary as a result of ohmic heating. This problem was not encountered to the same extent with the drawn packed capillaries due to the fact that the thicker glass walls are able to conduct the heat away from the liquid core, better than the thin walled fused silica capillaries used for slurry packed capillaries. Although this makes absolutely no difference to the radial temperature profile within the capillary, the absolute temperature would be expected to be lower in a thicker walled capillary. This argument obviously only applies to a situation like the one here where the capillary is not forcibly cooled.

The slurry packed capillaries used for electrochromatography were identical to those used in the previous section with one important difference. Because the force acting on the packing material acts in the opposite direction to that of the flow, it is only necessary to have a retaining frit at the inlet side of the capillary. Thus, the capillaries intended for use in electrochromatography were packed from the outlet side with the retaining frit at the end which would eventually become the inlet. The reason for this is that the formation of a second frit after



packing could not be carried out without leaving a small gap of ca.200 $\mu\text{m}$  between the top of the packing and the frit, which would result in the entire packed bed shifting down to fill the gap on the application of the electric field.

### 6.3.2 Plate Height Measurements

In most cases the plate heights in electrochromatography were determined from rising and falling fronts formed at the interface between the pure eluent and eluent containing dissolved fluorene. All tabulated data for unretained compounds on normal phase silica were obtained in this way.

#### 6.3.2.1 Drawn Packed Capillaries

Table 6.6 shows the reduced plate height and mobile phase linear velocities measured for a drawn packed capillary packed with 5 $\mu\text{m}$  diameter Hypersil for several values of the applied field. In this case an electrolyte of 90:10 (v/v) methanol:water containing sodium dihydrogenphosphate at a concentration of 0.002mol.dm<sup>-3</sup>, was used.

From a comparison of these data with those in table 6.1 it is clear that the column efficiencies obtained in the electrically driven case are vastly superior to those obtained from the conventional pressure driven system with the same type of capillary. Typical values of the minimum reduced plate height for such columns were approximately 1.4. However, as table 6.7 shows, some batches of drawn capillaries displayed even higher efficiencies. Table 6.7 shows that for a particular batch of such capillaries reduced plate heights as low as 0.7 could be achieved in the electrically driven system. This point is further illustrated by



figure 6.4 which shows a graph of plate height against reduced velocity for both the pressure driven and electrically driven cases. In both cases the mobile phase was 70:30 (v/v) acetonitrile:water and in the electrically driven case this contained sodium dihydrogenphosphate at concentrations of 2mM and 6mM.

Using a curve fitting program which was developed for this purpose on the BBC microcomputer, the  $A$ ,  $B$ , and  $C_s$  coefficients of the plate height equation,  $h = B/v + C_s v + A v^{1/3}$ , were estimated from both curves. The program is based on a least squares method and is listed in Appendix I. For the data in table 6.1, the pressure driven case, values of  $B=2.4$ ,  $C_s=0.01$  and  $A=1.43$  were calculated. If  $B$  and  $C_s$  are fixed at their typical values of 2 and  $0.1^{15}$  respectively, allowing only  $A$  to be optimised, the estimated value of  $A$  is 1.13.

If the same procedure is carried out for the data in table 6.7, i.e. the electrically driven case, the estimated values are  $B=2.8$ ,  $C_s=0.13$  and  $A=-0.21$ . If  $B$  and  $C_s$  are set at the same typical values, as before, a value of  $-0.07$  for  $A$  results. Although the value of  $A$  can obviously never be negative, these results do suggest that in the electrically driven case, the eddy diffusion term, for this particular batch of capillaries, is very close to zero.

The same effect on changing from pressure driven to electrically driven flow for the  $5\mu\text{m}$  diameter particles was also observed for  $30\mu\text{m}$  i.d. drawn packed capillaries packed with  $3\mu\text{m}$  diameter particles, i.e. the electrically driven capillaries show smaller plate heights than their pressure driven equivalents. For the  $3\mu\text{m}$  material in  $30\mu\text{m}$  i.d. drawn capillaries, a minimum reduced plate height of ca. 1.2 was observed, corresponding to a plate number of 140,000 from

a 50cm length of capillary. The data for the 3 $\mu$ m particles are tabulated in table 6.8.

The plate height verses linear velocity data for the drawn capillaries packed with 3 $\mu$ m and 5 $\mu$ m with both types of flow are summarised by figure 6.5

### 6.3.2.2 Slurry Packed Capillaries

Electrochromatographic efficiencies of slurry packed columns were measured only with fused silica capillaries having internal diameters of 50 $\mu$ m and 75 $\mu$ m. When larger bore capillaries were used it was not possible to maintain a stable electroosmotic flow due to the formation of dry patches within the packed bed (cf subsection 6.3.1). Table 6.9 shows typical plate height values for a capillary packed with 5 $\mu$ m diameter Hypersil. The reduced plate heights are similar to those obtained from typical batches of drawn packed capillaries with the same material, i.e.,  $h_{\min}$  of ca. 1.3. For the slurry packed capillaries packed with 3 $\mu$ m diameter Hypersil, as shown by table 6.10, the minimum reduced plate height was about 2.3, which, although larger than with the drawn capillaries, is considerably smaller than the values obtained with pressure driven slurry packed capillaries with the same particle diameter (cf. table 6.4).

TABLE 6.6

Drawn Packed Capillary 40μm i.d. Electrically Driven Mode.

Stationary Phase - Hypersil ( $d_p = 5\mu\text{m}$ )  
Mobile Phase - 90% methanol in water (by volume).  
Electrolyte - 2mM  $\text{NaH}_2\text{PO}_4$   
Total Length 70cm (length to detection zone = 52cm)

$\Delta V/\text{kV}$	$E/\text{kVm}^{-1}$	$t_m/\text{s}$	$u/\text{mm.s}^{-1}$	$v$	$h$
10	14.3	3388	0.16	0.78	2.13
15	21.4	2055	0.25	1.26	1.70
20	28.6	1426	0.36	1.82	1.44
25	35.7	1082	0.48	2.40	2.13
30	42.9	854	0.61	3.04	1.70
30	42.9	838	0.62	3.10	1.38
30	42.9	835	0.63	3.11	1.39
30	42.9	826	0.63	3.15	1.92
35	50.0	695	0.75	3.74	2.07
40	57.1	568	0.92	4.58	1.86
45	64.3	482	1.08	5.39	2.07
50	71.4	411	1.26	6.32	2.34
55	78.6	366	1.42	7.11	2.45

These data are consistant with a  $(\gamma\zeta)$  of 32mV,  
assuming  $\epsilon_r = 40$  and  $\eta = 0.75 \times 10^{-3} \text{Nm}^{-2}\text{s}$ .  
Estimated  $\kappa a = 240$ .

TABLE 6.7

**Drawn Packed Capillary 40 $\mu$ m i.d. Electrically Driven Mode.**

Batch with a particularly high efficiency.  
Electrically Driven Mode.

Stationary Phase - Hypersil ( $d_p = 5\mu\text{m}$ )  
Mobile Phase - 70% acetonitrile in water (by volume).  
Electrolyte - 2mM  $\text{NaH}_2\text{PO}_4$   
Total Length 77cm (length to detection zone = 60cm)

$\Delta V/\text{kV}$	$E/\text{kVm}^{-1}$	$u/\text{mm.s}^{-1}$	$v$	$h$
25	32.5	0.72	3.62	1.32
30	39.0	0.87	4.36	0.94
30	39.0	0.88	4.39	0.77
30	39.0	0.89	4.47	0.77
35	45.5	1.07	5.35	0.83
40	52.0	1.37	6.84	0.93
45	58.4	1.60	7.98	0.92
50	64.9	1.87	9.37	1.45

Electrolyte - 6mM  $\text{NaH}_2\text{PO}_4$   
Total Length 70cm (length to detection zone = 52cm)

20	28.6	0.42	2.11	1.27
25	35.7	0.61	3.06	0.98
25	35.7	0.70	3.48	0.93
30	42.9	0.72	3.59	0.80
30	42.9	0.76	3.82	0.77
30	42.9	0.78	3.89	0.82
35	50.0	0.83	4.17	0.73
40	57.0	1.03	5.13	0.71



TABLE 6.8

Drawn Packed Capillary 30 $\mu$ m i.d. Electrically Driven Mode.

Stationary Phase - Hypersil ( $d_p = 3\mu$ m)  
 Mobile Phase - 70% acetonitrile in water (by volume).  
 Electrolyte - 2mM NaH<sub>2</sub>PO<sub>4</sub>  
 Total Length 65cm (length to detection zone = 50cm)

$\Delta V/\text{kV}$	$E/\text{kVm}^{-1}$	$t_m/\text{s}$	$u/\text{mm.s}^{-1}$	$v$	$h$
15	23.1	1204	0.42	1.25	2.22
20	30.8	843	0.59	1.78	1.71
25	38.5	644	0.78	2.33	1.53
30	46.2	539	0.93	2.78	1.47
30	46.2	525	0.94	2.83	1.33
30	46.2	526	0.95	2.86	1.65
30	46.2	520	0.96	2.89	1.58
30	46.2	516	0.97	2.91	2.03
35	53.8	441	1.13	3.40	2.06
35	53.8	443	1.13	3.39	1.91
40	61.5	335	1.49	4.47	1.63
40	61.5	375	1.33	4.00	1.57
40	61.5	350	1.43	4.28	2.12
40	61.5	343	1.45	4.36	2.03
45	69.2	275	1.82	5.45	2.20
50	76.9	249	2.01	6.03	2.18
55	84.6	219	2.28	6.84	2.44
58	89.2	199	2.52	7.55	2.67

These data imply a  $\gamma\zeta$  of 33mV.  
 ( $\epsilon_r = 43, \eta = 0.6 \times 10^{-3} \text{Nm}^{-2}\text{s}$ )  
 Estimated  $\kappa a = 170$ .

Electrolyte - 6mM NaH<sub>2</sub>PO<sub>4</sub>

15	23.1	1368	0.37	1.11	2.32
20	30.8	901	0.56	1.67	1.67
30	46.2	598	0.84	2.51	1.19
30	46.2	591	0.84	2.54	1.22
35	53.8	485	1.03	3.10	1.29
40	61.5	383	1.30	3.91	1.37
45	69.2	305	1.64	4.92	1.71
50	76.9	269	1.86	5.58	1.51
55	84.6	236	2.12	6.36	1.49

TABLE 6.9

Slurry Packed Capillary 75µm i.d. Electrically Driven Mode.

Stationary Phase - Hypersil ( $d_p = 5\mu\text{m}$ )  
Mobile Phase - 70% acetonitrile in water (by volume).  
Electrolyte - 2mM  $\text{NaH}_2\text{PO}_4$   
Total Length 65cm (length to detection zone = 50cm)

$\Delta V/\text{kV}$	$E/\text{kVm}^{-1}$	$t_m/\text{s}$	$u/\text{mm.s}^{-1}$	$v$	$h$
10	15.4	2316	0.22	1.08	1.91
15	23.1	1374	0.36	1.82	1.17
20	30.8	954	0.52	2.61	1.20
25	38.5	742	0.67	3.37	1.23
30	46.2	572	0.87	4.37	1.76
30	46.2	548	0.91	4.56	1.65
35	53.8	453	1.10	5.52	1.58
40	61.5	353	1.42	7.09	1.87
50	76.9	303	1.66	8.28	3.09

Data imply a  $\gamma\zeta$  of 32mV.  
Estimated  $\kappa a = 140$ .

TABLE 6.10

**Slurry Packed Capillary 50 $\mu$ m i.d. Electrically Driven Mode.**Stationary Phase - Hypersil ( $d_p = 3\mu\text{m}$ )

Mobile Phase - 70% acetonitrile in water (by volume).

Electrolyte - 6mM  $\text{NaH}_2\text{PO}_4$ 

Total Length 72cm (length to detection zone = 55cm)

$\Delta V/\text{kV}$	$E/\text{kVm}^{-1}$	$t_m/\text{s}$	$u/\text{mm.s}^{-1}$	$v$	$h$
30	41.7	1659	0.33	0.99	2.40
30	41.7	1620	0.34	1.02	2.77
35	48.6	1500	0.37	1.10	2.74
35	48.6	1405	0.39	1.17	2.23
40	55.6	1163	0.47	1.42	2.39
45	62.5	1030	0.53	1.60	2.24
50	69.4	945	0.58	1.75	3.12
50	69.4	906	0.61	1.82	2.58
60	83.3	742	0.74	2.22	2.90
60	83.3	671	0.82	2.46	3.19

Data imply a  $\gamma\zeta$  of 12mV.Estimated  $\kappa a = 104$ .Total Length 74cm, 75 $\mu$ m i.d. (Length to detection zone = 57cm)Electrolyte 2mM  $\text{NaH}_2\text{PO}_4$ 

30	40.5	1182	0.48
35	37.5	974	0.52
40	54.1	826	0.69

Data imply a  $\gamma\zeta$  of 19mV.Estimated  $\kappa a = 60$ .

FIGURE 6.4

Comparison of  $h$  versus  $v$  Plots for  $5\mu\text{m}$  Diameter Particles in Drawn Packed Capillaries for Pressure and Electrically Driven Flow

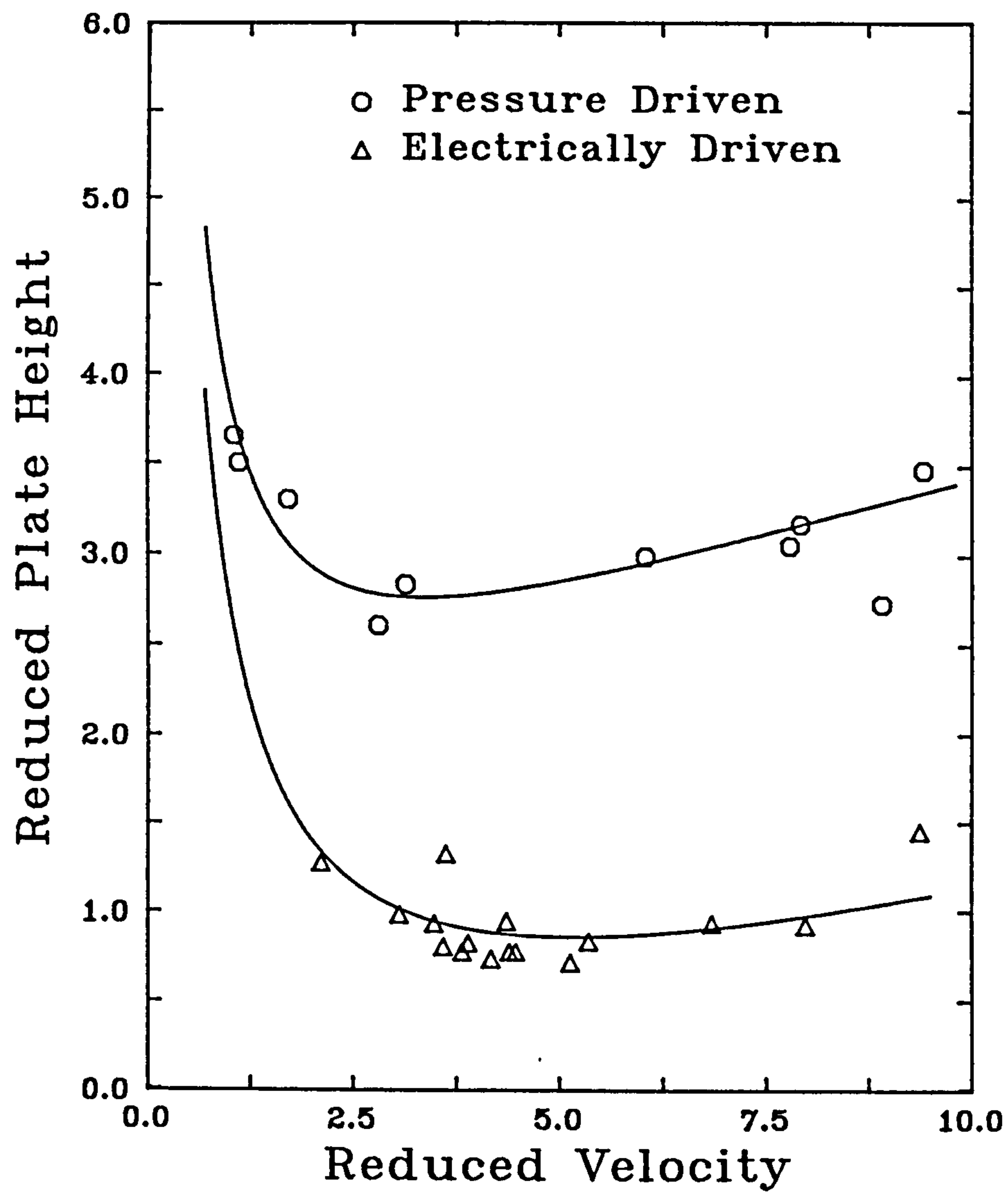
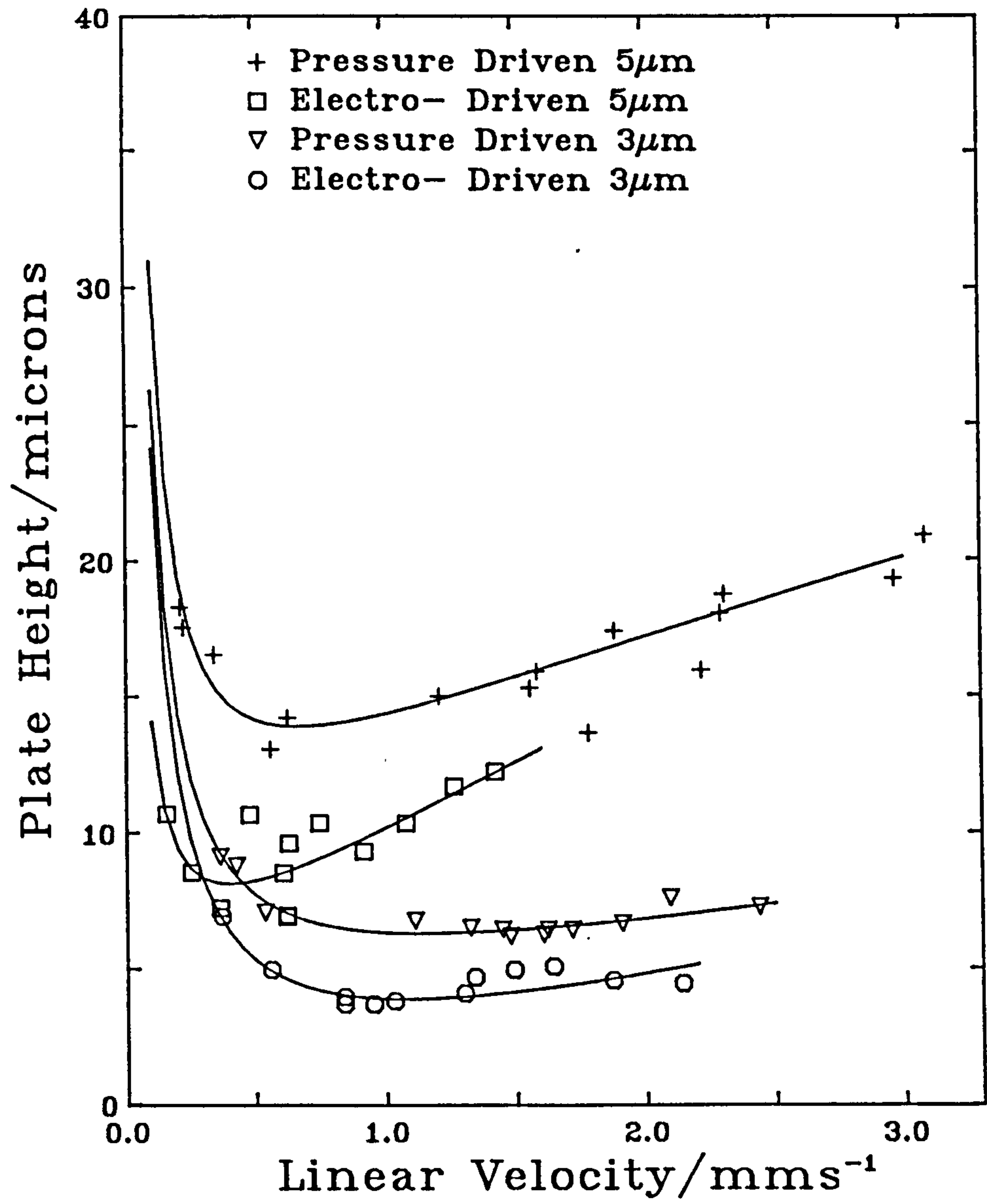




FIGURE 6.5

Summary of H verses u Data for Drawn Packed Capillaries  
Packed with 3 $\mu$ m and 5 $\mu$ m Diameter Particles

For each particle diameter the results obtained using both electroosmotic flow and pressure driven flow are shown. Data for 5 $\mu$ m particles are taken from tables 6.1 and 6.6, and for 3 $\mu$ m particles from tables 6.3 and 6.8.



### 6.3.3 Separations by Electrochromatography

Figure 6.6 shows the electrochromatographic separation of several polycyclic aromatic hydrocarbons on an ODS-derivatised drawn packed capillary (40 $\mu$ m i.d.) packed with 5 $\mu$ m diameter particles. The capillary was derivatised according to the procedure outlined in section 5.2. The separation of a similar mixture on the same type of capillary, but with pressure driven flow, is shown, for comparison, in figure 6.7. The electrochromatogram, which was obtained with a 50cm length of capillary, shows an efficiency of between 80,000 and 100,000 theoretical plates, corresponding to a reduced plate height of between 1.00 and 1.25.

The pressure driven chromatogram in figure 6.7 was obtained from a 60cm length of capillary, which with an efficiency of 47,000, despite being slightly longer, exhibits less than half the number of theoretical plates.

Figure 6.8 shows an overlay of the third peaks, fluorene, from typical separations of the same mixture, in electrochromatography and pressure driven chromatography, with the time axis expanded. The data were taken from two runs, on the same capillary, with similar linear velocities. The time scale for the pressure driven case, for which the linear velocity was slightly smaller, was multiplied by the ratio of retention times, making the peak appear narrower, in order to compensate for the slight difference in retention times. This procedure effectively converts the time axis to a length (along the migration path) axis, allowing the actual peak widths within the column to be compared. The reduced plate heights for the pressure driven and electrically driven peaks are 1.6 and 2.7

respectively. As can be seen from the graph, the signal from the electrochromatographic separation lies completely within that from the pressure driven case. This result clearly indicates that in electrochromatography, the flow term in the plate height equation has a much smaller contribution to the overall plate height than in normal pressure driven LC.

In addition, the traces shown in figure 6.8 show that in both cases symmetrical Gaussian shaped peaks are obtained. This demonstrates that, as a result of the 'on-column' detection and injection procedures, the effect of extra column disturbances is negligible. This point is further illustrated by figure 6.9 which shows a typical electrochromatogram together with the first derivative, with respect to time, of the fluorescence signal. The fact that for all peaks, with the exception of the last, which is slightly fronted due to a non-linear partition isotherm, the derivative signal deflects above and below the zero value to the same extent, suggests a high degree of peak symmetry.

Figures 6.10 and 6.11 show the separations of aromatic hydrocarbons on an 'in-situ' ODS derivatised capillary packed with 3 $\mu$ m diameter Hypersil, with pressure and electrically driven flow respectively. In this case, in contrast to the situation with 5 $\mu$ m particles, the reduced plate heights for both types of flow induction show no significant difference. In both cases the reduced plate height was determined to be ca. 3.3.

FIGURE 6.6

Separation of Polycyclic Aromatic Hydrocarbons on an ODS-Derivatised  
Drawn Packed Capillary by Electrochromatography

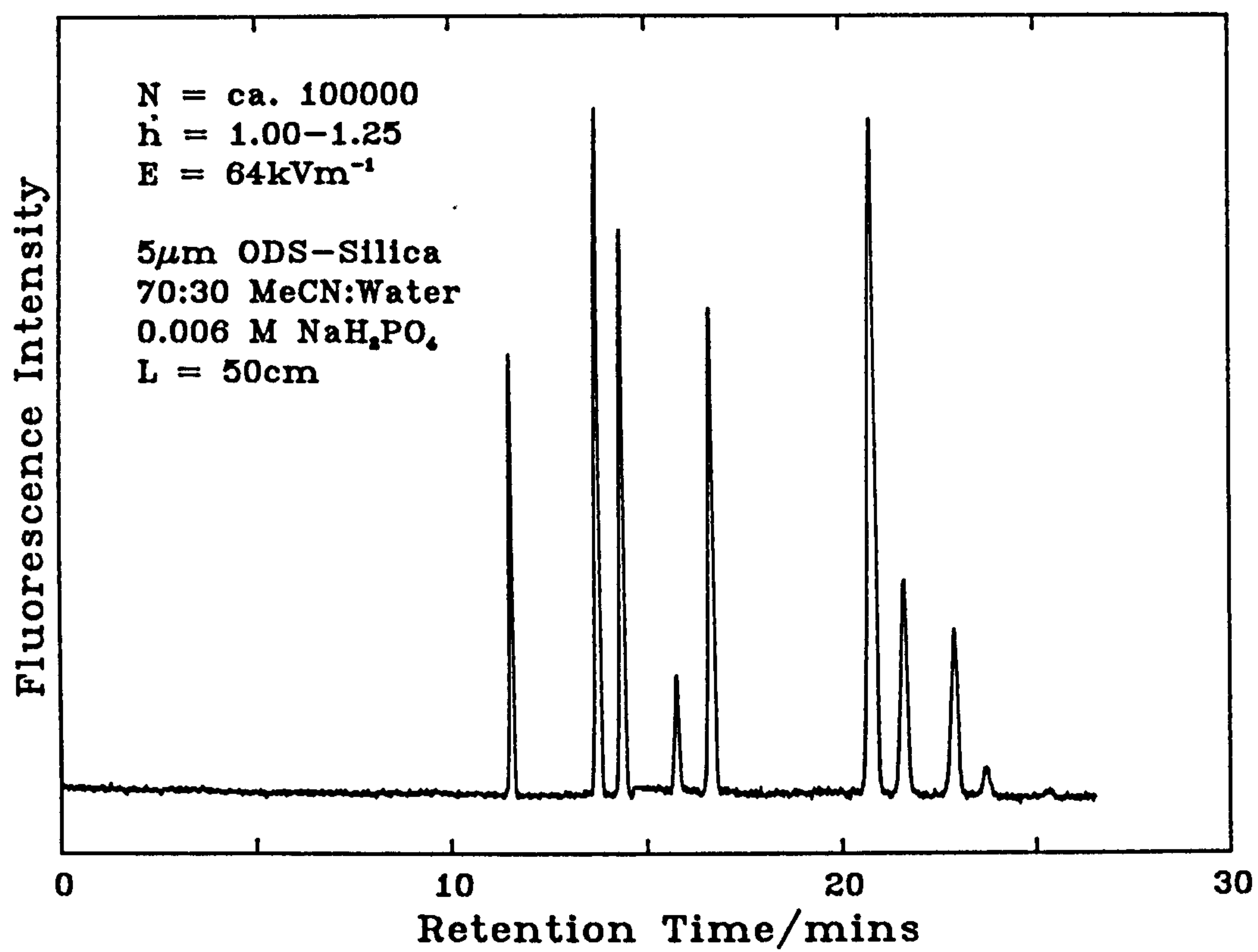




FIGURE 6.7

Separation of Polycyclic Aromatic Hydrocarbons on an ODS-Derivatised Drawn Packed Capillary by Pressure Driven Chromatography

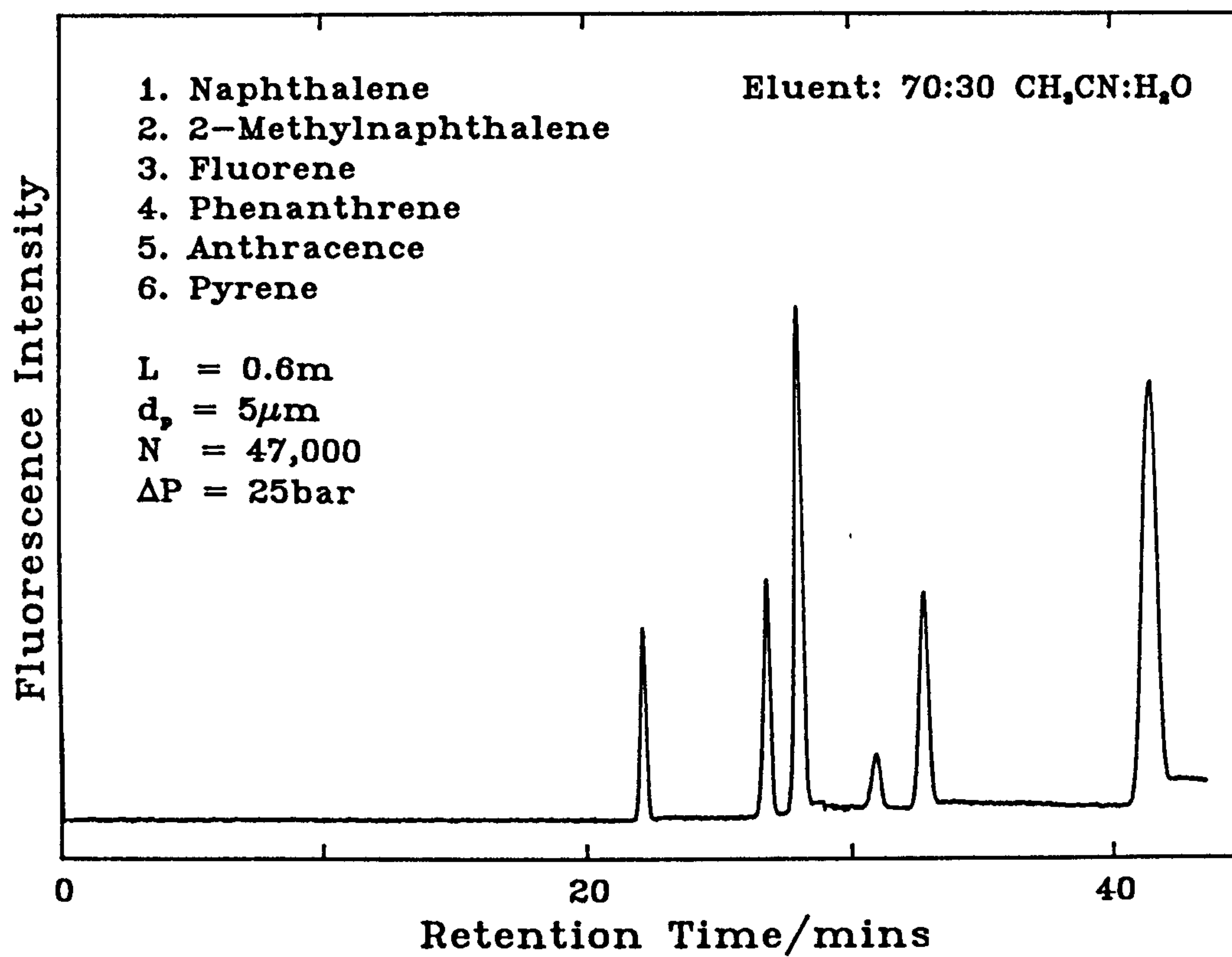


FIGURE 6.8

### Overlay of Fluorene Peaks from Electrochromatography and Pressure Driven Chromatography

The graph shows the peaks obtained for fluorene in the *same* capillary column using both methods of flow induction. Column Length=0.60m (Total Length=0.78m),  $d_p = 5\mu\text{m}$ ,  $d_c = 40\mu\text{m}$ .

A. Pressure Driven:  $\Delta P = 25\text{bar}$ ,  $t_r = 28\text{mins}$ ,  $\sigma^2 = 8.1\text{mm}^2$ ,  $h = 2.7$

B. Electrochromatography:  $E = 38.5\text{kVm}^{-1}$ ,  $t_r = 26\text{mins}$ ,  $\sigma^2 = 4.8\text{mm}^2$ ,  $h = 1.6$

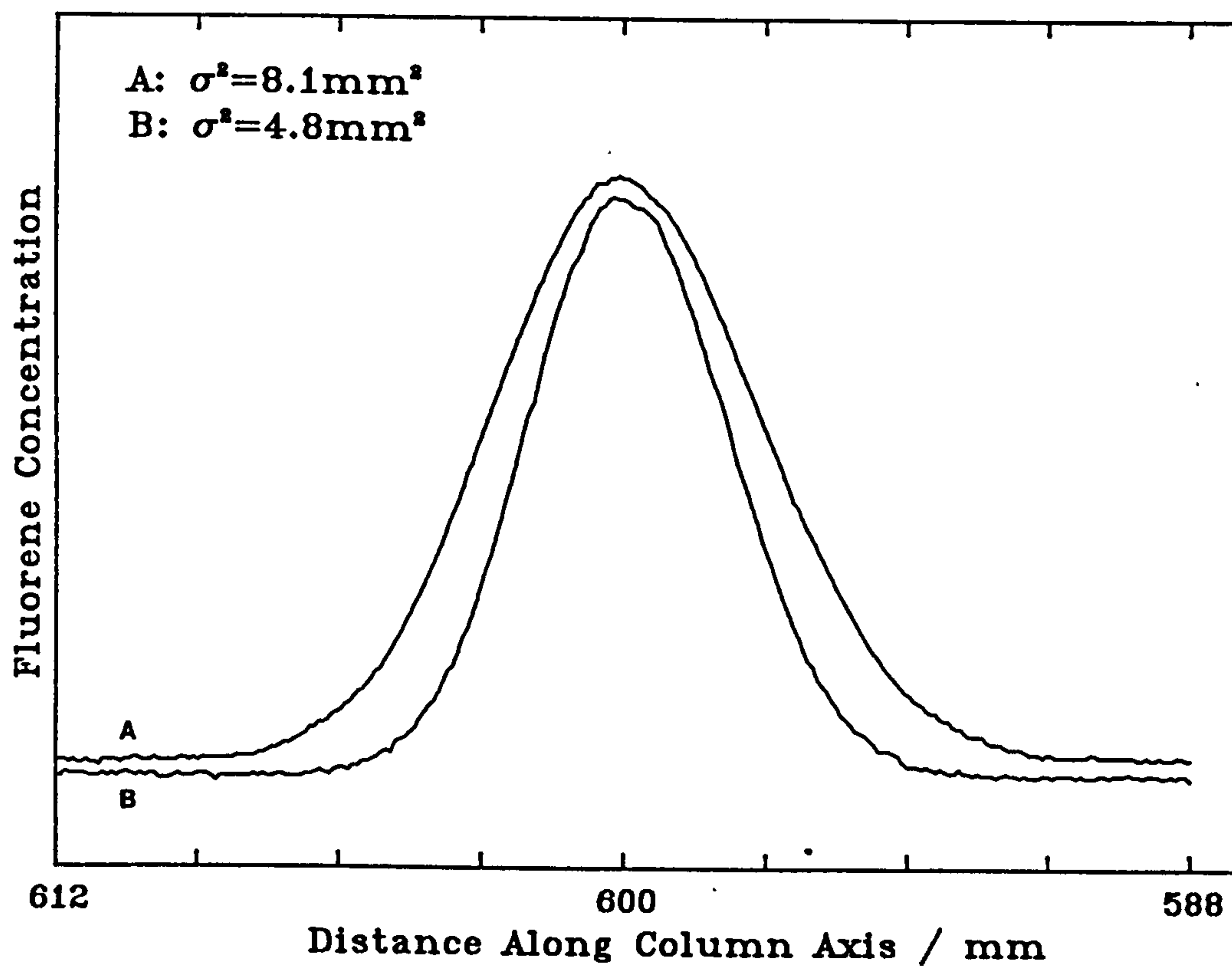


FIGURE 6.9

Electrochromatogram together with the First Derivative of the Fluorescence Signal with Respect to Time

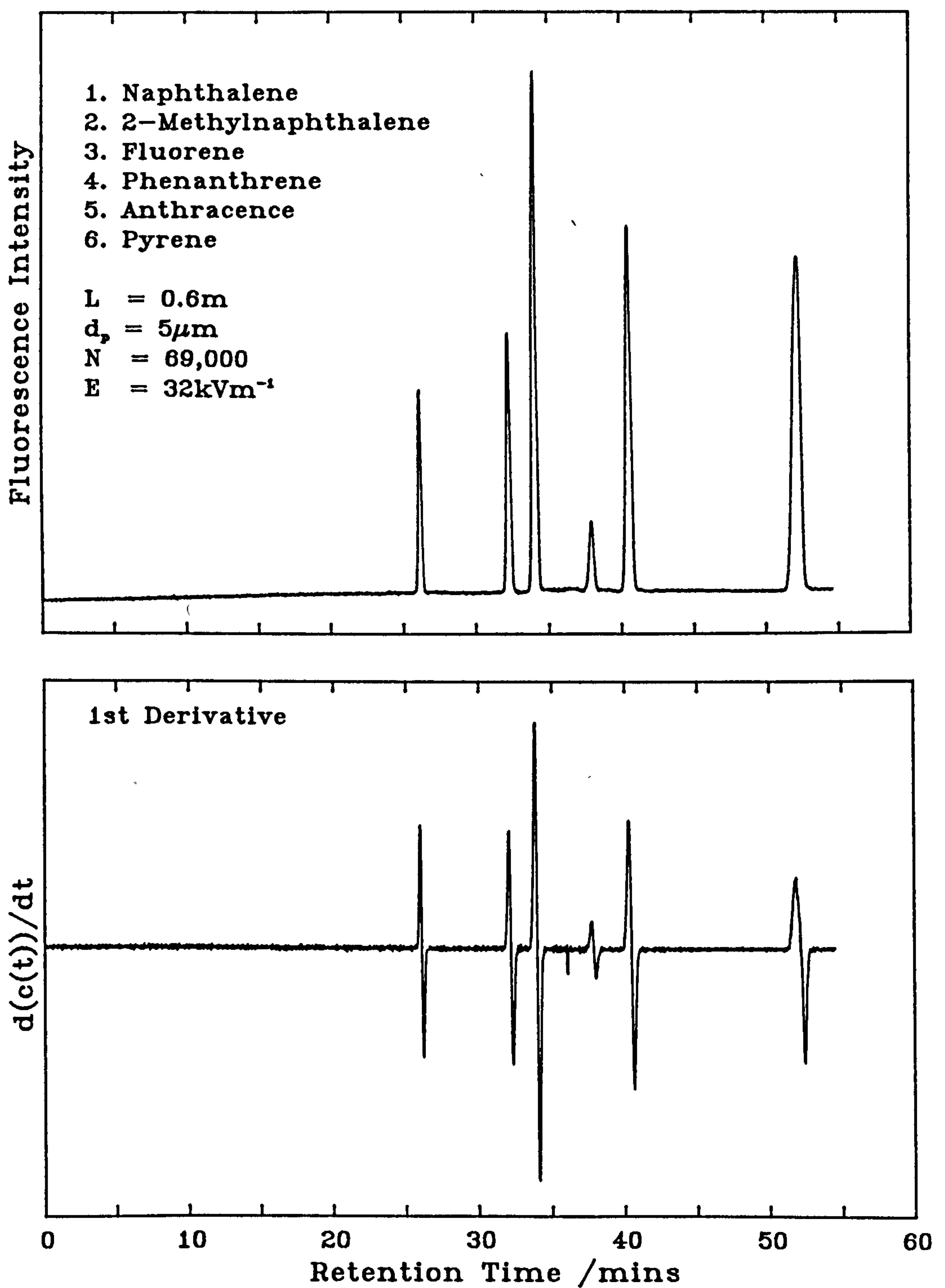


FIGURE 6.10

Pressure Driven Separation on an ODS-Derivatised  
Drawn Packed Capillary ( $d_p = 3\mu\text{m}$ )

Column Length = 0.90m,  $d_p = 3\mu\text{m}$ ,  $d_c = 30\mu\text{m}$ . Mobile Phase - MeCN:Water  
70:30(v/v),  $N \simeq 100,000$ ,  $h = 3.29$

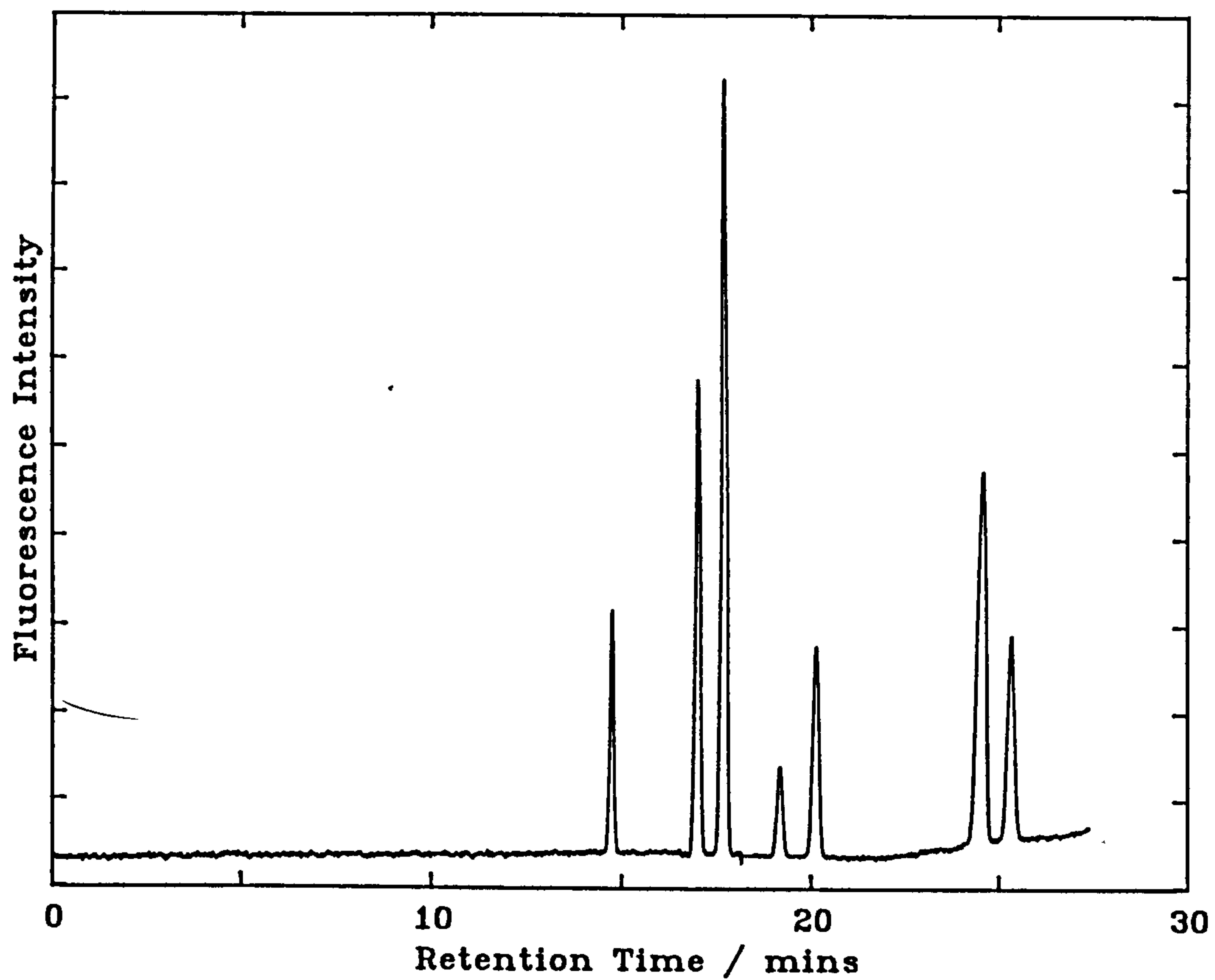
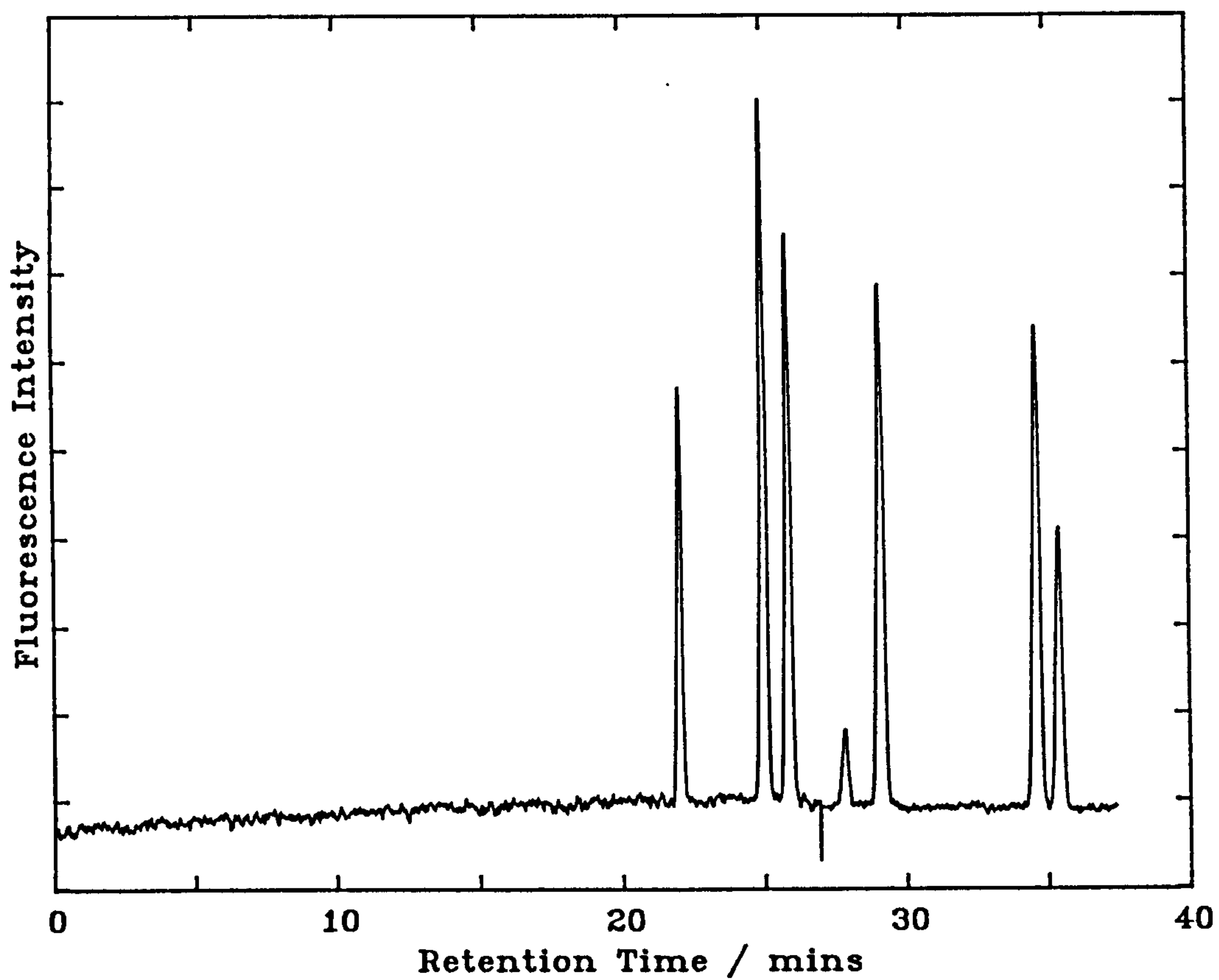




FIGURE 6.11

Electrochromatographic Separation on an ODS-Derivatised  
Drawn Packed Capillary ( $d_p = 3\mu\text{m}$ )

Column Length = 0.80m,  $d_p = 3\mu\text{m}$ ,  $d_c = 30\mu\text{m}$ . Mobile Phase - MeCN:Water  
70:30(v/v),  $N \approx 80,000$ ,  $h = 3.33$



### 6.3.4 Effect of Particle Size on Electroosmosis

A very important aspect of this work has been the elucidation of the effect of the particle diameter on the electroosmotic flow velocity. The data obtained for both types of capillaries packed 5 $\mu\text{m}$  particles, and for a drawn packed capillary packed with 3 $\mu\text{m}$  diameter particles are plotted in the form of linear velocity against the applied field in figure 6.12. For the measurements shown in the graph, the eluent composition was held constant at 70% acetonitrile and the salt concentration at  $2 \times 10^{-3} \text{ mol.dm}^{-3}$  sodium dihydrogen phosphate. From equation 3.11 the reciprocal double layer thickness  $\kappa$  can be calculated, for this ionic concentration, to be  $1.99 \times 10^8 \text{ m}^{-1}$ . In accordance with equation 3.29 the mean  $\kappa a$  value for a packed bed of 5 $\mu\text{m}$  diameter particles, where  $\phi = 380$  (slurry packed capillary), can be estimated to be ca. 145. Similarly for 5 $\mu\text{m}$  diameter particles where  $\phi = 150$  (drawn packed capillary),  $\kappa a$  is approximately 230.

From the graph in figure 6.12 there is no indication of a connection between the particle diameter or packing method and the velocity of electroosmotic flow and certainly nothing to indicate a trend towards lower velocities for smaller particles, despite the range of  $\kappa a$  values. This is not entirely unexpected, for the graph in figure 3.6 indicates that a significant loss of electroosmotic flow velocity will not be encountered unless the value of  $\kappa a$  falls below 10.

Linear velocity measurements were also taken from drawn packed capillaries packed with relatively large particles of 20 $\mu\text{m}$  (Lichrosphere, Merck GmbH, Germany.) and 50 $\mu\text{m}$  (Yamamura 40/60, Yamamura, Japan) diameter. The observed velocities and plate heights are tabulated in tables 6.11 and 6.12. These

data show no increase in flow velocity, for a given field strength, for capillaries packed with the larger particles. For the columns packed with 50 $\mu$ m diameter particles, the mean  $\kappa a$  value for the same electrolyte was estimated to be 3000

FIGURE 6.12

### Linear Velocity as a Function of Applied Field ( $d_p = 3\mu\text{m}$ and $5\mu\text{m}$ )

The graph below shows the linear velocity as a function of applied electric field for slurry packed and drawn packed capillaries packed with  $5\mu\text{m}$  diameter particles, and a drawn capillary with  $3\mu\text{m}$  particles. Mobile Phase: MeCN:Water 70:30(v/v)  $2 \times 10^{-3} \text{ mol dm}^{-3} \text{ NaH}_2\text{PO}_4$ .

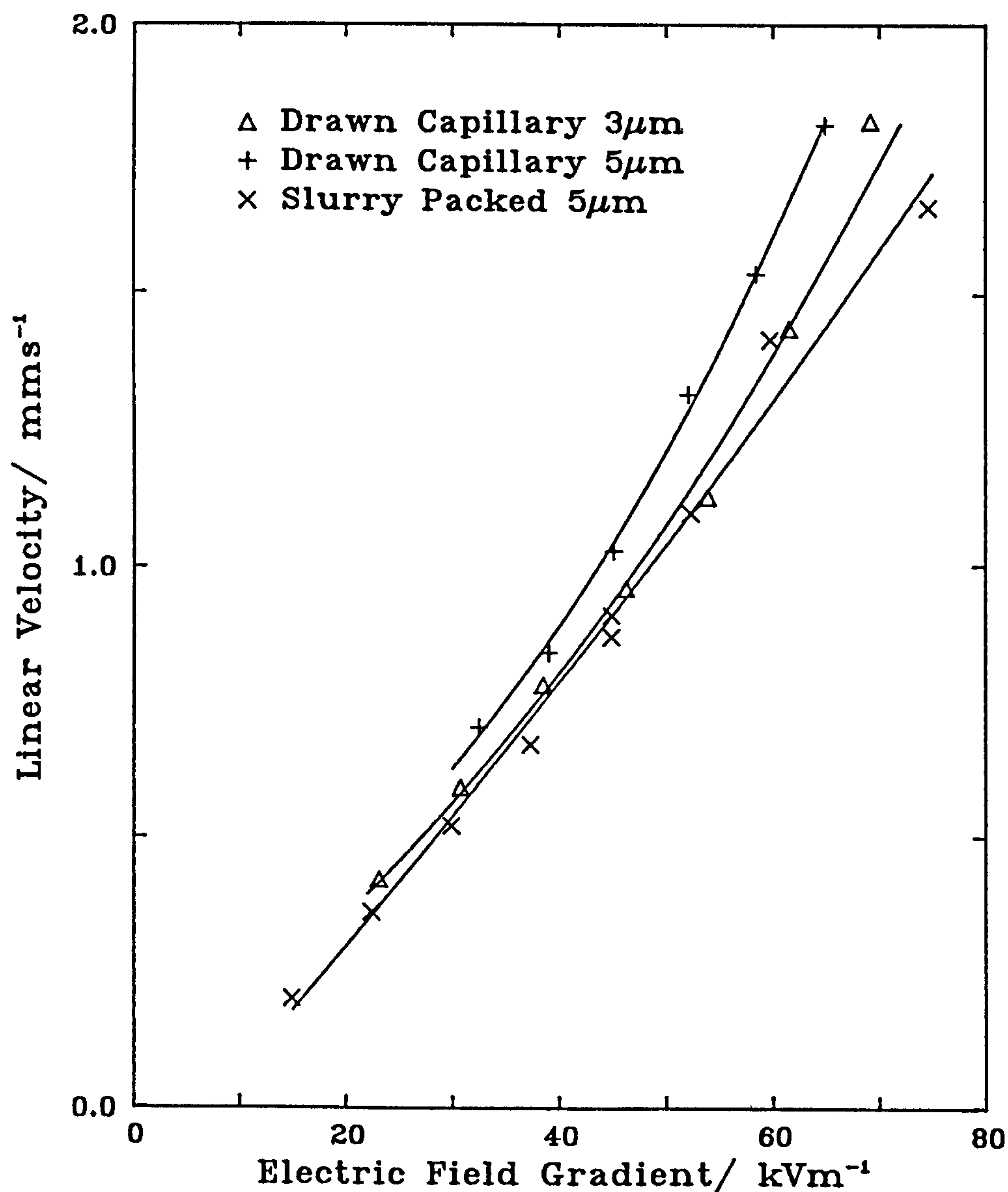




TABLE 6.11

**Drawn Packed Capillary 100μm i.d. Electrically Driven Mode.**

Stationary Phase - Lichrosphere ( $d_p = 20\mu\text{m}$ )  
Mobile Phase - 70% acetonitrile in water (by volume).  
Electrolyte - 2mM  $\text{NaH}_2\text{PO}_4$   
Total Length 68cm (length to detection zone = 50cm)

$\Delta V/\text{kV}$	$E/\text{kVm}^{-1}$	$t_m/\text{s}$	$u/\text{mm.s}^{-1}$	$v$	$h$
20	29.4	1637	0.31	6.11	1.21
25	36.8	1131	0.40	8.84	1.62
30	44.1	1059	0.47	9.44	1.61
40	58.9	731	0.68	13.7	2.10
45	66.2	683	0.73	14.6	4.20

Estimated value for  $\gamma\zeta = 12\text{mV}$ .

TABLE 6.12

Drawn Packed Capillary 200μm i.d. Electrically Driven Mode.

Stationary Phase - Yamamura 40/60 ( $d_p = 50\mu\text{m}$ )  
Mobile Phase - 70% acetonitrile in water (by volume).  
Electrolyte - 2mM  $\text{NaH}_2\text{PO}_4$   
Total Length 108cm (length to detection zone = 90cm)

$\Delta V/\text{kV}$	$E/\text{kVm}^{-1}$	$t_m/\text{s}$	$u/\text{mm.s}^{-1}$	$v$	$h$
25	23.2	3341	0.27	13.5	1.40
30	27.8	2554	0.35	17.6	1.56
30	27.7	2459	0.37	18.3	2.13
30	27.8	2436	0.37	18.5	1.43
35	29.6	2128	0.42	21.4	1.62
40	37.0	1774	0.51	25.4	2.13

Estimated value for  $\gamma\zeta = 16\text{mV}$ .

### 6.3.5 Results for 1.5 $\mu$ m Diameter Particles

The results described above suggested that adequate electroosmotic flow rates could still be obtained with even smaller particles. The smallest particles presently available are 1.5 $\mu$ m diameter Monospher particles (Merck GmbH, Mainz, Germany). The production of drawn packed capillaries with such particles is precluded by the need for the inner diameter to be no greater than ten particle diameters. This would have required the drawing of capillaries down to 15 $\mu$ m internal diameter or less. However, it was possible to produce columns with this material using the slurry packing method.

Table 6.12 shows the plate heights and linear velocities measured for various values of applied field for a 50 $\mu$ m ID capillary packed with Monospher 1.5 $\mu$ m. If these data are added to figure 6.12 it is quite evident, as can be seen from figure 6.13, that no reduction in electroosmotic flow velocity is observed even for particles as small as 1.5 $\mu$ m. In fact the measured velocity for this material is greater than for all other materials tested, which probably reflects more the fact that the material is non porous resulting in the velocity measured being  $u_0$  and not  $u$ , i.e.  $\gamma$  closer to unity, than any particle size dependence. Figure 6.13 also includes the data obtained from capillaries packed with the 20 $\mu$ m and 50 $\mu$ m particles.

Figure 6.14 shows, that in addition to high linear velocities, the very low values of reduced plate heights obtained for 3 $\mu$ m and 5 $\mu$ m material were also obtained for the 1.5 $\mu$ m materials. Reduced plate heights as low as 1.33 were obtained, which corresponds to an absolute plate height of only 2 $\mu$ m. This result is most

significant since since publications involving the use of very small particles, in pressure driven experiments, have not yet demonstrated the chromatographic performance expected for particles smaller than  $3\mu\text{m}$  in diameter. The plate heights quoted were measured using the frontal method (cf 5.4). Figures 6.15 and 6.16 show the signal from a typical experimental run with this material for both a rising and a falling front. From these the symmetry of the rising and falling fronts is readily apparent, which rules out the possibility of self sharpening fronts giving rise to deceptively high plate numbers. After a migration distance of 620mm, front standard deviations of 1.25mm and 1.24mm were measured for the rising and the falling front respectively, corresponding to plate numbers of 246,000 and 250,000. Both runs were carried out at the same linear velocity, of  $1.1\text{mm.s}^{-1}$  induced by a field of  $56\text{kVm}^{-1}$ .

The low values of reduced plate height mean that astonishingly large numbers of theoretical plates can be obtained, and as table 6.12 implies, plate numbers in excess of 300,000 were obtained from a 620mm column within five minutes. Unfortunately, it was not possible to obtain comparison data for the  $1.5\mu\text{m}$  material with pressure driven flow because of the very high pressures which would have been required. A single run was carried out at a pressure gradient of  $190\text{bar.m}^{-1}$  resulting in a linear velocity of  $0.017\text{mm.s}^{-1}$ , corresponding to a reduced velocity of only 0.025, and a reduced plate height of 13. This indicates a  $\phi$  value of approximately 700. This result is of great significance in the assessment of electroosmosis as an alternative to pressure driven flow, for this result alone, demonstrates the ease with which adequate linear velocities can be achieved in a chromatographic bed, which is effectively impermeable to pressure driven flow.



The realisation, in a chromatographic system, of 300,000 theoretical plates, in five minutes approaches even the performance of capillary GC and CZE, and could not be obtained with pressure driven flow. Working at optimum conditions, pressure driven LC, limited to 200bar with  $\phi = 500$ , could only produce 300,000 plates in approximately 3 hours 45 minutes, which would require a 5m length of column packed with  $7\mu\text{m}$  particles. The more efficient drawn packed capillaries would still require an unretained elution time of 45 minutes<sup>a</sup> for the same plate number. In fact, to obtain this plate number with pressure, in the same time, using  $1.5\mu\text{m}$  particles, assuming they could be adequately well packed, would require a pressure drop of  $1.5 \times 10^9$  bar ( $2.2 \times 10^{10} \text{ lb.in}^{-2}$ ), which is clearly unrealistic.

The estimated mean  $\kappa a$  value of this system is slightly over 30, which suggests that, with the same electrolyte concentration, the particle diameter can be reduced still further without loss of flow.

---

<sup>a</sup>  $d_p = 3\mu\text{m}$  and  $\phi = 110$ , see Appendix III

TABLE 6.13

Slurry Packed Capillary 50 $\mu$ m i.d. Electrically Driven Mode.

Stationary Phase - Merck monospher ( $d_p = 1.5\mu\text{m}$ )  
 Mobile Phase - 70% acetonitrile in water (by volume).  
 Electrolyte - 2mM  $\text{NaH}_2\text{PO}_4$   
 Total Length 80cm (length to detection zone = 62cm)

$\Delta V/\text{kV}$	$E/\text{kVm}^{-1}$	$t_m/\text{s}$	$u/\text{mm.s}^{-1}$	$v$	$h$
30	37.5	632	0.98	1.47	1.61
40	50.0	472	1.31	1.97	1.49
45	56.3	403	1.54	2.31	1.43
50	62.5	356	1.74	2.61	1.49
60	75.0	301	2.06	3.09	1.33

Electrolyte - 6mM  $\text{NaH}_2\text{PO}_4$

20	25.0	1251	0.49	0.74	2.87
25	31.3	857	0.73	1.09	2.25
30	37.5	772	0.80	1.20	2.01
35	43.8	724	0.85	1.28	2.01
40	50.0	670	0.93	1.39	2.07
40	50.0	648	0.96	1.44	1.92
42	52.5	602	1.03	1.54	1.64
45	56.3	573	1.08	1.62	1.66
45	56.3	569	1.09	1.63	1.69
48	60.0	537	1.15	1.73	1.57
50	62.5	495	1.25	1.88	1.53
55	68.8	460	1.35	2.02	1.41
58	72.5	448	1.39	2.08	1.75
58	72.5	436	1.42	2.13	1.48
60	75.0	409	1.51	2.27	1.38

Estimated  $\gamma\zeta$  for 2mM data = 43mV.  
 Estimated  $\kappa a = 30$ .

FIGURE 6.13

Linear Velocity as a Function of Applied Field (All Materials)

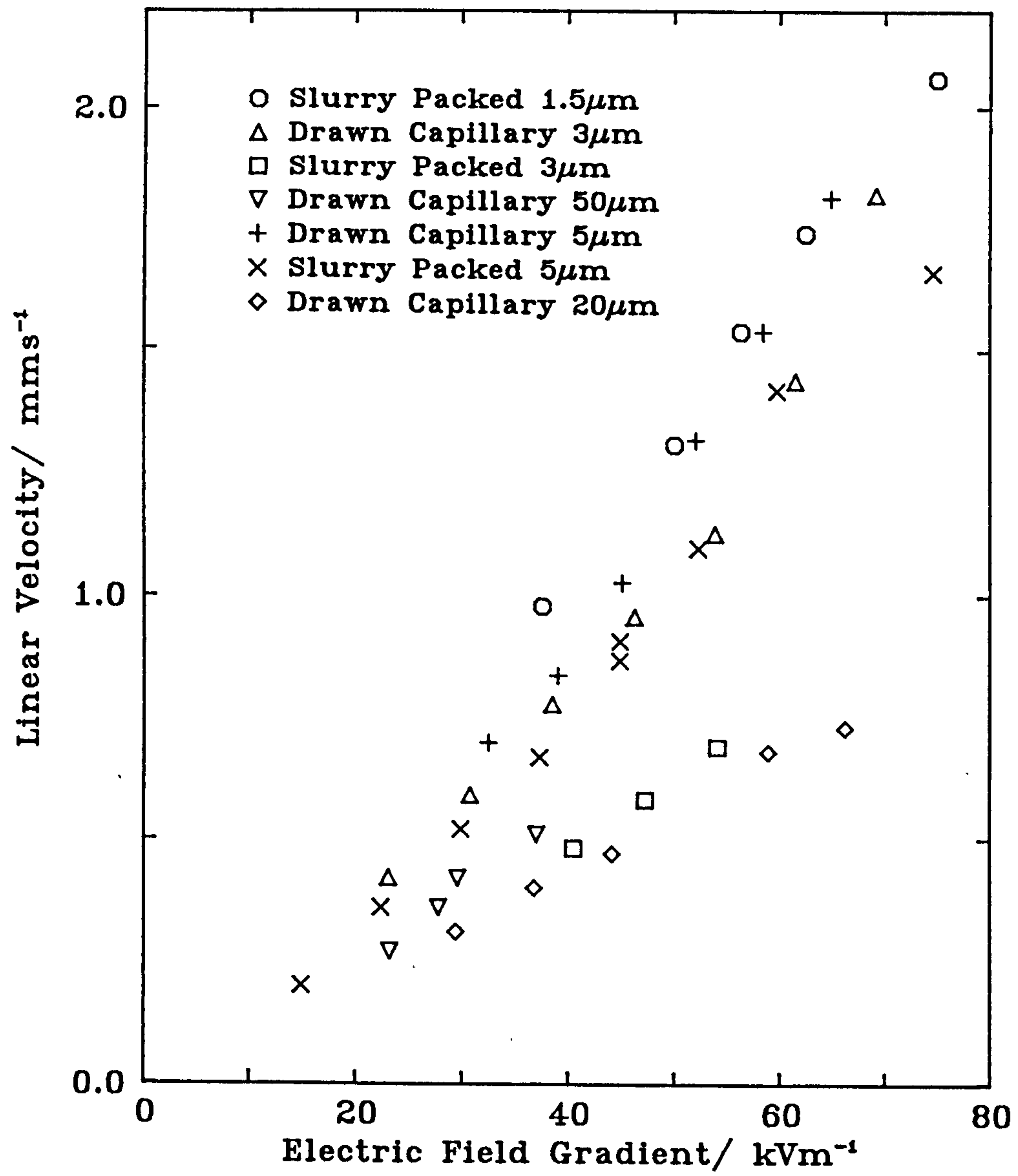


FIGURE 6.14

Reduced Plate Height (Electrically Driven) as a Function of  
Reduced Velocity for Monospher ( $d_p = 1.5\mu\text{m}$ )

Capillary:  $0.62\text{m} \times 50\mu\text{m}$  i.d.. All experimental points were determined at either  $6 \times 10^{-3} \text{mol dm}^{-3}$  or  $2 \times 10^{-3} \text{mol dm}^{-3}$   $\text{NaH}_2\text{PO}_4$  in 70:30 MeCN:Water.

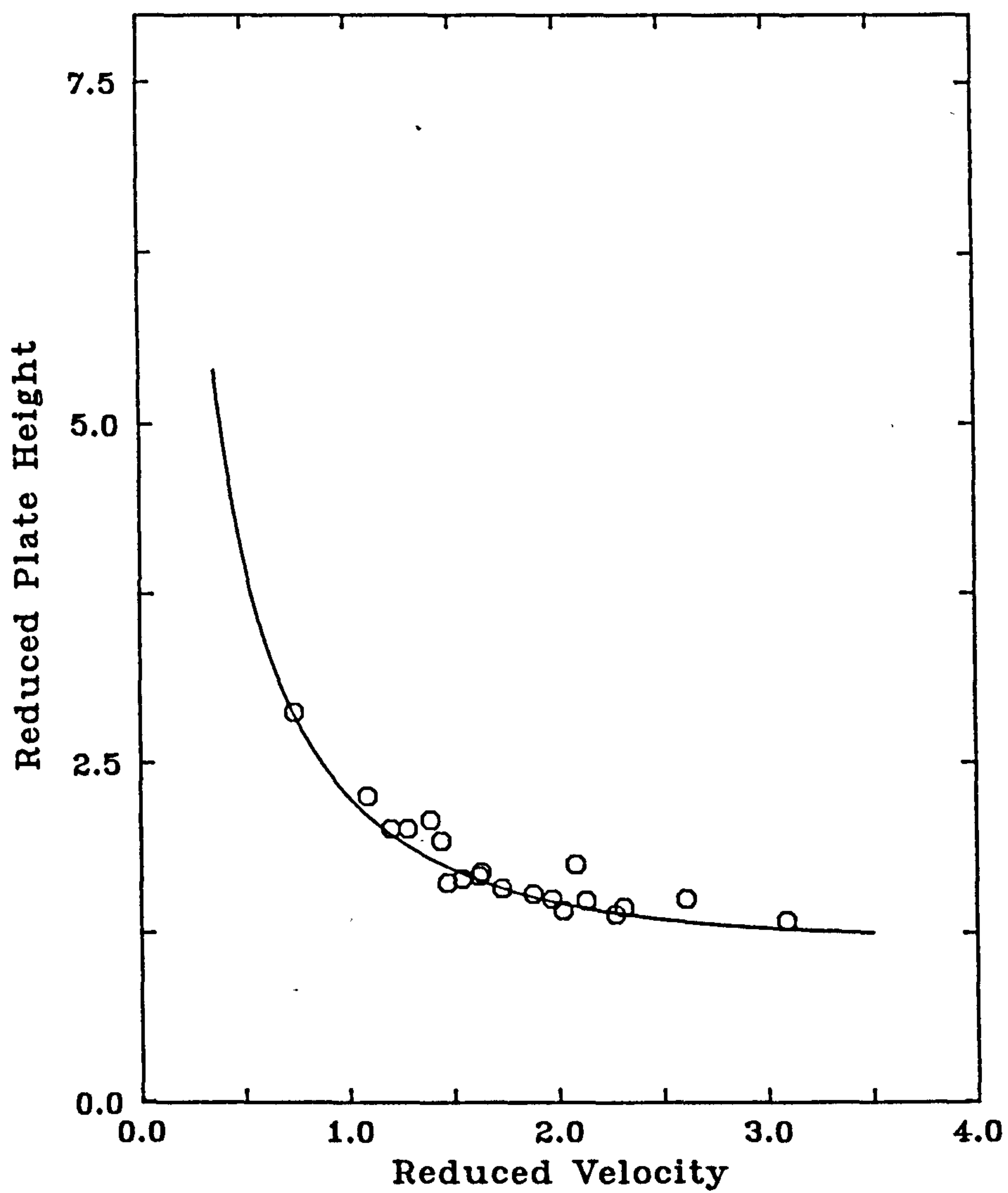




FIGURE 6.15

**Example of a Rising (or Leading) Front  
on Monospher 1.5 $\mu$ m Diameter Particles**

Capillary: 0.62m x 50 $\mu$ m i.d. (Total Length=0.80m) Mobile Phase:70:30  
MeCN:Water (v/v)  $6 \times 10^{-3} \text{ mol dm}^{-3}$   $\text{NaH}_2\text{PO}_4$  Applied Field=56.3kV $\text{m}^{-1}$ ,  
 $N=246,000$ ,  $h=1.68$ ,  $\sigma_L=1.25\text{mm}$ .

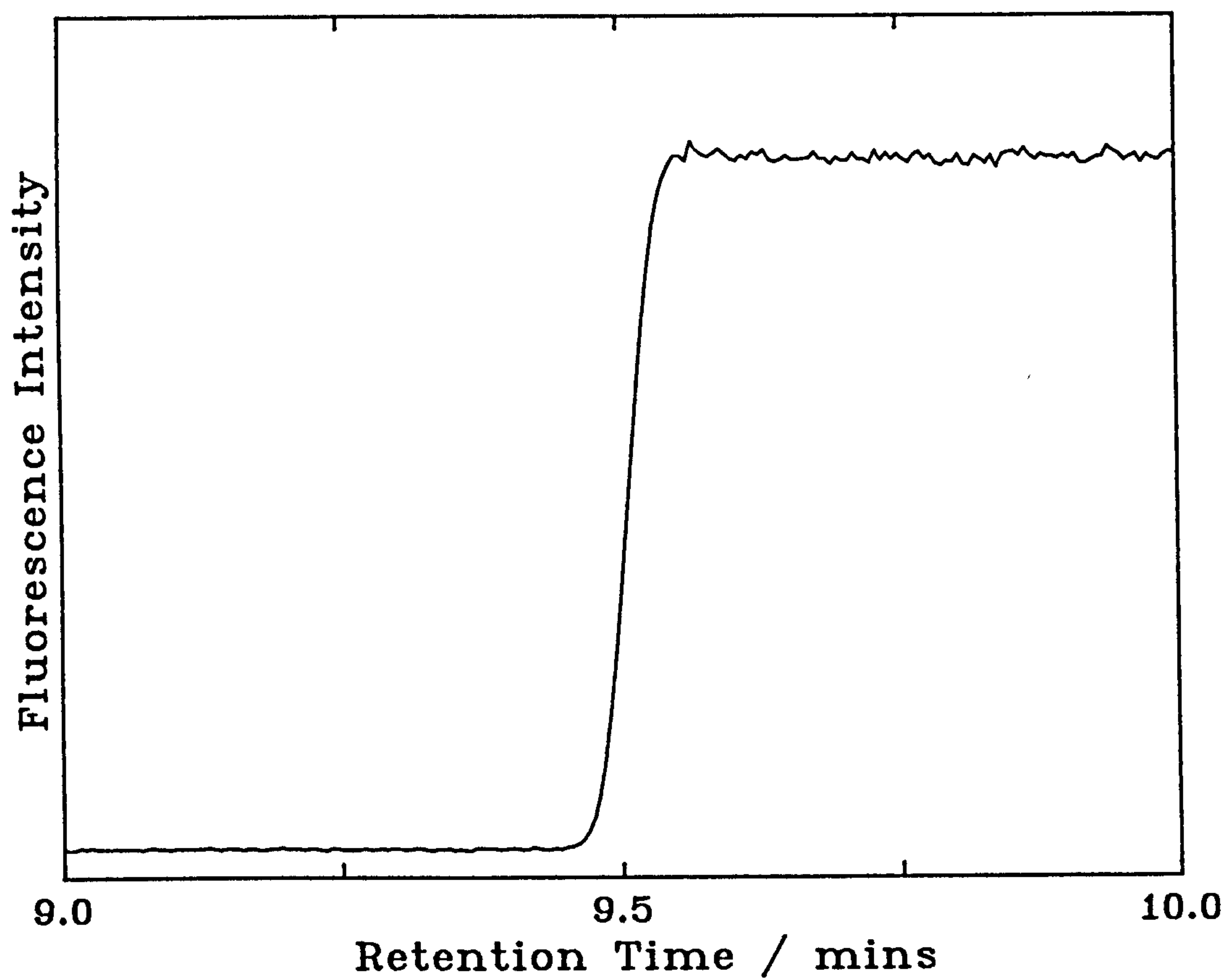
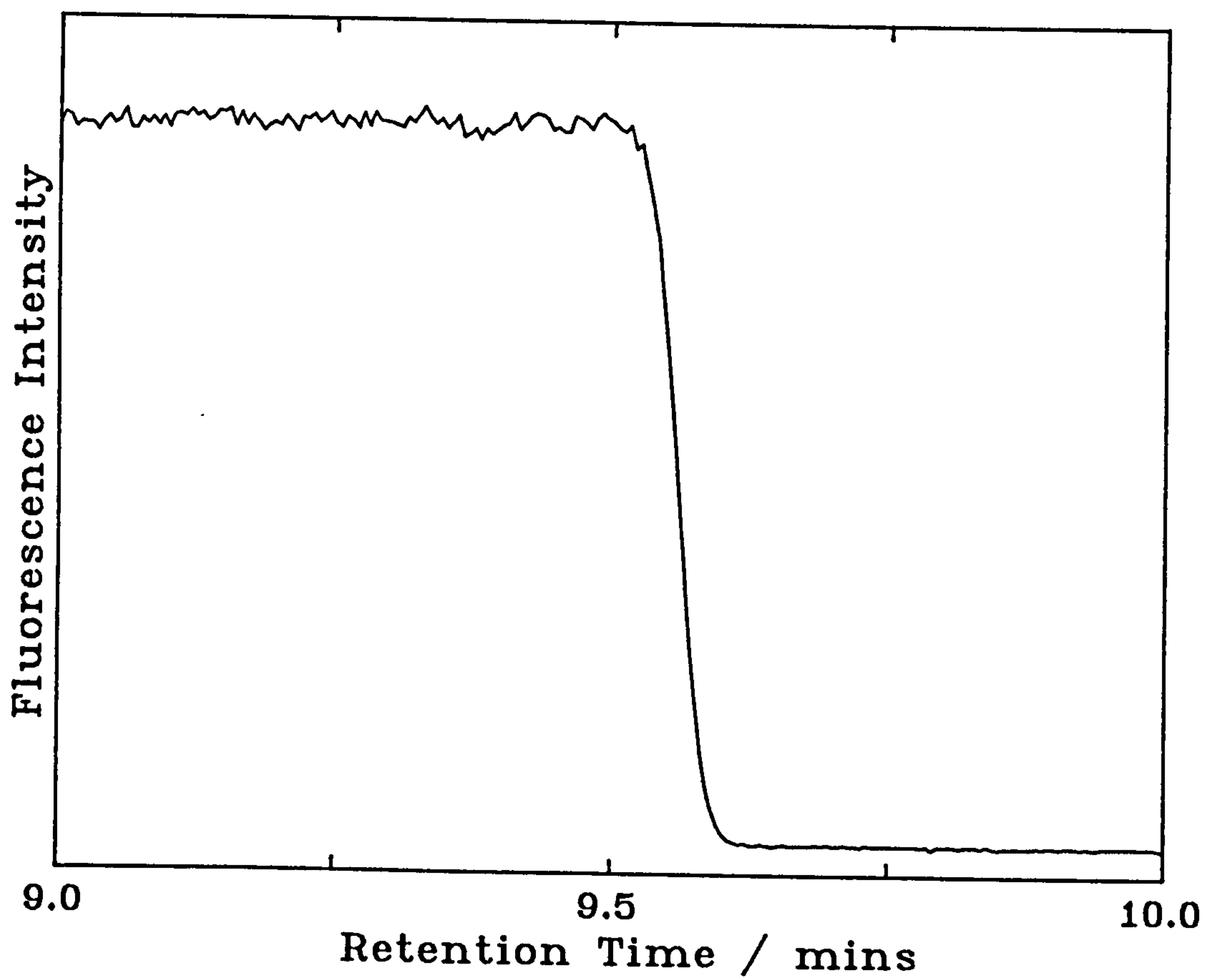


FIGURE 6.16

**Example of a Falling (or Trailing) Front  
on Monospher 1.5 $\mu$ m Diameter Particles**

Capillary: 0.62m x 50 $\mu$ m i.d. (Total Length=0.80m) Mobile Phase:70:30  
MeCN:Water (v/v)  $6 \times 10^{-3}$  moldm $^{-3}$   $\text{NaH}_2\text{PO}_4$  Applied Field = 56.3kVm $^{-1}$ ,  
 $N=249,000$ ,  $h=1.66$ ,  $\sigma_L=1.24$ mm.



### 6.3.6 Effect of Ionic Strength in Electrochromatography

According to equation 3.11, the reciprocal double layer thickness is a function of the electrolyte concentration. This provides a means of varying the value of  $\kappa a$  for a given particle diameter, by altering the ionic strength.

A series of experiments was carried out in which the electric field gradient was held constant and the ionic strength varied. The effect on plate height and flow rate was recorded. The electrolyte was changed electroosmotically by flooding the injection system with the new eluent and allowing electroosmosis to take place until a new stable value of the current was obtained. The passage of 10-20 column volumes was normally required.

Table 6.14 shows the data obtained from three capillaries packed with 5 $\mu\text{m}$ , 3 $\mu\text{m}$ , and 1.5 $\mu\text{m}$  diameter particles. The reduced plate heights as a function of concentration are shown graphically in figure 6.17.

For all particle sizes the same general trend was observed. At low electrolyte concentrations plate heights typical of those observed in pressure driven chromatography were observed, whereas at higher concentrations, results typical of the electrically driven method were obtained. The most notable effect was that observed for the capillary packed with the 5 $\mu\text{m}$  material, for which the reduced plate height was seen to drop from over three to less than one as a result of a ten-fold increase in ionic strength. The variation of the electrolyte concentration had little effect on the velocity of electroosmotic flow in the range investigated, for all particle sizes.

For the 1.5 $\mu\text{m}$  particles, assuming  $\phi = 700$ , the estimated  $\kappa a$  value ranges from less than 10 for  $c = 10^{-4} \text{ mol.dm}^{-3}$ , to 55 for  $c = 6 \times 10^{-3} \text{ mol.dm}^{-3}$ . Thus, even for a  $\kappa a$  value of 10 it is still possible to achieve adequate electroosmotic flow velocities. As can be seen from figure 6.17 larger plate heights are obtained, with the 1.5 $\mu\text{m}$  diameter particles, for  $\kappa a$  values of 10 or less. This can be explained by the fact that for small values of  $\kappa a$ , the velocity of electroosmotic flow shows a dependence on the diameter of the internal channels, in accordance with the predictions based on the equations of Rice and Whitehead. As a result of this, the A-term would be expected to increase, and as  $\kappa a$  tends towards zero the value of the coefficient A would tend towards its pressure driven value. Figure 6.18 shows the predicted percentage change in electroosmotic velocity for a one percent change in channel diameter as a function of  $\kappa a$ , and shows clearly that variations in the channel diameter, should have little effect on the velocity within these, for  $\kappa a$  values of greater than 10. It also demonstrates that the electroosmotic flow velocity can never be more sensitive to change in channel diameter than pressure driven flow. The effect for pressure driven flow is shown by the dotted line in figure 6.18 and demonstrates that the A-term for electrochromatography can never be larger than that for pressure driven LC no matter how small  $\kappa a$  is.

However, for the 3 $\mu\text{m}$  and 5 $\mu\text{m}$  diameter particles, the reduced plate heights continue to decrease with increasing concentration until  $\kappa a$  is greater than ca. 150, by which time the eddy diffusion term should have long since reached its residual value, due to the random orientation of the channels. In contrast to the Monospher material, Hypersil is a totally porous structure with a mean pore



diameter of 12nm. If flow were to occur within the particle, theoretically this would lead to a further fall in plate height due to a reduction of the  $C_s$ -term, since less of the "stationary zone" would actually be stationary. However, the value of  $\kappa a$  within the particles for  $c=2 \times 10^{-3} \text{ mol.dm}^{-3}$  is only 1.2, and therefore, the flow within the particles should be negligible.

The fact that enhanced plate heights, with respect to conventional pressure driven flow, are obtained for some materials only at higher than expected ionic strengths is nevertheless overshadowed by the fact that very small particles can be used. The utility of electrochromatography is not dependent on obtaining these enhanced values of reduced plate height.

TABLE 6.14

## Effect of Ionic Strength on Column Efficiency

Slurry Packed Capillary packed with Merck monosphere 1.5 $\mu$ m  
 Field Strength = 37.5kVm<sup>-1</sup>  
 Mobile Phase - 70% acetonitrile in water.  
 c denotes concentration of NaH<sub>2</sub>PO<sub>4</sub>.

$10^3 c/\text{mol.l}^{-1}$	$u/\text{mm.s}^{-1}$	$v$	$h$	$\kappa a$
0.06	1.14	1.71	3.73	
0.20	1.11	1.67	2.34	10
1.0	0.99	1.48	1.78	23
2.0	0.98	1.47	1.61	32
6.0	0.72	1.09	1.88	55

Drawn Packed Capillary packed with Hypersil 3 $\mu$ m  
 Field Strength = 43kVm<sup>-1</sup>  
 Mobile Phase - 70% acetonitrile in water.

$10^3 c/\text{mol.l}^{-1}$	$u/\text{mm.s}^{-1}$	$v$	$h$	$\kappa a$
0.40	0.91	2.74	2.53	75
1.0	0.92	2.76	2.44	120
2.0	0.92	2.76	1.55	170
6.0	0.72	2.17	1.45	290

All  $h$  and  $v$  values in the above table are the mean of at least three determinations at the quoted concentration.

TABLE 6.14 (continued)

Drawn Packed Capillary packed with Hypersil 5µm  
Field Strength = 38.5kVm<sup>-1</sup>  
Mobile Phase - 70% acetonitrile in water.  
c denotes concentration of NaH<sub>2</sub>PO<sub>4</sub>.

$10^3 c/\text{mol.l}^{-1}$	$u/\text{mm.s}^{-1}$	$v$	$h$	$\kappa a$
0.04	0.77	3.85	3.78	
0.10	0.75	3.78	2.52	60
0.20	0.77	3.85	3.01	90
0.20	0.77	3.85	2.68	90
0.30	0.81	4.05	2.20	110
0.50	0.81	4.05	1.41	140
1.0	0.80	4.00	1.04	200
2.0	0.82	4.10	0.93	280
2.0	0.78	3.90	0.91	280
6.0	0.69	3.45	0.81	490
20	0.52	2.60	1.03	890

All h and v values in the above table are the mean of at least three determinations at the quoted concentration.

FIGURE 6.17

Effect of Ionic Strength on the  
Plate Height in Electrochromatography

The graph below shows the reduced plate height as a function of the concentration of sodium dihydrogen phosphate in the mobile phase, for 5 $\mu\text{m}$  and 3 $\mu\text{m}$  diameter particles in drawn capillaries and for 1.5 $\mu\text{m}$  diameter particles in a slurry packed capillary.

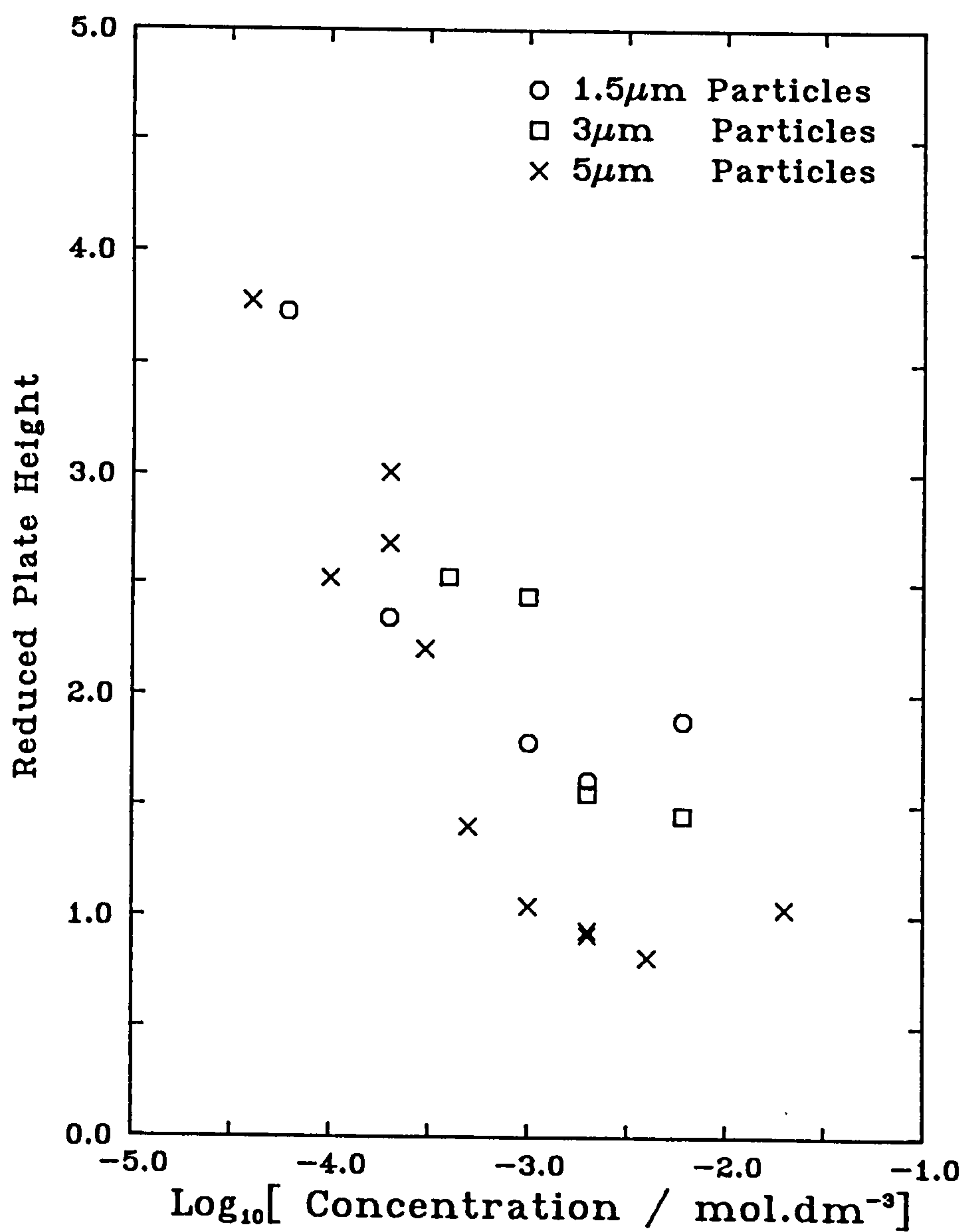
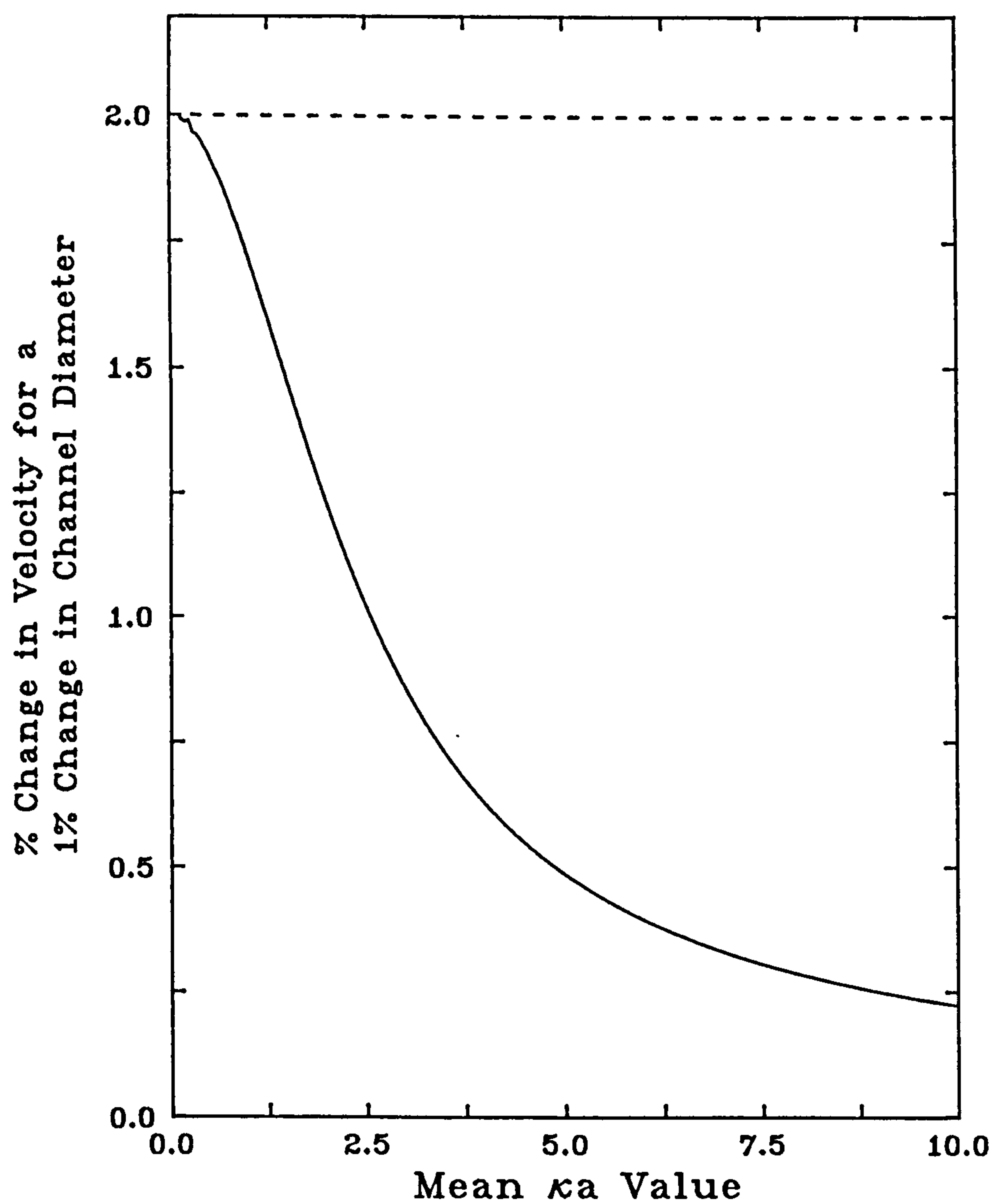




FIGURE 6.18

**%Change in Flow Velocity for a 1%  
Change in  $\kappa a$  as a Function of  $\kappa a$**

The graph indicates the sensitivity of the flow velocity to deviations from the mean channel diameter as a function of  $\kappa a$  and is predicted from equation 3.28. The dashed line indicates the expected behaviour for pressure driven flow.



## **CHAPTER 7**

### **DISCUSSION AND CONCLUSIONS**

## Chapter 7

### DISCUSSION AND CONCLUSIONS

#### 7.1 Introduction

In this chapter the scientific consequences of the experimental results will be discussed together with the conclusions which can be drawn from these. The future potential of electrochromatography as an analytical separation method, including its limitations, will also be discussed.

#### 7.2 Electroosmotic Flow Rates

A previous attempt to measure electroosmotic flow velocities, in chromatographic media, was made by Stevens and Cortes<sup>87</sup> in 1983. Experiments were carried out in 2cm long tubes 1mm i.d. packed with 10 $\mu$ m, 50 $\mu$ m and 100 $\mu$ m diameter particles. In contrast to the results described in the previous chapter, it was found that a drop in the predicted electroosmotic flow velocity was encountered on changing from 100 $\mu$ m to 50 $\mu$ m particles and a drastic reduction of the linear velocity was observed when using 10 $\mu$ m particles. At first sight these data would appear contradictory, however, it must be borne in mind that the initial experiments of Stevens and Cortes were carried out using pure organic mobile phases (methanol and acetonitrile) and distilled water. In these media the electrical double layer thickness would be expected to be large (ca. 1 $\mu$ m) and thus, leads to a small value of  $\kappa a$ . For this reason the electroosmotic flow velocities would be expected to show a strong dependence on

the particle diameter. However, even with water containing KCl at  $10^{-3} \text{ mol.dm}^{-3}$ , surprisingly low flow rates were reported for the  $10\mu\text{m}$  material. These were consistent with a zeta potential of only  $4\text{mV}$ , as opposed to  $37\text{mV}$ <sup>a</sup> for  $5\mu\text{m}$  Hypersil estimated from flow rates obtained in this work. The difficulties experienced in this work in maintaining electroosmotic flow in  $100\mu\text{m}$  bore, or larger, capillaries without the formation of partially dried out areas of the packed bed, suggest that the low velocities observed by Stevens and Cortes, could be due to incomplete saturation of the packed bed, a fact which would also explain the low electrical conductivity reported. Whatever the reason, it is clear from the results listed in the previous chapter for  $3\mu\text{m}$  and  $1.5\mu\text{m}$  diameter particles, that there is no significant drop in electroosmotic flow velocity with decreasing particle size, right down to an estimated  $\kappa a$  value of 10. This is indeed in full agreement with the predictions based on the work of Rice and Whitehead (cf. section 3.3).

Equation 3.28 for the mean velocity as a function of  $\kappa a$  predicts that for a  $\kappa a$  of 5, the mean velocity will be sixty four percent of the velocity predicted by the von Smoluchowski equation. If this value is arbitrarily chosen as the maximum acceptable deviation from the von Smoluchowski equation, it is possible to define a minimum particle diameter for a given ionic strength and relative permittivity. The mean value of  $a$  for a given particle diameter is given by equation 3.29 as  $(8/\phi)^{1/2} d_p$ . Thus, if the value of  $\kappa a$  must always be greater than 5, the minimum particle diameter is given by,

---

<sup>a</sup>More precisely  $\gamma\zeta = 37\text{mV}$ , i.e. a lower limit for  $\zeta$ .



$$d_{pmin} = 1.78\phi^{1/2} / \kappa \quad 7.1$$

Thus, for an electrolyte concentration of  $10^{-3} \text{ mol.dm}^{-3}$  in 70:30 acetonitrile water, for which  $\kappa = 1.4 \times 10^8 \text{ m}^{-1}$ , the minimum value of  $d_p$  is  $0.33 \mu\text{m}$ .

### 7.3 Comparison of Electrochromatography with HPLC

Comparison of the results obtained from both types of capillary with both pressure driven flow and electroosmotic flow, show clearly the superiority of electroosmosis over pressure, as a means of propelling solvent through a chromatographic bed. The fact that reduced plate heights as low as 0.7 have been observed (cf. table 6.7), together with the values estimated for the coefficient A in the plate height equation, indicate that for well packed capillaries the dispersion due to flow can, in the electroosmotic case, be effectively zero. This result suggests that for such columns, the residual eddy diffusion term resulting from the random directions of the interparticle channels, is small enough to be negligible. For the  $3 \mu\text{m}$  and  $5 \mu\text{m}$  diameter particles this results in a significant increase in efficiency, although the plate numbers obtained with these materials, could, in principle be obtained using pressure, with similar elution times, although longer capillaries would be required. However, the strength of the electroosmotic method lies in the fact that, as discussed in the previous chapter, smaller particles can be used. As has been demonstrated in chapter 6, for  $1.5 \mu\text{m}$  diameter particles, plate numbers of up to 300,000 can be obtained in approximately five minutes, from a column, which is effectively impermeable to pressure driven flow. This performance ( $N/t \simeq 1000 \text{ s}^{-1}$ ) could only be achieved,

in HPLC, for relatively small values of  $N$ , e.g., 3000 or less.

In contrast to HPLC, for which the maximum number of plates, for a given pressure drop, is unlimited, the maximum allowed plate number in electrochromatography is given by an expression analogous to equation 3.39, where axial diffusion is considered to be the sole contributor to band spreading. In the case of electrochromatography the electrophoretic mobility is replaced by the coefficient of electroosmotic flow ( $\mu_{eo}$ ) which is equivalent to  $\epsilon_r \epsilon_0 \gamma \zeta / \eta$ , leading to,

$$N_{\max} = V \cdot \epsilon_r \epsilon_0 \gamma \zeta / 2 D_m \cdot \eta \quad 7.2$$

assuming that  $B$  in the plate height equation is 2.

This expression states the maximum plate number which may be obtained in electrochromatography, regardless of the particle size. However, for particles of a finite size, this efficiency can never actually be achieved. Rather, it can only be approached asymptotically through the use of columns long enough for axial diffusion to become dominant. For a plate number of less than  $N_{\max}$  the analysis time, disregarding the self-heating effect, is proportional to the square of the particle diameter, since a reduction of the particle diameter accompanied by the same relative reduction in capillary length will produce the same reduced velocity. Thus, the same number of plates will be produced in a time proportional to the square of the length.

## 7.4 Comparison of Electrochromatography with CZE

Compared with CZE systems the efficiencies and performances reported for the  $3\mu\text{m}$  and  $5\mu\text{m}$  diameter materials are relatively poor, due to the fact that the introduction of a stationary phase, introduces dispersion due to the resistance to mass transfer in the stationary zone. However, the results for  $1.5\mu\text{m}$  diameter particles are close to the efficiencies, which are typical of CZE, with a similar analysis time.

The realisation of a chromatographic system with the efficiency and speed of analysis of CZE would be of enormous advantage in separation science. In many analytical problems where the separation of structurally similar charged species must be carried out, the selectivity of zone electrophoresis is often insufficient<sup>55</sup> to produce an adequate separation, despite the enormous efficiency, although, in many cases, the same species may be easily separated in HPLC with a smaller plate number.

## 7.5 Potential of Electrochromatography

This section attempts to predict the theoretical performance limits of electrochromatography, assuming ideal behaviour, in order to give some idea of its future potential.

Equation 7.1 tends to suggest that the performance of electrochromatography can be increased by reducing the particle diameter until the condition set by equation 7.1 is no longer satisfied. Increasing  $\kappa$  by increasing the ionic strength



would permit the use of still smaller particles. However, the effect of ohmic heating, for a given diameter of capillary, becomes more significant as the particle size and column length are reduced, due to the increasing field strength. Reduction of the particle diameter to significantly below the value of the plate height due to the combined effect of ohmic heating and axial diffusion will clearly not bring about any further significant increase in performance.

In the ideal case where the particle diameter is small enough for the residual A-term and the resistance to mass transfer in the stationary zone to be negligible, the plate height in electrochromatography, for a given column diameter, can be expressed as,

$$H = 2D_m/u + (\epsilon_r \epsilon_0 \cdot \gamma \zeta \cdot E^5 \cdot d_c^6 / 98304 D_m) \cdot (\epsilon \cdot \alpha_V \cdot c/K)^2 \quad 7.3$$

which is obtained simply by adding equation 3.66, for the self heating term (cf section 3.8), to the term for axial diffusion. It can be shown from equation 7.3 that the minimum value for the plate height in the ideal case, is obtained when the field is equivalent to,

$$E_{Hmin} = (5.83/d_c) \cdot (D_m \cdot \eta / \epsilon_r \epsilon_0 \cdot \gamma \zeta)^{1/3} \cdot (K/\Lambda c \alpha_V \epsilon)^{1/3} \quad 7.4$$

This equation can be considered an electrochromatographic analogue of the expression derived by Bocek<sup>36</sup> for the field corresponding to the minimum plate height in ideal CZE.



The minimum value of the plate height is given by,

$$H_{\min} = (d_c/2.4) \cdot (D_m \cdot \eta / \epsilon_r \epsilon_0 \gamma \zeta)^{2/3} \cdot (\Lambda c \alpha_V \epsilon / K)^{1/3} \quad 7.5$$

which is equivalent to 1.2 times the plate height due to axial diffusion alone  $(2D_m \eta / E \epsilon_r \epsilon_0 \gamma \zeta)$ , at a field of  $E_{H\min}$ . Thus, the minimum plate height can also be expressed as,

$$H_{\min} = (2.4 D_m \eta / E_{H\min} \epsilon_r \epsilon_0 \gamma \zeta) \quad 7.6$$

For this value of  $H$ , the plate number corresponds to 87% of the maximum permitted by equation 7.2, and represents the smallest plate height which may be obtained using a capillary with a diameter  $d_c$ , and an electrolyte concentration  $c$ .

In a real case where particles of a finite diameter are present, the effect on the overall plate height of resistance to mass transfer in the stationary zone, will be at its most severe at the field strength corresponding to  $H_{\min}$ . Thus, the minimum value of  $H$  in the hypothetical case can be used as a guideline in calculating the most appropriate particle diameter, for a given capillary diameter, which will allow efficiencies approaching the ideal case to be obtained.

If one imposes the condition that the plate height due to slow mass transfer introduced by the stationary phase, should be no greater than 10% of the plate height predicted by equation 7.4, it would be possible to predict a particle size, which would produce ca. 90% of the plate number obtained from an ideal capillary packed with hypothetical particles of zero size.

The plate height due to slow mass transfer, which is equivalent to  $C_s u d_p^2 / D_m$ , is given by equation 7.7 as,

$$H_{mt} = C_s d_p^2 E \epsilon_r \epsilon_0 \gamma \zeta / D_m \eta \quad 7.7$$

By imposing the condition that  $H_{mt}$  is equivalent to 10% of  $H_{min}$  and taking a typical value, for porous particles, of 0.1 for  $C_s$ , one can derive, from equations 7.6 and 7.7, the following expression for  $d_p$ .

$$d_p = 0.645 H_{min} \quad 7.8$$

In the separation of ionic species the electrolyte concentration required is determined by the need for ionic buffering, which ensures an approximately constant field gradient within a sample zone containing charge carrying analytes. The effect of ionic concentration in zone electrophoresis has been discussed in detail by Everaerts et al<sup>34</sup>. In CZE, for  $d_c = 50\mu\text{m}$ , the salt concentration in the electrolyte is typically ca.  $3 \times 10^{-2} \text{mol} \cdot \text{dm}^{-3}$ . In an  $50\mu\text{m}$  i.d. ideal capillary, where  $\gamma \zeta = 30\text{mV}$  the application of  $60\text{kV}$ , could lead to the generation of 530000 theoretical plates in a  $27\text{cm}$  capillary with an analysis time of 82 seconds, where  $E$  corresponds to the value given by equation 7.3. The plate height under these conditions is equivalent to  $0.61\mu\text{m}$ . For the sake of this calculation  $D_m$  is assumed to be  $10^{-9} \text{m}^2 \text{s}^{-1}$ ,  $\Lambda = 0.015 \text{m}^2 \cdot \text{mol}^{-1} \Omega^{-1}$ ,  $\eta = 10^{-3} \text{Nm}^{-2} \text{s}$ ,  $\epsilon = 0.4$ ,  $\alpha_V = 0.026 \text{K}^{-1}$ , and  $K = 0.4 \text{Wm}^{-1} \text{K}^{-1}$ .

The application of equation 7.8 leads to a recommended value of  $0.39\mu\text{m}$  for the particle diameter, in order to achieve 90% of the theoretical maximum efficiency.

Thus, for a column packed with  $0.39\mu\text{m}$  diameter particles 480000 plates would be obtained in only 82 seconds, for a voltage drop of 60kV. Further reduction of the particle diameter would not significantly improve on this performance. This calculation clearly demonstrates that electrochromatography with submicron particles can easily match, or surpass the efficiency and performance of capillary zone electrophoresis. Furthermore the problem of sample interaction with the capillary wall which often leads to a serious loss of efficiency in CZE would not be expected to cause problems in electrochromatography.

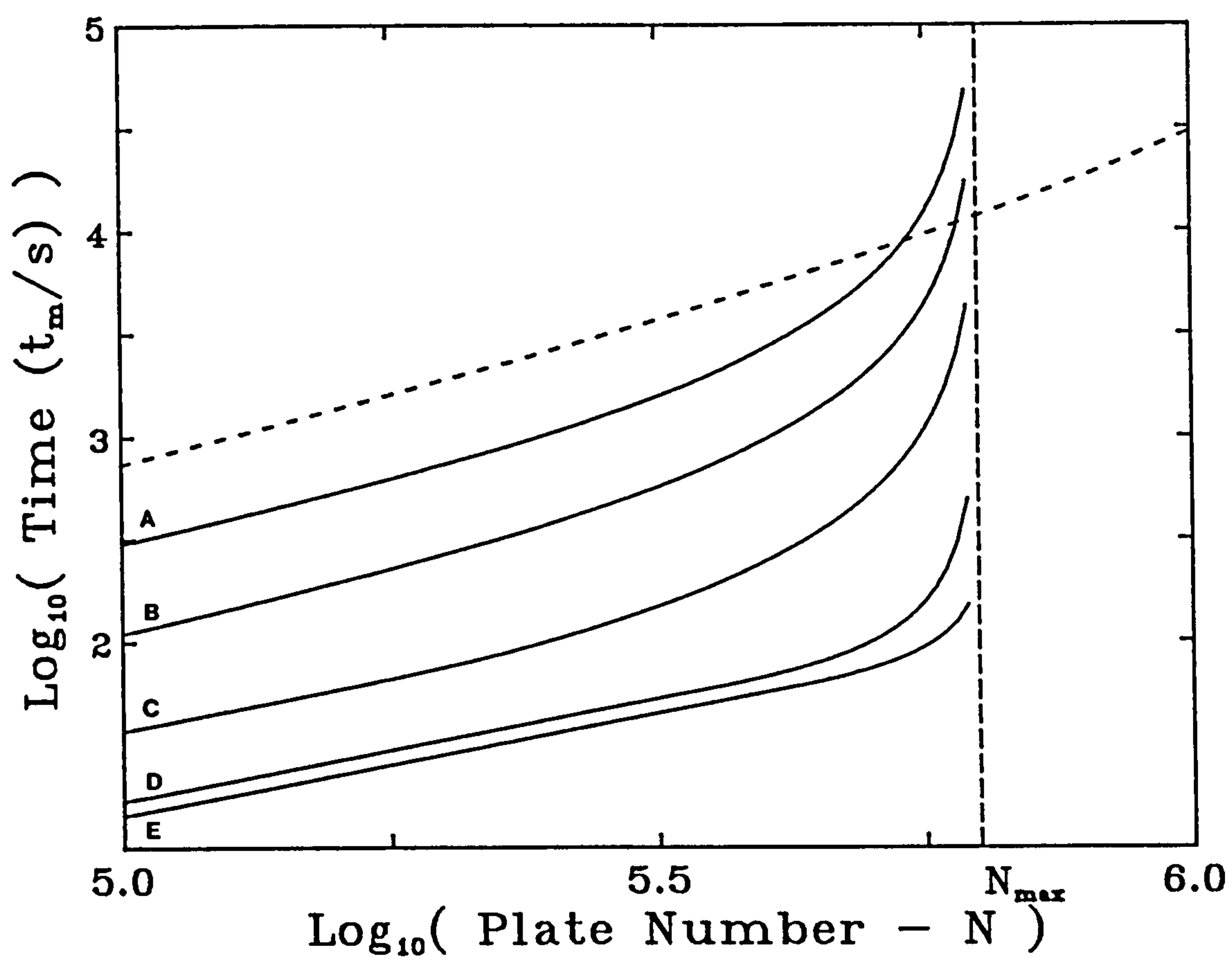
Figure 7.1 shows the minimum elution times possible in electrochromatography as a function of the desired plate number  $N$  for a  $50\mu\text{m}$  i.d. capillary, for  $c=0.03\text{mol.dm}^{-3}$  and with the same values as the previous case for all other parameters. The theoretical minimum analysis times were calculated using an iterative method, which is discussed in appendix III for particles sizes ranging from  $5\mu\text{m}$  diameter to  $0.5\mu\text{m}$ . The graph illustrates the effect of particle size on the analysis time. The curve for  $0.5\mu\text{m}$  particles demonstrates that for the chosen ionic strength, there is no need to reduce the particle diameter to much less than one hundredth of the capillary internal diameter, since this curve lies very close to that for the ideal capillary packed with particles of infinitesimal diameter indicated by the lowest curve on the graph. For the sake of comparison the optimum unretained times for a drawn packed capillary packed with  $5\mu\text{m}$  particles, limited to a pressure drop of 200bar, are shown by the dotted line in figure 7.1.



FIGURE 7.1

Minimum Analysis Times (for an Unretained Species) in  
Electrochromatography as a Function of Plate Number

The theoretical minimum analysis times were calculated based on the optimum value of  $N/t$  provided the optimum field can be achieved, otherwise an iterative method is used as discussed in appendix III. A: $d_p = 5\mu\text{m}$ , B: $d_p = 3\mu\text{m}$ , C: $d_p = 1.5\mu\text{m}$ , D: $d_p = 0.5\mu\text{m}$ , E: $d_p = \text{infinitesimal}$ .





For the separation of non-ionic species by electrochromatography there is no need for ionic buffering. However, the ion concentration must be sufficient to ensure a large enough value of  $\kappa a$ . The concentration necessary to ensure a  $\kappa a$  value of at least 5 is given by equation 7.9.

$$c = \phi \epsilon_r \epsilon_0 RT (1.78)^2 / 2 d_p^2 F^2 \quad 7.9$$

which can be obtained by combining equations 7.1 and 3.12.

If  $c$  in equation 7.5 is substituted by the above, and by making use of equation 7.7, an expression for  $d_p$  can be obtained. This leads to,

$$d_p^{5/3} = (D_m \eta / \epsilon_r \epsilon_0 \gamma \zeta)^{2/3} \cdot (\Lambda \alpha_V \epsilon / K)^{1/3} \cdot (\phi \epsilon_r \epsilon_0 RT / 2 F^2)^{1/3} \cdot (d_c / 2.56) \quad 7.10$$

Inserting the values of all constants,  $\gamma \zeta = 30 \text{ mV}$ ,  $\phi = 500$ , together with the same typical values for all other parameters, as used in previous calculations, leads to,

$$d_p = 7.52 \times 10^{-5} \cdot d_c^{3/5} \quad 7.11$$

Using this particle size plus the field gradient indicated by equation 7.3 75% of  $N_{\text{max}}$  will be obtained, provided that  $c$  satisfies equation 7.9

The performances predicted for a 50, 100, and 200  $\mu\text{m}$  i.d. capillary are listed in table 7.1.

The data in the table show that for the separation of electrically neutral species 480000 theoretical plates can be obtained in only 110 seconds, even with a 200  $\mu\text{m}$

i.d. capillary. This treatment suggests that fast electrochromatography, of neutral species could be carried out with efficiencies close to the theoretical maximum for CZE, but without the need to use such narrow capillaries.

In the previous chapter however it was stated that some difficulty was experienced, especially with slurry packed capillaries, for which the ratio of the outer to the inner diameter was very small, in maintaining a constant electroosmotic flow rate in capillaries larger than 75 $\mu$ m i.d.. However, all the experimental data presented in chapter 6 was obtained without thermostating or cooling of the capillary. As a result the absolute temperature in the capillary increases with increasing  $d_c$ ,  $c$  and  $E$ , which explains the clear positive curvature in graphs of linear velocity verses the applied field (cf. figure 6.13). Thus, it is clear that in order to obtain performances approaching those predicted above, the capillary must be cooled in order to prevent the formation of dried out areas or even boiling of the mobile phase.

TABLE 7.1

**Theoretical Analysis Times for Non-Ionic Species in Electrochromatography**

The particle diameter quoted is calculated according to equation

7.10. Following the assumptions listed below 90% of the ideal efficiency for zero sized particles corresponds to 480000 plates.

$d_e/\mu\text{m}$	$d_p/\mu\text{m}$	$10^3 c/\text{mol.dm}^{-3}$	$L/\text{cm}$	$t_m/\text{s}$
200	0.45	0.73	37.3	110
100	0.30	1.77	24.6	48
50	0.20	3.82	16.2	21

The values are calculated assuming an A-term of zero, and a  $\kappa a$  of 5. The following assumptions were made:  $\eta = 10^{-3} \text{Nm}^{-2}\text{s}$ ,  $D_m = 10^{-9} \text{m}^2\text{s}^{-1}$ ,  $\Lambda = 0.015 \text{m}^2 \text{mol}^{-1} \Omega^{-1}$ ,  $\epsilon = 0.4$ ,  $\gamma\zeta = 30 \text{mV}$ ,  $K = 0.4 \text{Wm}^{-1}$ ,  $\alpha_V = 0.026 \text{K}^{-1}$ ,  $\phi = 500$  and  $V = 60 \text{kV}$ .

## 7.6 Limitations of Electrochromatography

### 7.6.1 Dependence on $\zeta$ -Potential

An obvious prerequisite for electrochromatography is a significant  $\zeta$ -potential at the interface between the stationary and mobile phases.

The absolute value of the zeta potential influences the performance of electrochromatography in two ways.

The maximum number of theoretical plates which can be obtained for a given voltage drop is directly proportional to the zeta potential in accordance with equation 7.2.

In addition it can be shown, from equation 3.63 by replacing  $\mu_{ep}$  by  $\mu_{eo}$ , that the theoretical minimum analysis time for an unretained analyte in electrochromatography is given by,

$$t = 3ND_m^{1/3} \cdot (\epsilon \Lambda c \alpha_v / K)^{2/3} \cdot (\eta / \epsilon_r \epsilon_0 \gamma \zeta)^{4/3} \quad 7.12$$

Thus, the analysis time is proportional to  $\zeta^{-4/3}$ .

For the reasons discussed above it is clear that the smaller the zeta potential in electrochromatography, the poorer the performance. Thus, the mobile phase in electrochromatography is subject to restrictions as regards pH and ionic strength.

The measurements of linear velocity as a function of applied field, at an ionic



strength of  $2 \times 10^{-3} \text{ mol.dm}^{-3}$ , discussed in the previous chapter imply a value of between 12 and 43mV for the product of the zeta potential and the factor  $\gamma$  which accounts for the tortuosity of the bed and the internal porosity of the particles. The separations by electrochromatography on in-situ ODS derivatised capillaries suggest that the zeta potential is not significantly reduced by the derivatisation procedure. Measurements of the zeta potential on ODS Hypersil by Knox and Kaliszan<sup>88</sup> using particle electrophoresis have shown that at an ionic concentration of  $10^{-3} \text{ mol.dm}^{-3}$  the zeta potential is 43mV. Given that for a packed bed of porous particles the value of  $\gamma$  could be expected to be 0.5 or less, this value is in approximate agreement with the flow rates obtained in this work. From the point of view of  $\gamma$  it would be preferable to work with non-porous particles. However, the need for a large internal surface area to ensure adequate retention dictates the use of porous materials.

From the above it is clear that the assumption of a  $\gamma\zeta$  of 30mV, used in the previous section is not unreasonable.

Knox and Kaliszan have also shown that the zeta potential on ODS Hypersil drops to a negligible value at a pH of less than ca. 3. However, the combined electrochromatography/electrophoresis of charged species would still be possible in the absence of a zeta potential provided that the charges carried by the analytes were all of the same sign.

### 7.6.2 Detection

The enforced miniaturisation of the system places heavy demands on the detection method. It is this aspect which most severely limits the application of capillary electrophoresis and electrochromatography to real analytical problems.

The detection methods which exhibit a good concentration sensitivity in capillaries, such as fluorescence<sup>52</sup> or electrochemical<sup>86</sup> detection are unfortunately very specific and thus, the excellent sensitivity is only achieved for certain classes of compounds. The more general method of UV absorption, which is often the method of choice in liquid chromatography, does not, in many cases, exhibit the sensitivity required for capillary zone electrophoresis, a fact which would also apply to electrochromatography.

Many alternative detection methods such as mass spectrometric<sup>89</sup> or thermal lens detection<sup>90</sup> are in the course of development, however, it is clear that the widespread application of electrochromatography and indeed of capillary electroseparation methods in general awaits further developments in detector technology.

## 7.7 Conclusions

The main conclusions which can be drawn from the work described within this thesis can be summarised as,

1. Electroosmosis can be used to provide adequate flow velocities for liquid chromatography in typical chromatographic media. The flow velocity, unlike for pressure driven flow, does not show a dependence on the particle size, in the size range investigated.
2. Electroosmotic flow makes a smaller contribution to the A-term in the plate height equation than does pressure driven flow.
3. Electrochromatography with small particles (e.g. 1.5 $\mu\text{m}$  diameter) can produce plate numbers approaching those of capillary zone electrophoresis with similar analysis times.
4. It can be expected that further reduction of the particle diameter to below 1 $\mu\text{m}$  will further improve the performance of electrochromatography.

Finally it can be concluded that electrochromatography has the potential to unify the exceptionally high performance of capillary zone electrophoresis with the versatility and the vast range of possible applications of HPLC.

## LITERATURE CITED

1. Tswett, M., *Ber. der Deut. Botan. Ges.*, 24 (1906) 316.
2. Lodge, O., *British Association Reports*, 1886.
3. Michaelis, L., *Biochem. Zeit.*, 16 (1909) 81.
4. Wieland, T. and Fischer, E., *Naturwiss.*, 37 (1950) 25
5. Condsen, R., Gordon, A. M., and Martin, A. J. P., *Biochem. J.*, 40 (1946) 29.
6. Strain, H. H., *J. Amer. Chem. Soc.*, 61 (1939) 1292.
7. Synge, R. L. M. and Tiselius, A., *Biochem. J.*, 46 (1950) xli.
8. Lecoq, H., *Bull. de la Soc. Roy. des Sci. (de Liège)*, 13 (1944) 20.
9. Synge, R. L. M., and Martin, A. J. P., *Biochem. J.*, 35 (1941) 1358.
10. Wilson, J., *J. Amer. Chem. Soc.*, 62 (1940) 1583.
11. Van Deemter, J. J., Zuiderweg, F. J. and Klinkenberg, A., *Chem. Eng. Sci.*, 5 (1956) 271.
12. Dal Nogare, S. and Juvet, R. S. in *"Gas Liquid Chromatography"*, Interscience, New York (1962).
13. Giddings, J. C., *J. Chromatogr.*, 13 (1964) 301.
14. Giddings, J. C., *"Dynamics of Chromatography"*, Part 1, Dekker, New York (1965).
15. Knox, J. H., in *"Techniques in Liquid Chromatography"*, Ed. Simpson., Wiley Heyden, U.K. (1982) p.35.
16. Giddings, J. C., *Anal. Chem.*, 37 (1965) 60.
17. Knox, J. H., *J. Chem. Soc.* (1961) 433.
18. Knox, J. H. and Saleem, M. *J. Chromatogr. Sci.*, 7 (1969) 614.
19. Jorgenson, J. W. and Lukacs, K. D., *J. of HRC & CC*, 4 (1981) 230.



20. Golay, M. J. E., in *"Gas Chromatography 1958"*, Ed. Desty, Butterworths, London, 1959, P.36.
21. Knox, J. H. and Gilbert, M. T. *J. Chromatogr.*, 186 (1979) 405.
22. Helmholtz, H. L. F. von, *Wiedemanns Ann. (Ann. Phys. Leipzig)*, 7 (1877) 337.
23. Goüy, M., *J. Phys.*, 9 (1910) 457.
24. Chapman, D. L., *Phil. Mag.*, 25 (1913) 475.
25. Stern, O., *Zeit. Elektrochem. Angew. Phys. Chem.*, 30 (1924) 508.
26. Debye, P. and Hückel, E., *Physik. Z.*, 24 (1923) 185.
27. Eversole, W. G. and Boardman, W. W., *J. Phys. Chem.*, 46 (1942) 914.
28. Smoluchowski, M. von, in *"Handbuch der Elektrizität und des Magnetismus. Vol. II"* Ed. Graetz, Leipzig. (1914) 366.
29. Rice, C. L. and Whitehead, R., *J. of Phys. Chem.*, 69 (1965) 4017.
30. Hückel, E., *Physik. Z.* 25 (1924) 204.
31. Henry, D. C., *Proc. Roy. Soc. (London)*, 133 (1931) 106.
32. Giddings, J. C., *Separation Sci.*, 4 (1969) 181.
33. Jorgenson, J. W. and Lukacs, K. D., *Anal. Chem.*, 53 (1981) 1298.
34. Mikkers, F. E. P., Everaerts, F. M. and Verheggen, Th. P. E. M., *J. of Chromatogr.* 169 (1979) 11.
35. Tiselius, A., *Naturwiss.*, 37 (1950) 25.
36. Tiselius, A., Hjerten, S., and Jerstedt, S., *Arch. Ges. Virusforsch.*, 17 (1965) 512.
37. Virtanen, R., *Acta Polytech. Scand.*, 123 (1974).
38. Taylor, Sir G. I., *Proc. Roy. Soc. (London)*, A219 (1953) 186.
39. Foret, F., Deml, M. and Bocek, P., *J. of Chromatogr.*, 452 (1988) 613.
40. Tiselius, A., *Trans. Faraday Soc.*, 333 (1937) 524.

41. Gordon, A. H., in *"Electrophoresis of Proteins in Polyacrylamide Gels"*, North Holland, London, 1969.
42. Ed. Hames B. D. and Rickwood, D., *"Gel Electrophoresis of Proteins"*, IRL, Washington DC, 1983.
43. Kolin, A., *Methods Med. Res.* 12 (1970) 326.
44. Stegemann, H, *Zeit. Analyt. Chem.* 350 (1969) 917.
45. Haglund, H., *Science Tools* 17 (1970) 2.
46. Gilbert, M. T., Knox, J. H. and Kaur, B., *Chromatographia* 16 (1982) 138.
47. Wall, R. A., *J. Chromatogr.* 60 (1971) 195.
48. Knox, J. H., and Jurand, J., *J. Chromatogr.* 125 (1976) 89.
49. Horváth, C., Melander, W., Molnar, I. and Molnar, P., *Anal. Chem.* 49 (1977) 2295.
50. Yau, W. W., Kirkland, J. J., and Bly, D. D., *"Modern Size Exclusion Chromatography"*, Wiley, New York, 1979.
51. Horváth. C., Lee, A., Liao, A. and Valayudhan, A., *Int. Symp. on Column Liquid Chromatography, Amsterdam, NL., 28th June - 3rd July 1987.*
52. Guthrie, E. and Jorgenson, J. W., *Anal. Chem.* 56 (1984) 483.
53. Rose, D. J. and Jorgenson, J. W., *J. Chromatogr.* 44 (1988) 117.
54. Walbroehl, Y. and Jorgenson, J. W., *J. Chromatogr.* 315 (1984) 135.
55. Erni, F., Steuer, W. and Grant, I. H., *J. Chromatogr.* 507 (1990) 125.
56. Aris, R., *Proc. Roy. Soc. (London)*, A235 (1953) 67.
57. Martin, M. and Guiochon, G., *Anal. Chem.* 56 (1984) 614.
58. Lauer, H. H. and McManigill, D., *Anal. Chem.* 58 (1985) 166.
59. Bushey, M. M. and Jorgenson, J. W., *J. Chromatogr.* 480 (1989) 301.
60. Green, J. S. and Jorgenson, J. W., *J. Chromatogr.* 478 (1989) 63.
61. Hjerten, S., *J. Chromatogr.* 347 (1985) 191.

62. Hoyt, A. M. Jr. and Sepaniak M. J., *Anal. Lett.* 22(4) (1989) 861.
63. Grossman, P. D., Wilson, K. J., Petrie, G. and Lauer, H. H., *Anal. Biochem.* 173 (1988) 265.
64. Tsuda, T., Takagi, K., Watanabe, T. and Satake, T., *J. of HRC and CC*, 11 (1988) 721.
65. Walbroehl, Y. and Jorgenson J. W., *Anal. Chem.* 58 (1986) 479.
66. Cohen, A. S., Paulus, A. and Karger, B. L., *Chromatographia* 24 (1987) 15.
67. Cohen, A. S. and Karger, B. L., *J. Chromatogr.* 397 (1987) 409.
68. Guttman, A., Paulus, A., Cohen, A. S., Grinberg, N., and Karger, B. L., *J. Chromatogr.* 448 (1988) 41.
69. Terabe, S., Otsuka, K., Ichikawa, K., Tsuchiya, A. and Ando, T., *Anal. Chem.* 56 (1984) 111.
70. Terabe, S., Otsuka, K. and Ando, T., *Anal. Chem.* 57 (1985) 834.
71. Fujiwara, S. and Honda, S., *Anal. Chem.* 59 (1987) 2773.
72. Tsuda, T., *Anal. Chem.* 59 (1987) 521.
73. Tsuda, T., *Anal. Chem.* 60 (1988) 1677.
74. Pretorius, V., Hopkins, B. J., and Schiecke, J. D., *Journal of Chromatography*, 99 (1974) 23.
75. Jorgenson, J. W. and Lukacs, K. D., *J. Chromatogr.* 218 (1981) 209.
76. Tsuda, T., Nomura, K. and Nakagawa, G., *J. Chromatogr.* 248 (1982) 241.
77. Ishii, D. and Takeuchi, T., *J. Chromatogr.* 255 (1983) 349.
78. Gluckman, J. C., Hirose, A., McGuffin, V. L. and Novotny, M., *Chromatographia* 17 (1983) 303.
79. Tsuda, T. and Novotny, M., *Anal. Chem.* 50 (1978) 271.
80. Tsuda, T., Tanaka, I. and Nakagawa, G., *Anal. Chem.* 56 (1984) 1249.



81. Tanaka, N., Kinoshita, H., Araki, M., and Tsuda, T.,  
*Int. Symp. on HPLC, Kyoto, Japan, Jan. 28th-30th, 1985.*  
*Abs. No. 50128.*
82. Alborn, H. and Stenhagen, G., *J. Chromatogr.* 323 (1985) 47.
83. Novotny, M., *Anal. Chem.* 5 (1983) 580.
84. Huang, X., Gordon, M. J. and Zare, R. N., *Anal. Chem.* 60 (1988)  
377.
85. Huang, X., Gordon, M. J. and Zare, R. N., *J. Chromatogr.*,  
425 (1988) 385.
86. Wallingford, R. A. and Ewing, A. G., *Anal. Chem.* 60 (1988) 1975.
87. Stevens, T. S. and Cortes, H. J., *Anal. Chem.* 55 (1983) 1365.
88. Knox, J. H., Kaliszan, R. and Kennedy, G. J., *Faraday Discussions*  
*of the Roy. Soc. of Chem.* 15 (1980) 113.
89. Smith, R. D., Olivares, J. A., Nguyen, N. T., and Udseth, H. R.,  
*Anal. Chem.* 60 (1988) 436.
- 90 Yu, M. and Dovichi, N. J., *Anal. Chem.* 61 (1989) 37.



## **APPENDICES**

# APPENDIX I

## Calculation of h, v curve Coefficients

The estimation of the A,B and C terms in the Knox h,v equation can be obtained from experimental data by calculating the co-efficients required to give the minimum variance between experimental points and the approximating function,

$$h = B/v + C_s v + A v^{1/3}$$

One method<sup>1</sup> of obtaining these co-efficients is illustrated below.

First the data is written in matrix form as  $(n \times 3) \times (3 \times 1) = (n \times 1)$ , where the  $(n \times 3)$  matrix contains the reduced velocities at the appropriate powers, the  $(3 \times 1)$  the coefficients A,B and  $C_s$  and the  $(n \times 1)$  the measured plate heights. Consider the example below where n represents the total number of plate height determinations (typically 15-20).

$$\begin{pmatrix} v_1^{1/3} & v_1^{-1} & v_1 \\ v_2^{1/3} & v_2^{-1} & v_2 \\ v_3^{1/3} & v_3^{-1} & v_3 \\ v_4^{1/3} & v_4^{-1} & v_4 \\ \vdots & \vdots & \vdots \\ v_n^{1/3} & v_n^{-1} & v_n \end{pmatrix} \times \begin{pmatrix} A \\ B \\ C \end{pmatrix} = \begin{pmatrix} h_1 \\ h_2 \\ h_3 \\ h_4 \\ \vdots \\ h_n \end{pmatrix}$$

If both sides of this equation are multiplied by the transpose of the reduced velocity matrix, i.e. a  $(3 \times n)$  matrix, this will give rise to a  $(3 \times 3) \times (3 \times 1) = (3 \times 1)$ . This equation can then be solved by Gaussian elimination to give an upper triangular  $(3 \times 3)$  matrix allowing the optimum values of A,B and  $C_s$  to be readily calculated.

The microcomputer routine listed below was developed for this application on the BBC microcomputer and is written in BBC basic. Line numbers have been omitted for clarity, except where these are required.

---

<sup>1</sup>Savitzky, A. & Golay, M. J. E., Anal. Chem. 36 (1964) 1627.

```

REM Curve fit routine for h,v plots
REM For BBC model B/B+ and Acorn Electron
REM 10/12/85 I H Grant
MODE 0
PRINT""Column Details""
INPUT"Column Length/m="L
INPUT"Particle Diameter/um="dp:dp=dp/1E6
PRINT"Diffusion Coefficient=1E-9 m ^ 2/s (Y/N) ?"
Dm=1E-9
REPEAT:ANSS=GET$:UNTIL INSTR("yYnN",ANSS)
IF INSTR("Yy",ANSS) THEN INPUT"Diffusion Coefficient="Dm
FACX=(L*dp)/(Dm*60)
FACY=L/dp
INPUT"Number of data points="N:N%=N:CLS
PRINT""Input times in minutes and number of plates observed"
DIM X(N,3),Y(N,1),TRANS(3,N),A(3,3),C(3,3),B(3)
REM Form data matrix containing velocities

FOR I%=1 TO N
  PRINT TAB(10,I%+2);"tm(";I%;"")=";
  INPUT""X(I%,1):X(I%,1)=FACX/X(I%,1)
  PRINT TAB(30,I%+2)"N(";I%;"")=";
  INPUT""Y(I%,1):Y(I%,1)=FACY/Y(I%,1)
  X(I%,2)=X(I%,1) ^ 0.33
  X(I%,3)=1/(X(I%,1))
NEXT I%

PROCtable
PROCtrans("X")
PROCmultiply("TRANS","X",3,3,N)
REM Subroutine returns product in array C

FOR I%=1 TO 3
  FOR K%=1 TO 3
    A(I%,K%)=C(I%,K%)
  NEXT K%
NEXT I%

PROCmultiply("TRANS","Y",3,1,N)
REM Y values now in matrix C from subroutine
PROCeliminate(3)
PROCsolve(3)
PRINT""A="";B(2)
PRINT"B="";B(3)
PRINT"C="";B(1)
END

```

```

DEFPROCmultiply(A$,B$,m,q,n)
REM Multiplies matrices A$xB$, (m x n) x (p x q)
REM Returns a matrix m x q, n=p -number of operations per point
A$=A$+"(I%,f)*"+B$+"(f,K%)"
FOR I%=1 TO m
  FOR K%=1 TO q
    C(I%,K%)=0
    FOR f=1 TO n
      C(I%,K%)=C(I%,K%)+EVAL(A$)
    NEXT f
  NEXT K%
NEXT I%
ENDPROC

```

```

DEFPROCtrans(A$)
REM Returns the transpose of matrix
REM called A$
A$=A$+"(K%,I%)"
FOR I%=1 TO 3
  FOR K%=1 TO N
    TRANS(I%,K%)=EVAL(A$)
  NEXT K%
NEXT I%
ENDPROC

```

```

DEFPROCeliminate(N)
REM Performs Gaussian elimination on N x N array
REM Returns upper triangular matrix
FOR S=1 TO N-1
  FOR I=S+1 TO N
    QUOT=A(I,S)/A(S,S)
    FOR K=S TO N
      A(I,K)=A(I,K)-QUOT*A(S,K)
    NEXT K
    C(I,1)=C(I,1)-QUOT*C(S,1)
  NEXT I
NEXT S
ENDPROC

```



```

DEFPROCpivot(S)
REM Finds largest co-efficient before elimination
MAX=A(S,S)
FOR J=S TO N
  IF A(J,S)>MAX THEN MAX=A(J,S):R=J
NEXT J
IF R=S THEN ENDPROC
REM Exchange A(R,K) and A(S,K) for K=S TO N
FOR T=S TO N
  TEMP=A(S,T)
  A(S,T)=A(R,T)
  A(R,T)=TEMP
NEXT T
TEMP=C(S,1)
C(S,1)=C(R,1)
C(R,1)=TEMP
ENDPROC

DEFPROCsolve(N)
REM Performs triangular substitution
FOR I=N TO 1 STEP -1
  SUB=0
  IF I=N THEN 10
  FOR J=I+1 TO N
    SUB=SUB+A(I,J)*B(J)
  NEXT J
10  B(I)=(C(I,1)-SUB)/A(I,I)
NEXT I
ENDPROC

```

```

DEFPROCtable
CLS:VDU2:REM Produces tabulated data.
PRINT'TAB(5);"Column Length="";L;"m";
PRINT"  Particle Diameter="";dp*1E6;"um"
PRINT'
PRINT TAB(5) STRING$(68,"-")
PRINT TAB(5)"tm/mins";TAB(15)"|";TAB(20)"u/(m/s)";TAB(30)"|";
PRINT TAB(33)"Red. Vel.";TAB(45)"|";TAB(48)"Plate Height";
PRINT TAB(62)"|";TAB(65)"Red. Height"
PRINT TAB(5) STRING$(68,"-")
MAX=0
FOR I%=1 TO N
  TM=FACX/X(I%,1):u=L/(TM*60):H=Y(I%,1)*dp
  @%=&020205:PRINT TAB(8);TM;TAB(15)"|";
  @%=&010306:PRINT TAB(20);u;TAB(30)"|";
  @%=&020205:PRINT TAB(36);X(I%,1);TAB(45)"|";
  PRINT TAB(52);H*1000;TAB(62)"|";
  PRINT TAB(66);Y(I%,1)
  IF Y(I%,1)>MAX THEN MAX=Y(I%,1)
NEXT I%
VDU3
ENDPROC

```

## APPENDIX II

### Datasytem for Electrochromatography

The following listing gives details of the datasytem used for the collection and processing of the chromatographic data obtained in this work. The program is written in BBC BASIC and line numbers have been omitted for clarity except where these are necessary. The location of the data in the memory and the data collection method are based on LABMASTER, a chromatographic integration package by Dr. A. G. Rowley. The graphic display and scaling routines were taken directly from this program, as indicated in the listing. The function of each subroutine and the significance of important variables are explained in comment statements.

```

REM Electrochromatography Datasytem.
REM November 1986
REM Menu and Control Program
datastart%=&3008:HIMEM=&3000:C%=FALSE
*FX12,10
*FX4,1
*FX225,150
DIMdata(1),AREA(3):PROCcu(0)
ON ERROR CLOSE#0:IF ERR=17 THEN 110 ELSE REPORT:PRINT;" at line ";ERL:END
110 REPEAT VDU22,7:PROCcu(1)
    PRINTTAB(5);CHR$(141);"ELECTROCHROM DATA SYSTEM"
    PRINTTAB(5);CHR$(141);"ELECTROCHROM DATA SYSTEM"
    PRINT"
    PRINT";CHR$(129);"    1) Save Data"
    PRINT;CHR$(129);"    2) Load New Data"
    PRINT;CHR$(129);"    3) Analyse Data"
    PRINT;CHR$(129);"    4) Display Full Run"
    PRINT;CHR$(129);"    5) Acquire New Data"
    PRINT;CHR$(129);"    6) Return to Main Menu"
    PRINT";CHR$(129);"* Operating System Command"
    PRINT"" Please Enter Choice";
    *FX15,1
    X$=GET$
    IF X$="1" THEN PROCsave
    IF X$="2" THEN PROCsafe:IF INSTR("Yy",safe$) THEN PROCload
    IF X$="3" THEN PROCplot
    IF X$="4" THEN PROCwhole
    IF X$="5" THEN PROCsafe:IF INSTR("Yy",safe$) THEN PROCready:PROCread
    IF X$="6" THEN PROCsafe:IF INSTR("Yy",safe$) THEN CHAIN"MENU"
    IF X$="*" THEN CLS:INPUT"*"CM$:OSCLI(CM%):REPEAT:UNTIL GET=32
    SOUND 1,-10,200,1
    UNTIL FALSE
END

```

PROCread - Reads A/D convertor by calling BBC function ADVAL(1) every K%/100 seconds. Data is stored in RAM location defined by variable L%. 12bit Data samples are stored in two adjacent 8bit RAM locations. During data collection the signal and elapsed time are displayed numerically.

```

DEFPROCread
VDU22,7
@%=&90A:C%=TRUE
PROCcu(0):N%=-1:L%=datastart%:time%=0
PRINTTAB(0,1);CHR$(131);CHR$(157);TAB(11,1);CHR$(141);CHR$(132);"READING DATA"
PRINTTAB(0,2);CHR$(131);CHR$(157);TAB(11,2);CHR$(141);CHR$(132);"READING DATA"
PRINTTAB(4,6)"Time/secs";TAB(20,6)"Fluorescence"
PRINTTAB(0,23);"PRESS <ESC> TO STOP    ";100DIVK%;"Hz"
REPEAT
    TIME=0
    *FX17,1
    PRINT TAB(8,10);time%DIV100;TAB(25,10);Y%DIV64;" ~
    REPEAT:UNTIL ADVAL(0)DIV256=1

```

```

Y%=ADVAL(1)
?L%=Y%MOD256:?(L%+1)=Y%DIV256
L%=L%+2:N%=N%+1
REPEAT:UNTILTIME=K%
time%=time%+K%
UNTIL L%>=&B000
ENDPROC

```

PROCload and PROCsave enable the chromatographic data to be loaded from or saved to disk. pd%, cl%, N%, pdv% and K% are stored with the data file and represent particle diameter, column length, number of stored points, voltage drop and sampling interval respectively.

```

DEFPROCload
C%=TRUE
PRINTTAB(1,21);"
INPUTTAB(1,21);"Enter Filename ~f$
OSCLI("LOAD ~+f$)
pd%=?&3000
cl%=?&3001
K%=?&3002
N%=?&3003+?&3004*256
DELAY%=?&3005*10
pdv%=?&3006
ENDPROC

```

```

DEFPROCsave
IF C%=FALSE THEN ENDPROC
INPUTTAB(1,21);"Enter Filename ~f$
?&3000=pd%
?&3001=cl%
?&3002=K%
?&3003=N% MOD 256
?&3004=N% DIV 256
?&3005=DELAY% DIV 10
?&3006=pdv%
DEC%=&3006+N%*2-1
PROCgethex(DEC%)
OSCLI("SAVE ~+f$+" 3000 ~+hex$)
ENDPROC

```

PROCanalyse - Calculates number of plates from the width at half height and the statistical second moment. Recieves from PROCcursor tb% and te% defining the area of intrest. SUB% corresponds to the baseline background flourescence signal. Uses the function FNgetpoint(N%), from Labmaster, to recall the value of the sample with serial number N%. Call integration routine to integrate c(t) as "FNtruept(I%)" with respect to time, followed by "FNtruept(I%)\*I%" and "FNtruept(I%)\*(I%-TM%)^2" which represent t.c(t) and  $(t_m - t)^2 \cdot c(t)$  respectively. The peak area, the first moment and the second moment are stored in the variable AREA(1), AREA(2) and AREA(3) respectively.



```

DEFPROCanalyse
tb%=FNpt(data(0))
te%=FNpt(data(1))
SUB%=(FNgetpoint(tb%)+FNgetpoint(te%))/2
YMAX%=0
FOR I%=tb% TO te%
  IF FNgetpoint(I%)>=YMAX% THEN YMAX%=FNgetpoint(I%)
NEXT I%
PROCupslope(1.5)
PROCdownslope(1.5)
XMAX%=(XL%+XR%)/2
PROCupslope(2)
PROCdownslope(2)
PROCline(2)
fwhh=(XR%-XL%+1)*K%/100
PROCupslope(10)
PROCdownslope(10)
PROCline(10)
MOVE FNscx(XMAX%),SUB%*cf*vsc1%:PLOT 21,FNscx(XMAX%),YMAX%*cf*vsc1%
REM Find peak symmetry
PS=(XR%-XMAX%)/(XMAX%-XL%)
HZ=100/K%
PROC INTEGRATE("FNtruept(I%)",1)
SOUND1,-10,200,2:SOUND1,0,200,5:SOUND1,-10,250,2
PROC INTEGRATE("FNtruept(I%)*I%",2)
TM%=AREA(2)/AREA(1)
PROC INTEGRATE("FNtruept(I%)*((I%-TM%)^2)",3)
VAR=(AREA(3)/AREA(1))/(HZ^2)
TM=TM%/HZ+DELAY%
PROCreport
ENDPROC

```

PROCINTEGRATE(func\$,loc%) integrates the function contained in func\$ from tb% to te% using the trapezium rule. The result is stored in the array AREA; the location is specified by the variable loc%.

```

DEFPROC_INTEGRATE(A$,L%)
I%=tb%
SUM=EVAL(A$)*0.5
FOR I%=(tb%+1) TO (te%-1)
  SUM=SUM+EVAL(A$)
NEXT I%
I%=te%
SUM=SUM+0.5*EVAL(A$)
AREA(L%)=SUM
ENDPROC

```

PROCreport Prints a complete report for each chromatographic peak after the second moment has been calculated.

```

DEFPROCreport
CLS:VDU19,0,0,0,0,0
PRINT"Do you want printed results (Y/N) ?"
REPEAT:A$=GET$:UNTIL INSTR("YyNn",A$):CLS
IF A$="Y" OR A$="y" THEN VDU2
PRINT"TAB(30)"Peak Analysis Report"
@%=&02020A
PRINT TAB(30)"-----"
PRINTTAB(10)"First Moment/s=";TAB(50);TM
PRINTTAB(10)"Second Moment/s^2=";TAB(50);VAR
NP%=INT((TM^2/VAR)+0.5)
@%=10:PRINTTAB(10)"Number of Theoretical Plates=";TAB(50);NP%
PRINTTAB(10)"Number of Plates from FWHH=";TAB(50);INT(5.54*((TM/fwhh)^2)+0.5)
PRINTTAB(10)"Column Length/cm=";TAB(50);cl%
PRINTTAB(10)"Particle Diameter/um=";TAB(50);pd%
PRINTTAB(10)"Potential Drop/kV=";TAB(50);pdv%
@%=&02020A:PRINTTAB(10)"Peak Symmetry at 10% of Height=";TAB(50);PS
PRINTTAB(10)"Reduced Plate Height=";TAB(50);cl%/NP%/(pd%*1E-4)

```

```

PRINT TAB(10)"Reduced Velocity / (1+k')=";TAB(50);10*cl%*pd%/TM
PRINT:VDU3
PRINT TAB(27,28)"PRESS <SPACE> TO CONTINUE"
*FX15,1
REPEAT:UNTIL GET=32
@%=10:VDU19,0,4,0,0,0
ENDPROC

```

FNtruept is equivalent to  $c(t)$ . FNgetpoint represents the actual signal and SUB% the average background signal.

```

DEF FNtruept(n%)
=FNgetpoint(n%)-SUB%

```

Serial numbers to screen co-ordinate functions

```

DEF FNscx(n%)
=2*(n%-st%)/hsc1%

DEF FNscy(n%)
=INT(FNgetpoint(n%))*cf*vsc1%

```

PROCupslope(fract) returns the x co-ordinate of the point in a slope increasing with time, where the height is equivalent to  $1/\text{fract}$  of the maximum height. Returns XL% to PROCanalyse (equivalent to  $t_i$ ). PROCdownslope returns XR% (equivalent to  $t_r$ ) to PROCanalyse.

```

DEFPROCupslope(ph)
l%=tb%-1
REPEAT
  l%=l%+1
  UNTIL FNtruept(l%)>((YMAX%-SUB%)/ph)
XL%=l%
ENDPROC

```

```

DEFPROCdownslope(ph)
l%=te%+1
REPEAT
  l%=l%-1
  UNTIL FNtruept(l%)>((YMAX%-SUB%)/ph)
XR%=l%
ENDPROC

```

```

DEFPROCline(ph%)
MOVE FNscx(XL%),((YMAX%-SUB%)/ph%+SUB%)*cf*vsc1%
PLOT 21,FNscx(XR%),((YMAX%-SUB%)/ph%+SUB%)*cf*vsc1%
ENDPROC

```

```

DEFPROCsafe
IF C%=FALSE THEN safe$="Y":ENDPROC
*FX15,1
PRINT TAB(1,21);"Are you sure ? (Y/N)":VDU7
REPEAT:safe$=GET$:UNTIL INSTR("YyNn",safe$)
ENDPROC

```

PROCready is selected by data acquisition option. Reads in relevant parameters such as particle diameter, column length etc.. Calls PROCread following a sudden pulse in the input signal.

```

DEFPROCready
VDU22,7
PRINTTAB(0,1);CHR$(131);CHR$(157);TAB(9,1);CHR$(141);CHR$(132);"DATA ACQUISITION"
PRINTTAB(0,2);CHR$(131);CHR$(157);TAB(9,2);CHR$(141);CHR$(132);"DATA ACQUISITION"
PRINT:INPUT" Particle Diameter/um="pd%
INPUT" Column Length/cm="cl%:INPUT" Voltage/kV="pdv%
PRINT" Set time delay (y/n) ?":REPEAT:A$=GET$:UNTIL INSTR("YyNn",A$)
IF INSTR("Yy",A$) THEN INPUT" Delay time/mins="delay% ELSE DELAY%=0
INPUT" Sampling Rate/Hz="K%:K%=100DIVK%:VDU12
PRINTTAB(10,10);CHR$(141);"READY FOR DATA"
PRINTTAB(10,11);CHR$(141);"READY FOR DATA"
REPEAT:UNTIL ADVAL(1)DIV64>100:SOUND1,-15,200,1:SOUND1,-15,100,1
IF INSTR("Yy",A$) THEN PROCdelay
ENDPROC

```

```

DEFPROCgethex(DEC%)
hex$=""
FORI%=3TO0STEP-1
  he%=DEC% DIV 16 ^I%
  DEC%=DEC% MOD 16 ^I%
  IF he%<10 hex$=hex$+STR$(he%) ELSE he%=he%+55:hex$=hex$+CHR$(he%)
NEXT
ENDPROC

```

PROCdelay can be used to delay the recording of data for a set time after the injection. The delay time is automatically accounted for in subsequent calculations by the variable DELAY%. This allows data collection at a fast sampling rate (e.g. 33Hz) even for long elution times.

```

DEFPROCdelay
VDU22,7
PROCcu(0)
delay%=delay%*60:DELAY%=delay%
PRINT:PRINT" BEGIN RECORDING IN:"
REPEAT
  TIME=0
  dt%=delay% DIV 60
  sec%=delay% MOD 60
  PRINT TAB(12,9);CHR$(141);dt%;" : ";sec%; " min "
  PRINT TAB(12,10);CHR$(141);dt%;" : ";sec%; " min "
  PRINT" FLUORESCENCE SIGNAL":Y%=ADVAL(1)DIV64
  PRINT TAB(12,17);CHR$(141);Y%;" units "
  PRINT TAB(12,18);CHR$(141);Y%;" units "
  REPEAT:UNTIL TIME=100
  delay%=delay%-1
  UNTIL delay%=0
ENDPROC

```

The remaining procedures and functions were taken directly from LABMASTER by Dr. A. G. Rowley and are concerned with screen plotting and scaling and the selection of  $t_b$  and  $t_e$  using an on-screen cursor.

```

DEF FNgetpoint(n%)
LOCAL pointer%
pointer%=datastart%+n%*2
=(?pointer%+256*(pointer%+1)) DIV 64

```



```

DEFPROCplot
IF C%=FALSE THEN ENDPROC
VDU22,0
LOCALi%,hscI%,vscI%,cf,n%,a$,f%
VDU29,78;50;19,0,4;0;
hscI%=1:vscI%=1:cf=960/1023:st%=0:W%=(100/K%)*60
REPEAT CLG
  FORi%=0TO1200 STEP40:MOVEi%,970:DRAWi%,960:NEXT
  n%=st%:MOVE0,INT(FNgetpoint(n%)*cf)*vscI%
  FORi%=2TO1200 STEP 2
    DRAWi%,INT(FNgetpoint(n%)*cf)*vscI%
    n%=n%+hscI%:IF n%>N% i%=1500
  NEXT:f%=TRUE
780  PROClegend:*FX15,1
  REPEAT a$=GET$
  IF a$=CHR$(137)st%=st%+W%:IF st%>=N% st%=st%-W%
  IF a$=CHR$(136)st%=st%-W%:IF st%<0st%=0
  IF a$=CHR$(150)hscI%=FNinch(hscI%)
  IF a$=CHR$(151)hscI%=FNdech(hscI%)
  IF a$=CHR$(152)ANDvscI%<10vscI%=vscI%*2:IF vscI%=4vscI%=5
  IF a$=CHR$(153)ANDvscI%>1vscI%=vscI%DIV2
  IF a$=CHR$(154)W%=FNinc(W%):GOTO780
  IF a$=CHR$(155)W%=FNdec(W%):GOTO780
  IF a$=" " PROCcursor:IF f% THEN 780
  UNTIL FALSE

```

```

DEF FNinc(W%)
IF W%=(1000*60)/K% =W% ELSE =W%+1000/K%
DEF FNdec(W%)
IF W%=1000/K% =W% ELSE =INT(W%-1000/K%+0.5)
DEF FNinch(n%)
IF n%=1 =n%
IF n%=2 =1
IF n%=4 =2
=n%-4

```

```

DEF FNdech(n%)
IF n%=12 =n%
IF n%=1 =2
IF n%=2 =4
=n%+4

```

```

DEFPROClegend
PRINTTAB(0,31)STRING$(79," ");
PRINTTAB(0,31);INT(FNtime(0)+0.5);" to ";INT(FNtime(1200)+0.5);"s";
PRINTTAB(18,31);"Sp ";INT(W%*(K%/100)+0.5);"s";
PRINTTAB(0,0);100/vscI%
ENDPROC

```

```

DEFPROCcursor
LOCALa$,h%,dp%,p%:GCOL3,1
REPEAT
  MOVEh%,0:DRAWh%,1000:PRINTTAB(60,31)FNtime(h%);" secs.":p%=st%+(h%/2)*hscI%
  IFp%<=N% PRINTTAB(40,31)"Pk.Ht ";STRING$(4,CHR$(8));INT(FNgetpoint(p%)/1023*1000);
  REPEAT a$=GET$:UNTIL INSTR(" "+CHR$(135)+CHR$(136)+CHR$(137),a$)
  MOVE h%,0:DRAWh%,1200:PRINTTAB(46,31)" ";
  (IFa$=CHR$(135)ANDp%<=N%:GCOL0,1:MOVEh%,0:PLOT21,h%,1000:
  a$=CHR$(137):GCOL3,1:f%=FALSE:PROCrec)
  IF a$=CHR$(137)h%=FNup(h%):IF h%>1200 h%=0
  IF a$=CHR$(136)h%=FNdn(h%):IF h%<0 h%=1200
  UNTIL a$=" ":GCOL0,1
ENDPROC

```

```

DEF FNtime(n%)
LOCAL res:res=hscI%*(K%/100)
=st%*(K%/100)+((n%/2)*res)

```



```

DEFPROCrec
data(dp%)=h%:dp%=dp%+1:IF dp%=2 PROCanalyse:PROClegend:a$=" "
ENDPROC

```

```

DEFPROCcu(n%)
VDU23,1,n%;0;0;0;:ENDPROC

```

```

DEF FNpt(n)
=INT(st%+(n/2*hscl%))

```

```

DEFFNup(h%)
IF INKEY(-1)=TRUE =h%+16 ELSE =h%+2

```

```

DEFFNdn(h%)
IF INKEY(-1)=TRUE =h%-16 ELSE =h%-2

```

The above listing is concerned specifically with the analysis of Gaussian peaks. For fronts modified versions of PROCanalyse, PROCupslope and PROCdownslope are used.

## APPENDIX III

Minimum Chromatographic Analysis Times for a Fixed  $d_p$ .

## I. Electrochromatography

The minimum analysis time for a given number of theoretical plates will be realised by working at field corresponding to the maximum performance ( $N/t$ ). If the A-term is assumed to be negligible, the field at which  $N/t$  is a maximum is given by,

$$E_{opt} = (6.8/d_c) \cdot (D_m K / \mu_{eo} \epsilon \Lambda \alpha_v)^{1/3}$$

where  $\mu_{eo}$  is the coefficient of electroosmotic flow.

By again making the assumption that only the B and  $C_s$  terms contribute to the plate height, the maximum number of theoretical plates obtainable at this field is given by,

$$N_{Eopt} = V_{max} [3D_m / \mu_{eo} + 46C_s (d_p/d_c)^2 (\mu_{eo}/D_m)^{1/3} (K/\epsilon \Lambda \alpha_v)^{2/3}]^{-1}$$

where  $V_{max}$  represents the maximum voltage available. If  $N$  is less than  $N_{Eopt}$ , the maximum available voltage cannot be used, since this would lead to a field of greater than  $E_{opt}$ . For  $N=0$  to  $N=N_{Eopt}$  the shortest analysis time is given by,

$$t = V_{max} \cdot N / N_{Eopt} \cdot \mu_{eo} E_{opt}^2$$

If  $N > N_{Eopt}$  insufficient voltage is available for working at  $E_{opt}$ . The shortest analysis time for a given  $N$  will be achieved by working at  $V_{max}$  and adjusting the column length until  $N$  plates are achieved. For an available voltage  $V_{max}$  it can be shown that,

$$h\nu = \mu_{eo} \cdot V_{\max} / N \cdot D_m$$

If  $h$  is replaced by  $h = B/\nu + C_s \nu + D\chi^6 \nu^5$  one obtains,

$$C_s \nu^2 + B + D\chi^6 \nu^6 - (\mu_{eo} V_{\max} / ND_m) = 0$$

This equation can be solved for  $\nu$  using a Newton/Raphson iterative method. The analysis time is then given by,

$$t = Nd_p^2 h / \nu D_m$$

## II. Pressure Driven Chromatography

Similary for HPLC with a fixed particle diameter the maximum value of  $N/t$  for a given  $N$ , will be achieved by using the full available pressure and adjusting the length until  $N$  plates are obtained. By analogy with the electrochromatographic case one can write,

$$h\nu = \Delta P d_p^2 / \phi \eta N D_m$$

If  $h$  is replaced by  $h = A\nu^{1/3} + B/\nu + C_s \nu$  one obtains,

$$B + A\nu^{4/3} + C_s \nu^2 - (\Delta P d_p^2 / \phi \eta N D_m) = 0$$

As in the previous case the value of  $\nu$  can be obtained using an iterative method.

The above method is only relevant if  $d_p$  is fixed. Faster analyses are always possible if the particle size predicted by the Knox & Saleem method is used.

## APPENDIX IV

## Glossary of Symbols Used

- A Flow term coefficient in plate height equation.
- $A_c$  Capillary cross sectional area.
- $a$  Capillary or particle radius.
- $C_m$  Mobile zone mass transfer coefficient in plate height equation.
- $C_s$  Stationary zone mass transfer coefficient in plate height equation.
- $c$  Concentration of electrolyte.
- $D_m$  Diffusion coefficient of a species in the mobile zone ( $m^2 s^{-1}$ ).
- $D_s$  Diffusion coefficient of a species in the stationary zone ( $m^2 s^{-1}$ ).
- $d_p$  Particle diameter.
- $d_c$  Capillary diameter.
- $E$  Electric Field ( $Vm^{-1}$ ).
- $E$  Separation impedance (  $E = h^2 \cdot \phi$  ).
- $E_n$  Potential energy of state  $n$ .
- $e$  Charge on an electron ( $1.60 \times 10^{-19} C$ ).
- $\Delta G_0$  Change in electrical potential energy as a result of migration ( $Jmol^{-1}$ ).
- $H$  Absolute value of plate height.
- $h$  Reduced plate height (  $h = H/d_p$  )
- $I_0(x)$  Zero order modified Bessel function of the first kind.
- $I_1(x)$  First order modified Bessel function of the first kind.
- $I_n$   $n$ th statistical moment of a distribution.



- $k'$  Phase capacity ratio.  
 $k''$  Zone capacity ratio.  
 $K$  Distribution coefficient.  
 $K$  Thermal conductivity ( $\text{WmK}^{-1}$ ).  
 $k$  Boltzmann constant ( $1.38 \times 10^{-23} \text{JK}^{-1}$ )  
 $\kappa$  Reciprocal electrical double layer thickness.  
 $L$  Column length.  
 $l$  Length of injected sample zone.  
 $N$  Number of theoretical plates (dimensionless).  
 $\Delta P$  Pressure drop across column ( $\text{Nm}^{-2}$ ).  
 $Q$  Rate of heat generation (W).  
 $q$  Electrical charge (C).  
 $R$  Electrical resistance ( $\Omega$ ).  
 $R$  Universal gas constant ( $8.314 \text{Jmol}^{-1} \text{K}^{-1}$ ).  
 $t_b$  Effective peak or front start time.  
 $t_e$  Effective peak or front end time.  
 $t_m$  Elution time of an unretained species.  
 $u$  Mean linear flow velocity in mobile phase.  
 $u_0$  Mean linear flow velocity in mobile zone.  
 $V$  Voltage across full length of capillary.  
 $V_m$  Volume of mobile phase contained within a column.  
 $V_R$  Retention volume.  
 $v_A$  Hypothetical volume of mobile phase per plate in plate model.  
 $w$  Effective peak width ( $w = 4 \cdot \sigma_L$ ).  
 $w_{1/2}$  Peak width at half height.

$z$	General migration coordinate (in length units).
$z$	Charge Number.
$\alpha_V$	Coefficient of viscosity change with temperature ( $K^{-1}$ ).
$\alpha_e$	Coefficient of change in dielectric constant with temperature ( $K^{-1}$ ).
$\alpha_k$	Coefficient of change in $k'$ with temperature ( $K^{-1}$ ).
$\delta$	Thickness of the Stern layer.
$\epsilon_r$	Relative permittivity.
$\epsilon_0$	Permittivity of free space ( $8.85 \times 10^{-12} C^2 N^{-1} m^{-2}$ ).
$\epsilon$	Porosity of packed bed.
$\phi$	Dimensionless flow resistance parameter.
$\gamma$	Geometric constant for obstructed diffusion.
$\gamma$	Combined Tortuosity and Porosity Factor.
$\eta$	Coefficient of viscosity ( $Nm^{-2}s$ ).
$\lambda$	Geometric constant in Van Deemter equation.
$\lambda_{ex}$	Fluorescence excitation wavelength.
$\lambda_{em}$	Fluorescence emission wavelength.
$\Lambda$	Molar conductivity of electrolyte ( $m^2 mol^{-1} \Omega^{-1}$ ).
$\mu_{ep}$	Electrophoretic mobility ( $m^2 s^{-1} V^{-1}$ ).
$\mu_{eo}$	Coefficient of electroosmotic flow ( $\mu_{eo} = \epsilon_r \epsilon_0 \cdot \zeta / \eta$ ).
$v$	Reduced velocity ( $v = u_o \cdot d_p / D_m$ ).
$\rho$	Charge density ( $Cm^{-3}$ )
$\sigma$	Peak standard deviation.
$\sigma_0$	Surface charge density ( $Cm^{-2}$ ).

- $\tau$  Mean residence time in a particular zone denoted by subscript m or s.
- $\psi$  Electrical potential (V).
- $\psi_0$  Surface potential.
- $\psi_d$  Potential at Stern plane.
- $\chi$  Reduced column diameter ( $\chi = d_c/d_p$ ).
- $\zeta$  Zeta potential (V).

## APPENDIX V

### COURSES ATTENDED

In accordance with the University of Edinburgh regulations, in addition to attending regular departmental seminars in physical chemistry, the following postgraduate courses were attended.

1. Molecular Electronics
2. Microcomputers in the Laboratory
3. Signal Processing
4. EMAS Scribe Course
5. FORTRAN Programming
6. Industrial Chemistry
7. Chemical Technology and Industrial Chemistry
8. Mass Spectroscopy
9. All meetings of the East of Scotland HPLC Users Group during the period of study.
10. Course in Scientific German.

### Conferences Attended

9th International Symposium on Column Liquid Chromatography, Edinburgh, July 1985.